Designing fluorescent probes for the study of intracellular cholesterol metabolism

Master's Thesis
University of Jyväskylä
Department of Chemistry
20.2.2019
Jukka Hintikka

Abstract

Cholesterol is abundantly present in animal cells. It comprises a major portion of the lipids in mammalian cell membranes and is required for the synthesis of steroid hormones, lipoproteins and bile acids. Many characteristics of cellular membranes are highly affected by their cholesterol content. The intracellular transport and distribution of cholesterol is affected and controlled by many distinct and individual mechanisms, many of which are not fully understood. Fluorescent sterols or sterol-binding molecules are commonly utilized as probes to provide valuable data on cholesterol transport and distribution. Three new synthetic fluorophores, Fp1-Fp3, were provided by the Institute of Biotechnology of the Czech Academy of Sciences. Their applicability in the fluorophore-labeling of cholic acid and methyl lithocholate was investigated. A conjugate of Fp2 and cholic acid was successfully synthesized (yield 14 %) for further molecular biology studies.

Keywords: Cholesterol transport, sterols, bile acids, fluorescence, fluorescent probes

Tiivistelmä

Kolesteroli on yksi yleisimpiä eläinsolujen rakennusaineita. Eläinsolujen solukalvot koostuvat pääosin fosfolipideistä ja kolesterolista. Kolesterolin osuus solukalvon lipideistä voi olla jopa 40 %. Solukalvojen ominaisuudet, kuten läpäisevyys ja liikkuvuus, riippuvat vahvasti niiden sterolipitoisuudesta. Kolesterolia tarvitaan myös steroidihormonien, lipoproteiinien ja sappihappojen synteesiin. Kolesterolin solunsisäinen kuljetus ja jakautuminen riippuvat useiden itsenäisten homeostaattisten mekanismien yhteisvaikutuksesta. Suurinta osaa näistä mekanismeista ei vielä tunneta yksityiskohtaisesti. Kolesterolin solunisäistä kuljetusta ja jakautumista tutkitaan usein fluoresoivilla kolesterolianalogeilla tai steroleja sitovilla fluoresoivilla merkkiaineilla. Kolme uutta synteettistä fluoroforia, Fp1-Fp3, saatiin käyttöön Tsekin Tiedeakatemian Bioteknologian Instituutilta. Tässä työssä pyrittiin valmistamaan kolmen fluoroforin konjugaatit koolihapon kanssa. Konjugaattien oletetaan sitovan kolesterolia ja siten toimivan fluoresoivina merkkiaineina tarkasteltaessa kolesterolin kuljetusta ja jakautumista soluissa fluoresenssimikroskopian avulla. Fp2:n ja koolihapon konjugaatti syntetisoitiin onnistuneesti (saanto 14%). Se lähetetään molekyylibiologisiin jatkotutkimuksiin.

Asiasanat: Kolesteroli, kuljetus, steroli, sappihappo, fluoresenssi, fluoresoivat merkkiaineet

Preface

The experiments of the present thesis were conducted at the laboratories of Organic Chemistry at the Department of Chemistry, University of Jyväskylä from January 2018 to May 2018.

I would like to express my gratitude to my supervisor Elina Sievänen for the opportunity to work in her lab and for providing the truly interesting topic, guidance and support.

My thanks to my family, close friends and colleagues for their trust and encouragement. A special shoutout to Taija Kolehmainen for support throughout the process and notes on typography.

Jyväskylä, December 2018.

Jukka Hintikka

Contents

Abbreviations

ABC	ATP-binding cassette transporter
ACAT	Acyl-CoA cholesterol acyltransferase
ACN	Acetonitrile
apoA1	Apolipoprotein A1
ATP	Adenosine triphosphate
BODIPY	Boron dipyrromethene difluoride
cAMP	Cyclic adenosine monophosphate
CARS	Coherent anti-Stokes Raman scattering
CCD	Charge-coupled device
CTL	Cholestatrienol
dansyl	5-Dimethylamino-1-napthalenesulfonyl
DCM	Dichloromethane
DHE	Dehydroergosterol
DMPC	Dimyristoylphosphatidylcholine
DRM	Detergent resistant membrane
ER	Endoplasmic reticulum
ERC	Endocytic recycling compartment
EtOAc	Ethyl acetate
FCS	Fluorescence correlation spectroscopy
FLIP	Fluorescence loss in photobleaching
FRAP	Fluorescence recovery after photobleaching
GUV	Giant unilamellar vesicle
HDL	High density lipoprotein
HMGCR	3-Hydroxy-3-methylglutaryl CoA reductase
ld	Liquid-disordered
LDL	Low density lipoprotein
LDLR	Low density lipoprotein receptor
LE	Late endosome
lo	Liquid-ordered
LTP	Lipid transfer protein
LXR	Liver X receptor
Ly	Lysosome

MeOH	Methanol
MβCD	Methyl-β-cyclodextrin
MD	Molecular dynamics
NBD	Nitrobenzodiazole
NPC	Niemann-Pick type C
NPC1L1	Niemann Pick C1-Like 1
ORP	OSBP-related protein
OSBP	Oxysterol binding proteins
PFO	Perifringolysin O
PM	Plasma membrane
PtdCho	Phosphatidylcholine
PtdEtn	Phosphatidylethanolamine
PtdSer	Phosphatidylserine
Scap	SREBP cleavage activating protein
SIMS	Secondary ion mass spectrometry
SM	Sphingomyelin
SqMO	Squalene monooxygenase
SR-B1	Scavenger receptor B1
SREBP	Sterol response element-binding protein
StAR	Steroidogenic acute regulatory protein
VLDL	Very low-density lipoprotein

I Theoretical part

1. Introduction to the theoretical part

Cholesterol (Figure 1) is abundantly present everywhere in the animal kingdom. It comprises a major portion of the lipids in mammalian cell membranes and is required for the synthesis of steroid hormones, lipoproteins and bile acids. The shape, fluidity and permeability of cellular membranes are highly affected by their cholesterol content. The cholesterol concentration of cells is tightly controlled by homeostatic processes and the intracellular transport and distribution of cholesterol is affected and controlled by many distinct and individual mechanisms, many of which are not fully understood.

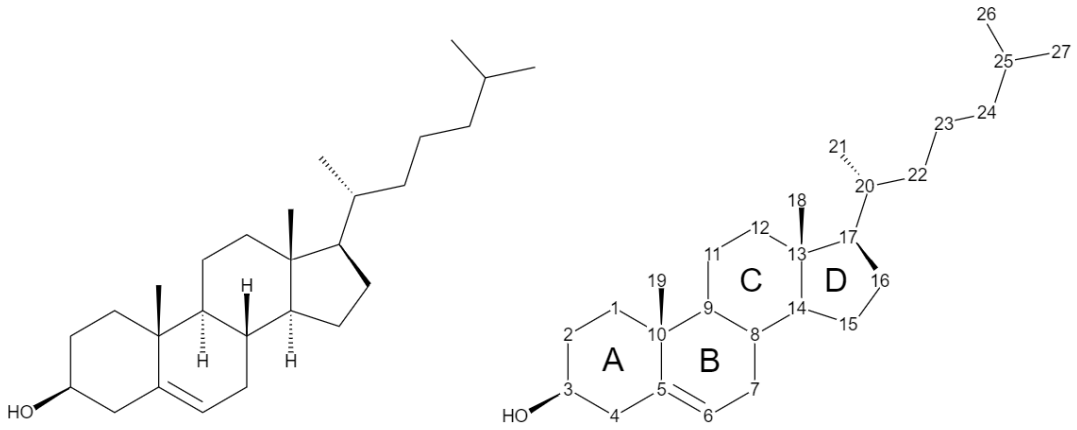

Figure 1. Structure of cholesterol without (left) and with (right) IUPAC-recommended carbon atom numbering and ring assignment. The cholesterol molecule consists of a steroid backbone with 3β-OH group, 5,6-double bond, and isooctyl sidechain branching from carbon 17.

Due to the many unanswered questions regarding intracellular cholesterol metabolism it has attracted a lot of interest in chemistry and pharmacology. Notably, the accumulation of cholesteryl ester droplets in macrophages is a key step in the formation of atherosclerotic lesions. Cardiovascular disease being globally the most prevalent cause of death[1] these mechanisms have understandably been subject to rigorous investigation.

Quantitative and qualitative characterization of intracellular sterol transport is a daunting and challenging task and no single method can be established for this task. Besides isolation of cell components (subcellular fractionation) and various methods to quantify cholesterol from these components, fluorometric techniques using fluorescent cholesterol analogs or sterol-binding molecules have been utilized to provide valuable data on cholesterol transport. The advantage of fluorometric methods is the possibility of using *in vivo* cells which would provide both steady-state and kinetic information on cholesterol distribution.[2]

This thesis takes a glance at the current knowledge on intracellular processes of cholesterol metabolism and fluorescent probes in analysis of cholesterol distribution. In addition, bile acids, which are naturally occurring sterol waste products and cholesterol analogs with steroid-binding properties, are investigated as potential fluorescent probes. So far, bile acids have been less focused on in current literature on fluorescent probes.

2. Cholesterol transport

2.1. Intracellular cholesterol distribution

Cells obtain cholesterol by either receptor mediated lipoprotein uptake or synthetic pathway. *De novo* cholesterol synthesis takes place in the endoplasmic reticulum (ER). Despite being the site of synthesis, cholesterol in the ER makes up of only about 0,5 – 1 % of cell cholesterol content. Cholesterol concentration is relatively higher in the neighboring Golgi apparatus, with increasing concentration when moving from the *cis*- to the *trans*-Golgi. Plasma membrane (PM), the outermost cellular wall, harbors the highest amount of cholesterol. In steady state, PM is estimated to contain 60-80 % of total cellular cholesterol. Also, up to 40 % of lipid molecules in the PM are estimated to be cholesterol. This pool undergoes rapid and continuous delivery to the cell interior and back to the PM, with an estimated half-time of 40 hours. In polarized epithelial cells, the apical membrane has higher sphingolipid and cholesterol content than the basolateral membrane.[3] Within the endocytic pathway, the route by which cells gain cholesterol from the extracellular environment, high amounts of cholesterol reside in the endocytic recycling compartment (ERC), which is a site for containment and redistribution of membrane proteins and lipids.

Cholesterol content in late endosomes (LEs) and lysosomes (Lys), which are the main sites of hydrolysis of low density lipoprotein (LDL) -derived cholesteryl esters, has not been well determined but is estimated to be lower than in the ERC.[4]

Several homeostatic processes tightly regulate cholesterol content and distribution in the cell (Figure 2). Cholesterol synthesis in the ER is highly sensitive to changes in the cholesterol concentration, despite its low steady-state levels. The sterol response element-binding protein (SREBP), along with its carrier proteins Scap and Insig activate upon reduced levels of cholesterol in the ER. This causes dissociation of Insig and the SREBP-Scap complex to migrate to the nucleus where it induces genes required for *de novo* synthesis and also the expression of low-density lipoprotein receptors (LDLR) to increase cholesterol uptake. As cholesterol levels return, the SREBP-Scap complex is reassociated with Insig and retained in the ER. Increased ER cholesterol levels cause the activation of liver X receptors (LXR), which induces a set of genes that work to decrease cholesterol load. These genes induce the expression of ATP-binding cassette transporters (ABC), which are cholesterol efflux pumps, expression of cytochrome P450 7A1, which is an enzyme involved in bile acid synthesis and breakdown of LDL-receptors. In addition, two main enzymes involved in cholesterol synthesis, 3-hydroxy-3-methylglutaryl CoA reductase (HMGCR) and squalene monooxygenase (SqMO), readily undergo degradation upon increase in ER cholesterol.[5,6] The ubiquitin-proteasome system is essential in regulating the expression of the aforementioned proteins and cholesterol homeostasis.[7] Conjugation of ubiquitin, a regulatory polypeptide, to target proteins results in the release of specific signals, which attracts proteasomes to subsequently degrade the targets. ER is also the site for esterification of excess cholesterol by acyl-CoA cholesterol acyltransferase (ACAT). Cholesteryl esters are stored into lipid droplets and hydrolyzed back to free cholesterol if cellular levels of cholesterol drop excessively. Esterification and storage of cholesterol is one of the main factors in the pathogenesis of atherosclerosis.

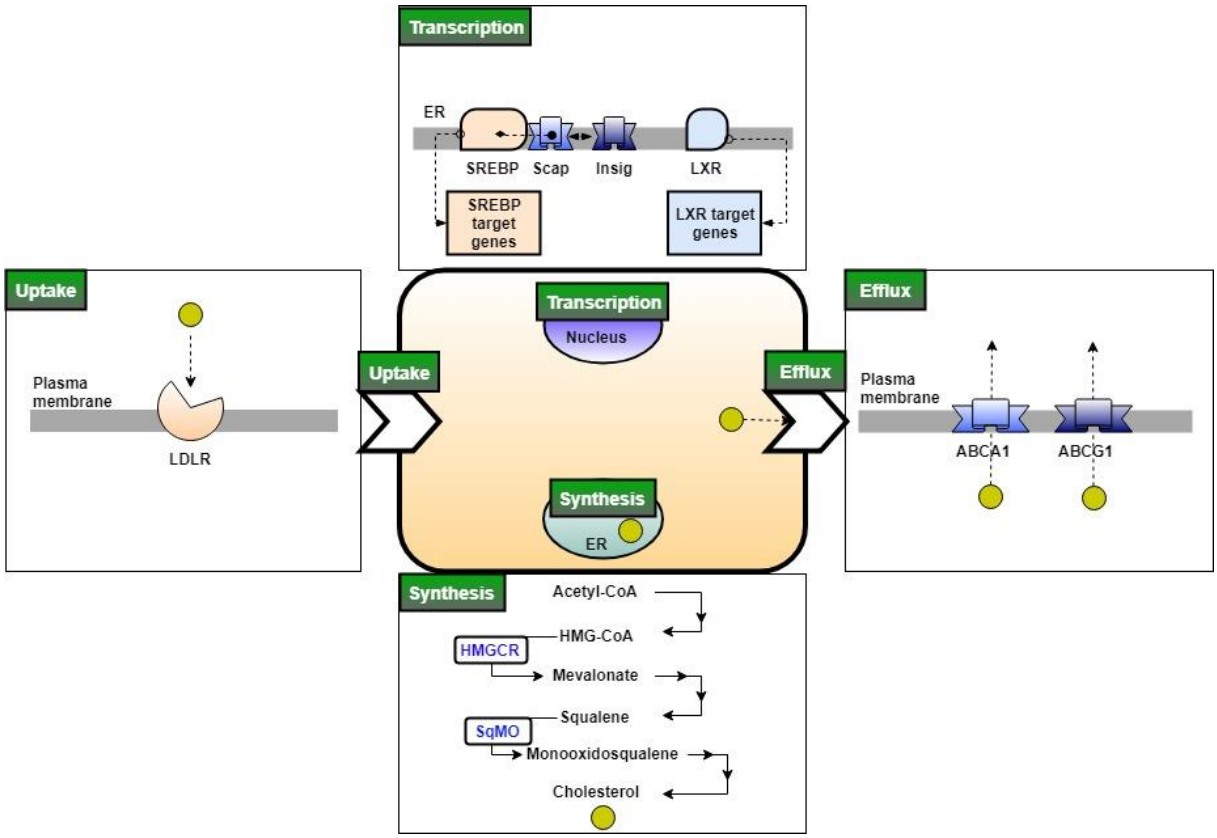

Figure 2. Overview of factors involved in cholesterol homeostasis. Abbreviations: (ABCA1) ATP-binding cassette transporter A1, (ABCG1) ATP-binding cassette transporter G1, (HMGCR) HMG CoA reductase, (LDLR) low-density lipoprotein receptor, (LXR) liver X receptor, (Scap) SREBP cleavage activating protein, (SqMO) squalene monooxygenase, (SREBP) sterol regulatory element binding protein.[7]

2.2. Plasma membrane and lipid asymmetry

The PM in animal cells is a two-leaflet wall consisting of phospholipids, cholesterol and membrane proteins. The hydrophilic ends of the phospholipid molecules point outwards creating a hydrophobic cavity, or core, between the two leaflets. Integral membrane proteins protrude into a single or through both leaflets whereas peripheral membrane proteins are attached to either surface of the PM. Cholesterol squeezes itself between the phospholipid acyl chains in either leaflet. The cholesterol portion of a leaflet dramatically alters membrane fluidity and structure through supramolecular interactions with the fatty acid chains of phospholipids, reducing the available space for hydrocarbon chain reconformation. Cholesterol has a slightly polar 3β-OH group that can form hydrogen bonds with adjacent lipid headgroups, and its steroid frame and sidechain are buried in the hydrophobic interior of the bilayer. Cholesterol molecules are shielded by the phospholipid

headgroups, their contact with water is minimized and they form tight van der Waals interactions with adjacent acyl chains. In this way, lipid bilayers have a reduced surface area in the presence of cholesterol. Thus, at low temperatures, cholesterol increases fluidity by keeping phospholipids from packing tightly together and at high temperatures, it reduces fluidity. Cholesterol in a biological membrane, along with unsaturated fatty acid chains, expands the range of temperatures at which the membrane maintains a functional fluidity. In addition to PM, phospholipids and cholesterol can form smaller entities as well. Vesicles are spherical membrane analogues, which have a bilayer shell containing an aqueous cavity. Micelles are spherical membranes that lack the inner leaflet, thus having a hydrophobic core[8] (Figure 3).

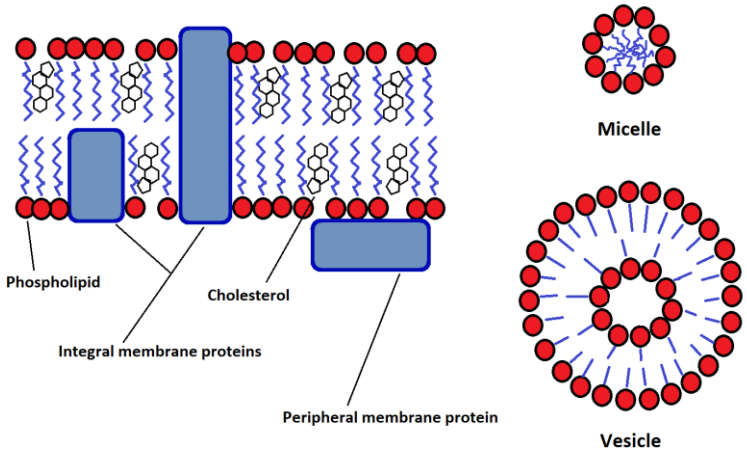

Figure 3. Plasma membrane constituents and derived organelles.

The composition of the two PM leaflets reflects their function (Figure 4). The inner leaflet is rich in amino-phospholipids phosphatidylethanolamine (PtdEtn) and phosphatidylserine (PtdSer), which have high portions of unsaturated fatty acids typically exhibiting low phase transition temperatures. The outer membrane on the other hand is enriched with phosphatidylcholine (PtdCho), sphingomyelin (SM) and glycosphingolipids, which are more rigid and have more saturated fatty acid chains.[9] This would hint at a less ordered inner leaflet, which retains higher fluidity and membrane fusion competency and a rigid, ordered outer leaflet, although findings supporting the opposite exist.[10] Model membranes demonstrate that cholesterol has a preferential affinity for SM over other saturated phospholipids among membrane constituents and this is supported by experiments finding

a larger portion of sterols in the SM-rich outer leaflet.[11] In this case also, there are contradicting findings associating a higher amount of sterols to the inner leaflet.[12,13]

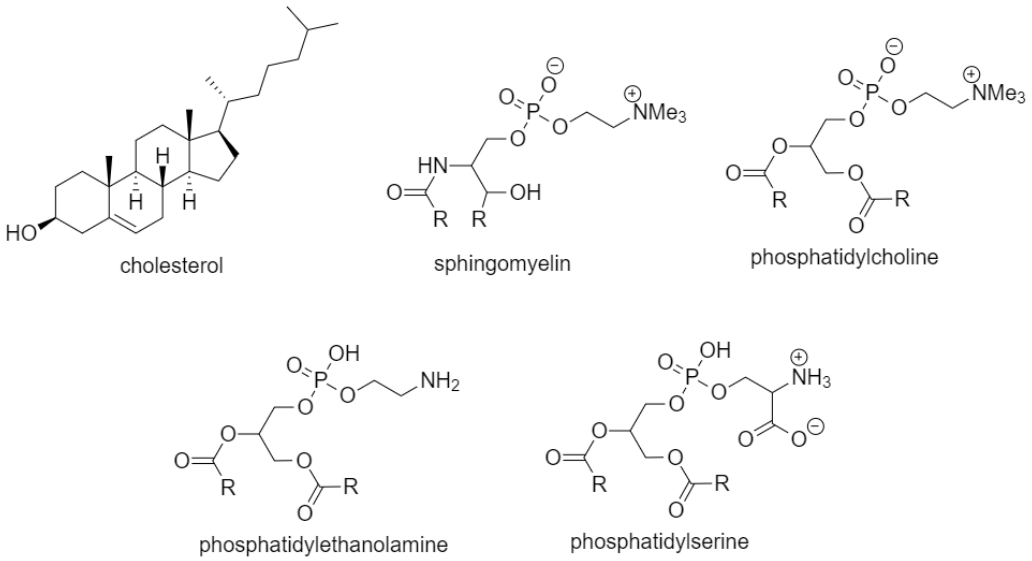

Figure 4. Lipids found in high concentrations in plasma membrane leaflets. R = fatty acid hydrocarbon chain.

Contradictory to the commonly referenced fluid mosaic model proposed in the 70's[14], where molecules are free to move in the plane of the membrane, lipid composition of a membrane is not homogenous and cholesterol and SM in particular appear to be enriched in particular lateral domains. Movement of PM proteins is inhibited by their attachment to cytoskeletal elements – these include actin filaments and glycophosphatidylinositol. Lateral lipid domains form in response to interactions between protein residues and the lipids. In the presence of sterols, biological membranes tend to divide into coexisting liquid-ordered (lo) and liquid-disordered (ld) phases. In lo phases, lipid acyl chains have a high degree of lateral mobility but are tightly condensed and very extended compared to ld phases, where the acyl chains have more lateral conformational space. Cholesterol, when introduced to highly ordered liquid crystalline bilayers, will increase fluidity and perturb lipid ordering. On the other hand, when introduced to an ld phase, cholesterol can induce an lo phase by its condensing effect.[15,16]

Lipid rafts are cholesterol- and SM-enriched lo phase lipid domains, which have a role in intracellular lipid traffic and cell signaling. Some models along with IR spectroscopy associate the condensing effect of cholesterol on hydrogen bonds between 3β-OH groups of cholesterol and SM (Figure 5).[17,18] Certain domains of the PM are not solubilized by detergents, such as Triton X-100 or CHAPS, at low temperatures. These were termed detergent resistant membranes (DRM) by Brown and Rose[19] in their hallmark research paper. DRMs are enriched in cholesterol and SM and are usually, but not always, associated with lipid rafts. However, because rafts in intact membranes undergo rapid exchange of lipid molecules with the ld phase and DRMs are characterized mainly in solubilized membranes, the terms raft and DRM are not to be used interchangeably.[20] One important type of detergent resistant domain are caveolae, deep membrane infoldings that are coated with caveolin protein and enriched in cholesterol, SM and signal transduction molecules. Caveolae are important sites of potocytosis, transient closure of the caveola and release of receptor-bound ligands into the cytoplasm. They are also involved in transcytosis between cells and cholesterol trafficking to the PM. They also seem to play a role in cell cycle by restricting cholesterol efflux during cell division.[21,22]

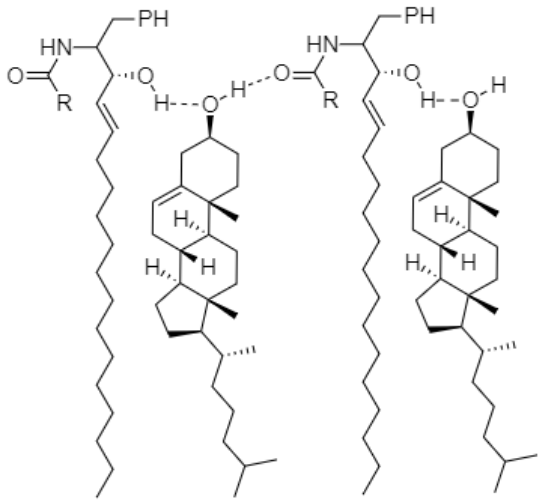

Figure 5. Packing of cholesterol and SM in lipid rafts by hydrogen bonds, as proposed by Simons and Ikonen.[17] PH = polar headgroup, R = hydrocarbon chain.

2.3. Lipid orientation in a bilayer

Molecular dynamics (MD) simulations and NMR measurements of model bilayer membranes have shed more light into the mechanisms underlying the condensing effects of cholesterol. In their 2006 study, Aittoniemi *et al.*[23] performed MD simulations on bilayers composed of either saturated or unsaturated phospholipids (dipalmitoyl or dioleoyl phosphatidylcholine). The bilayers were infused with a 20 molar % concentration of cholesterol, desmosterol, ketosterol or D-cholesterol (Figure 6). The group quantified molecular order parameters, average surface area per phospholipid unit and also a novel parameter called tilt, measured as the angle between the membrane normal and a vector connecting the sterol ring atoms C3 and C17, effectively characterizing sterol orientation in a bilayer (Figure 7). In both saturated and unsaturated bilayers, cholesterol exhibited the smallest average tilt angle, highest molecular ordering capacity and, consequently, the smallest area per phospholipid. This underlines the way how cholesterol has evolved to optimize its interactions with saturated lipids, such as the interactions between cholesterol and SM in lipid rafts.

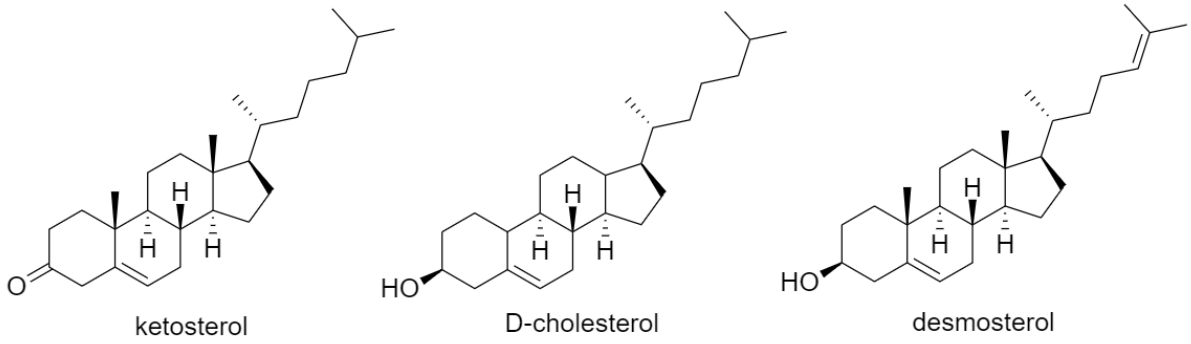

Figure 6. Structures of three cholesterol analogs: Ketosterol with a keto group instead of a OH-group, D-cholesterol with modified steroid frame and desmosterol with modified side chain.

Further MD studies[24,25] on hydrated dimyristoylphosphatidylcholine (DMPC) bilayers, much resembling the structures of lo domains, have elucidated the effect of cholesterol concentration on its orientation and ability to order phospholipid acyl chains. As the molar fraction of cholesterol in a membrane increases, conformational space and also the average tilt angle for both phospholipids and cholesterol decreases. The decreased surface area and

occupied volume per lipid molecule also lead to thickening of the bilayer. The cholesterol concentration is inversely correlated to change in cholesterol orientational entropy, which can be used to derive another measure, the tilt modulus. The tilt modulus is interpreted as quantitative measure of the force associated with tilting a molecule and is proportional to the cholesterol concentration. Also, the ability of cholesterol molecules to change their orientation with respect to each other, defined as splay deformation, decreases with increasing cholesterol molar fraction. These findings largely explain how cholesterol in biological membranes can maintain a healthy membrane fluidity as temperatures vary. Interestingly, probability density plots for lipid tilt angles, derived from MD simulations, reveal a nonzero probability for finding cholesterol molecules at very large tilt angles, even for the highest simulated sterol concentrations. This is not surprising, considering that experiments have shown that in unsaturated and polyunsaturated bilayers, particularly at low sterol concentrations, cholesterol molecules can orient themselves perpendicular to the bilayer normal with both the steroid frame and side chain immersed in the membrane core. At least transiently, cholesterol molecules can even appear in a flipped orientation, having the side chain point towards the phospholipid heads.

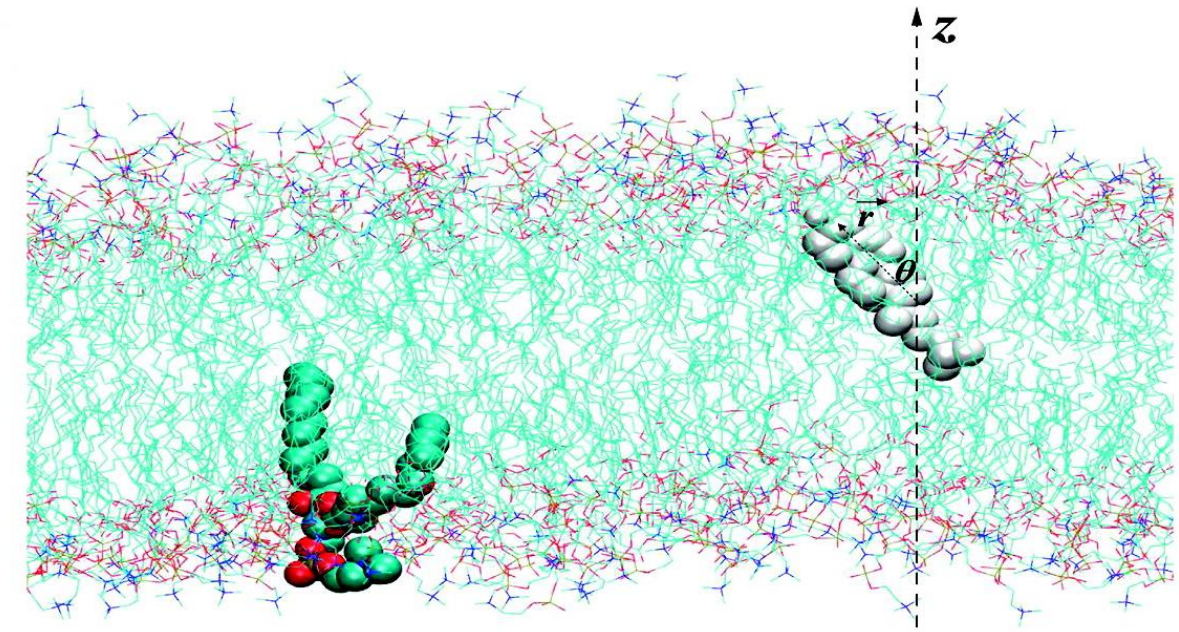

Figure 7. Cholesterol tilt angle (θ) in relation to the bilayer normal (z). One cholesterol molecule is shown in white, and water molecules are removed. One DMPC lipid molecule is also highlighted in space-fill. Adapted with permission from Khelasvili *et al.*[24] Copyright (2010) American Chemical Society.

2.4. Mechanisms of cholesterol transport

Several different, simultaneously working mechanisms transport cholesterol between cell organelles, which makes studying cholesterol transport challenging. Lipid bilayers can form vesicles that carry hydrophobic membrane constituents. They can also be transported through microtubules. Rapid desorption of cholesterol from membranes and the presence of sterol-binding proteins makes carrier-mediated diffusion important for cholesterol homeostasis. This is also apparent based on pharmacological studies where the inhibition of tubule or vesicle traffic does not impair cholesterol transport. Interestingly, the extreme hydrophobicity of cholesterol makes its desorption highly energy-intensive. Pulling cholesterol out of a bilayer into water requires an energy input of 80-90 kJ/mol, which corresponds to hydrolysis of 1-2 ATP-molecules.[26] This should indicate an efficient nonvesicular transport system involving carriers that can fuse into cell membranes. Non-specific lipid transfer proteins (LTPs) transfer sterols along with other lipids between cell membranes. Specific LTPs can bind only one or two types of lipids and include oxysterol binding proteins (OSBP) and steroidogenic acute regulatory (StAR) proteins. Another way in which cholesterol is transported is to have two membranes close to each other to overcome the energy barrier in cholesterol desorption. In some types of cells, the ER has regions very close to the PM. In addition, sophisticated models of the Golgi apparatus have revealed areas of close contact between the trans-Golgi network (TGN) and ER. With the aid of transfer proteins, the vicinity of two membranes could facilitate rapid transport of cholesterol and other lipids[27,28] (Figure 8).

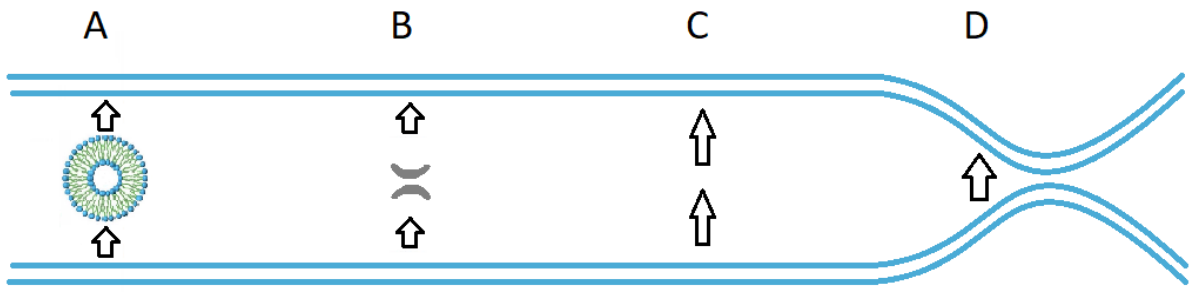

Figure 8. General mechanisms of cholesterol transport between membranes. Vesicular, ATP-dependent transport (A), diffusion through the cytoplasma either freely (C) or assisted by transfer proteins (B) and diffusion facilitated by close proximity of two membranes (D).

Sterol molecules will readily desorb and diffuse to a mean excursion distance d_m before resorption by the donor membrane. Transfer proteins can aid the transport of cholesterol between donor and recipient membranes in several different ways (Figure 9). Soluble proteins move within the cytosol and bind desorbed cholesterol. On the other hand, peripheral membrane proteins can bind cholesterol directly from the donor membrane. Transfer proteins can also reduce the distance between two membranes by tethering mechanisms. Non-vesicular sterol movement within distances below d_m is largely restricted by sterol fraction equilibrium between the membranes, which has been extensively reported by Wüstner and Solanko.[27] Cholesterol flux can therefore be promoted or limited by diffusional mechanisms. Less clear, however, is how two membranes can sustain thermodynamic equilibrium while having radically differing cholesterol fractions. As noted above, cholesterol exhibits partitioning preference for certain phospholipids and the lipid composition of two membranes has been proposed as an explanation.

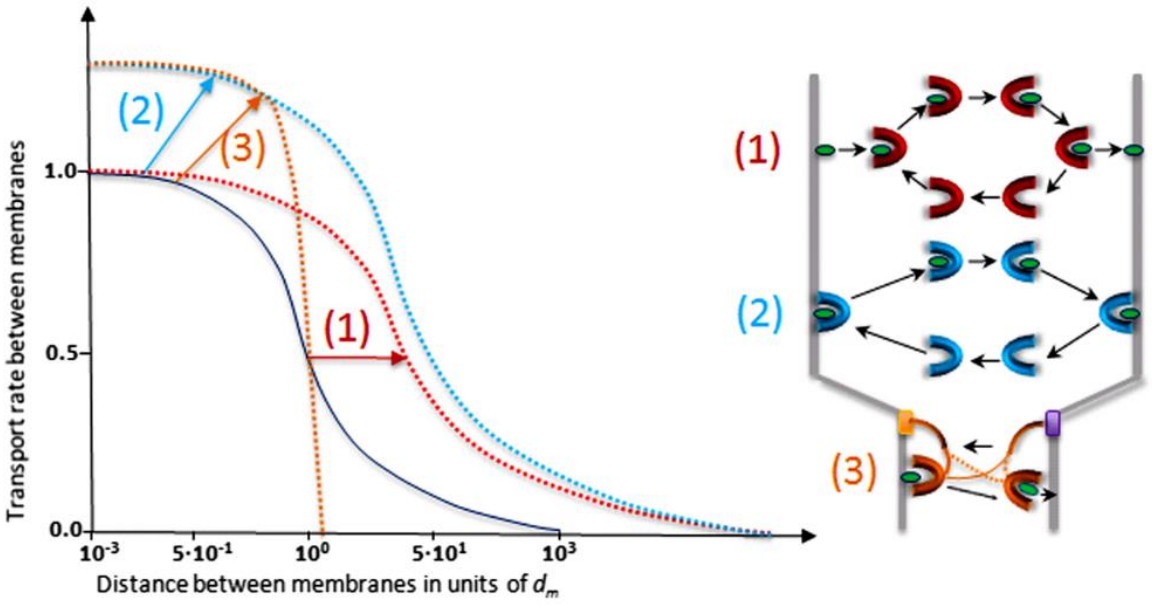

Figure 9. Nonvesicular cholesterol transport mechanisms. In case (1) soluble transfer proteins will increase effective transport distance d_t several fold without changing sterol flux J_{max}. In case (2), membrane-binding transfer proteins will increase both, d_t and J_{max}. In case (3), transfer proteins tether two membranes together, thereby increasing J_{max} and pulling the membranes to a distance ~ d_m, such that diffusion will never limit the net sterol flux between membranes. Adapted from Wüstner and Solanko[27] under Creative Commons (CC BY-NC-ND) license.

Cholesterol transport mechanisms have certain distinctions between nonpolarized and polarized cells (Figure 10). Many epithelial cells, including hepatocytes, develop distinct apical and basolateral PM domains that are oriented towards the lumen and extracellular matrix, respectively. These membrane domains differ in their function, lipid content and membrane proteins. Membrane constituents are transferred between different domains through energy-dependent mechanisms. Tight junctions, composed of transmembrane protein complexes, act as barriers against transmembrane diffusion and maintain the membrane asymmetry. Besides epithelial cells, in specialized cells such as immune cells and neurons, cell polarity enables the short-range and long-range transmission of electrical and biochemical signals. Cholesterol in the PM can bypass tight junctions by either protein-mediated transfer or by translocating between the PM leaflets. In addition, cholesterol destined for other membrane domains is trafficked in vesicles through a specialized cell organelle, the apical recycling compartment (ARC).[2,27]

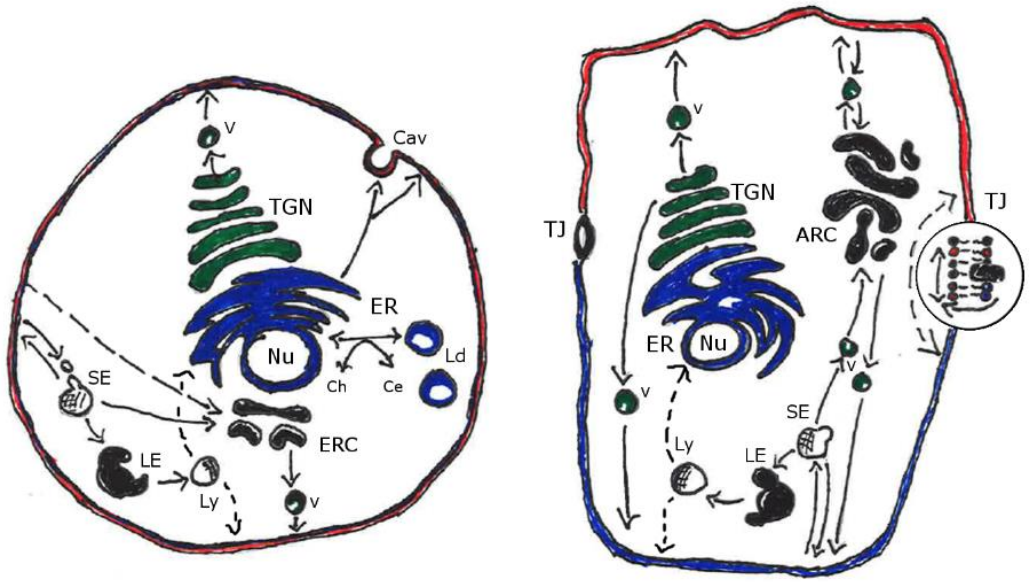

Figure 10. Cholesterol transport in nonpolarized (left) vs. polarized (right) cells. Polarized cells consist of apical (red) and basolateral (blue) membranes which are separated by tight junctions (TJ). Cholesterol can be transported between the membranes *via* ARC, protein mediated transport through the cytoplasm or diffusion along the inner leaflet. Abbreviations: (Cav) Caveolin, (Ch) cholesterol, (Ce) cholesteryl ester, (Ld) lipid droplets, (Nu) nucleus, (v) vesicle.

2.4.1. Transport from the endoplasmic reticulum

ER is an organelle consisting of a network of flattened, membrane-enclosed cavities that are continuous with the outer nuclear membrane. Rough ER is the main site of protein synthesis whereas smooth ER handles the synthesis of lipids and hormones in some cells. ER is also the site of *de novo* cholesterol synthesis, yet only a fraction of intracellular cholesterol is pooled in the ER in steady state. This indicates one or several energy-dependent, yet efficient, transport routes to channel cholesterol to other compartments. Most lipids leaving the ER take the biosynthetic secretory pathway through the Golgi apparatus and are transported in vesicles. However, pharmacological tests utilizing a vesicle-inhibiting drug brefeldin A demonstrate that this is not the main channel for cholesterol transport from the ER. Specific lipid transfer proteins that might be involved are StAR, OSBP and OSBP-related proteins (ORPs). In addition, a caveolin complex containing nascent cholesterol is suggested as a carrier, based on the observations that newly synthesized cholesterol is first found in caveolae-domains in the PM.[3,29] Spontaneous movement, facilitated by close membrane contants, between adjacent areas of the ER and the PM can play a role as well. Interestingly, the mechanisms delivering cholesterol from the ER to the PM are so efficient, that cholesterol precursors such as desmosterol are also transported to the cell surface.[3]

2.4.2. Transport from the plasma membrane

Dynamic data from studies with fluorophores show that cholesterol is constantly cycled from the PM to the cell interior and back. Less apparent is the mechanism by which cholesterol is taken into the intracellular organs. Transport is inhibited by a variety of factors, including progesterone, disruption of cytoskeletal elements and disruption of acidic compartments. In addition, plasma membrane SM fraction appears to be somewhat reversely correlated to cholesterol transport towards the cytoplasm and, simultaneusly, enzymatic breakdown of SM causes cholesterol to accumulate in membrane-derived vesicles.[3,30,31] Depletion of ATP causes the vesicles to remain close to the PM whereas when ATP is added, the vesicles deliver their contents to late endosomes and lysosomes. However, cholesterol transport to ER and subsequent esterification is not affected by energy depletion, which hints at another transport mechanism to the ER.

2.4.3. Endocytosis

Another way in which cells gain cholesterol is internalization from LDL and other lipoproteins. LDLs are particles that have a core of cholesteryl esters and apolipoproteins with a monolayer surface consisting of phospholipids and free cholesterol. LDL is the predominant carrier of serum cholesterol, containing approximately 60% of circulating cholesterol, delivering it to cells in need such as the adrenal glands, gonads, and other tissues. LDL-receptors on the cell surface diffuse into clathrin-coated pits, which in turn actively dissociate from the PM as vesicles, internalizing any receptor-bound LDL.

Endosomes are membrane-bound compartments consisting of a network of microtubules and vesicles. The main function of endosomes is to sort incoming material before degradation in lysosomes (Ly). Lipoprotein-derived cholesteryl esters first arrive in sorting endosomes (SE) in endocytic vesicles and are hydrolyzed to free cholesterol in late endosomes (LE) and lysosomes (Figure 11). Most of this free cholesterol, about 70 %, is transported to the caveolae domains in the PM. Transport from Lys to the PM seems to be inhibited by hydrophobic amines and brefeldin A, a disruptor of the Golgi apparatus, but not by disruption of cytoskeletal elements. About 30 % cholesterol in LEs and Lys is transported to the ER to be incorporated into cholesteryl esters, lipoproteins or bile acids. Brefeldin A treatment or disruption of microtubules does not affect this pathway but it is inhibited by hydrophobic amines, ATP-poisons, disruption of actin filaments or disruption of acidic compartments.[2]

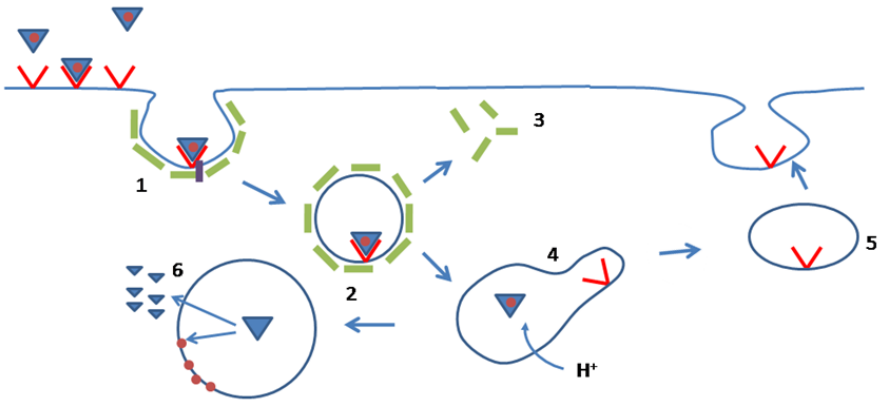

Figure 11. Cholesterol endocytosis. Receptor bound LDL in clathrin-coated pits (1) is internalized in vesicles (2). Clathrin is recycled to PM (3) and LDL is detached from the receptor in sorting endosomes (4) under acidic conditions. LDL-receptors are recycled to cell surface (5) and the LDL-derived cholesteryl esters are hydrolyzed to free cholesterol and acyl groups in lysosomes (6).[8]

In Niemann-Pick disease type C (NPC), a human genetic disease, cholesterol accumulates in storage organelles that are enriched in lipids and resemble late endosomes. These were thought to be lysosomes at first observations of the disease, but later studies have shown that initial export from LEs is not affected. The NPC genes encode at least two proteins, NPC1 and NPC2, which do not bind cholesterol directly but are thought to be integral membrane proteins that facilitate transport in vesicles. NPC-mutant fibroblasts are able to hydrolyze LDL-derived cholesterol normally but cannot elicit normal regulatory responses that would stimulate cholesterol storage and inhibit *de novo* synthesis. NPC and the function of its related proteins are yet to be fully understood. NPC-diseased cells have been useful in cell studies where the role of LEs and Lys in cholesterol transport has been of interest. [27,32]

2.4.4. Efflux

The concern over plasma concentrations of high-density lipoprotein (HDL) in healthcare is due to reverse correlation between plasma HDL levels and risk of cardiovascular disease. Reverse cholesterol transport is an important biological mechanism, where excess cholesterol is collected from peripheral tissues by HDL and transported to the liver to be recycled or excreted as bile acids (Figure 12). Apolipoprotein A1 (apoA1), secreted by the liver and intestine, receives cellular cholesterol in a process largely, but indirectly, dependent on ABC transporters ABCA1 and ABCG1. Of these proteins, at least ABCA1 appears to facilitate phospholipid transfer into apoA1, which is followed by cholesterol efflux into nascent HDL particles by an independent mechanism. Cholesterol is rapidly esterified in HDL, which increases free cholesterol flux from the cell interior. Scavenger receptor B1 (SR-B1) is a protein that facilitates HDL binding to cells and reorganization of lipids in PM domains. Overexpression of caveolin in human fibroblasts increases cholesterol efflux to HDL, which is evidence for another, caveolae-dependent pathway.[33–35] This is also apparent by tests where suppression of caveolin by antisense DNA defects cholesterol efflux.

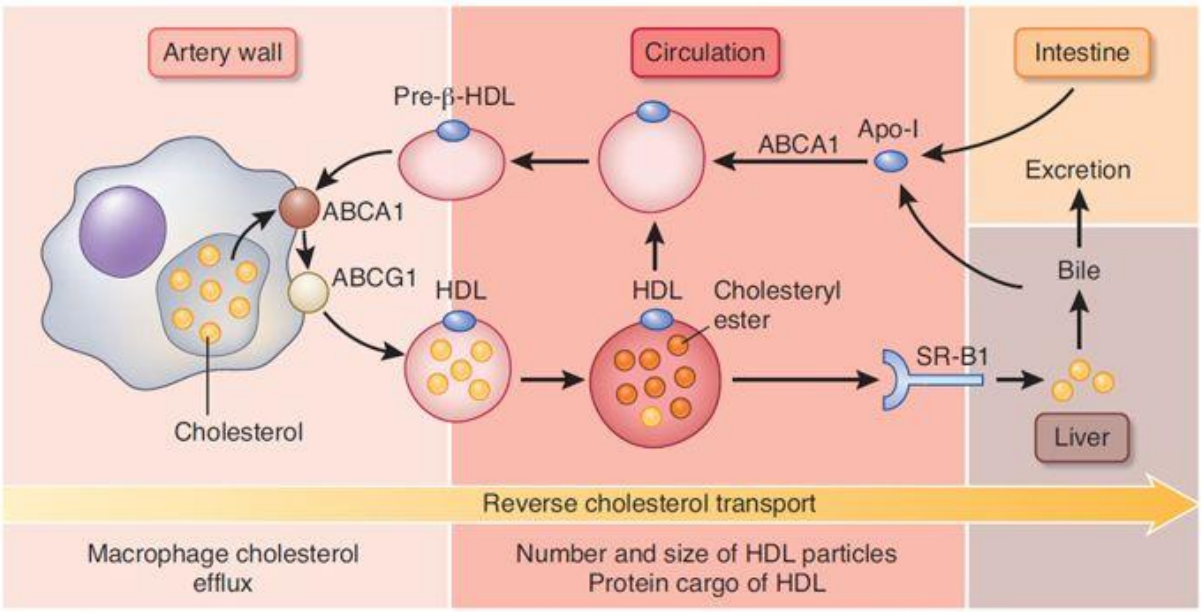

Figure 12. Overview of reverse cholesterol transport from macrophages by HDL, the primary mechanism inhibiting atherosclerosis. Reprinted with permission from Heinecke.[36] Copyright (2012) Springer Nature.

Tangier disease is a rare autosomal recessive disease, which is characterized by very low plasma HDL levels and accumulation of cholesteryl esters in macrophages in several tissues. Although Tangier patients have a heightened risk of cardiovascular disease, this is somewhat compensated by simultaneous decreased levels of LDL. In diseased individuals, the ABCA1-coding gene is mutated, and cells have impaired cholesterol efflux to apoA1, which indirectly leads to reduced HDL levels. Consistently, in Tangier cells efflux to other apoA1-like lipoproteins is also defective but efflux to vesicles and cyclodextrin carriers is inaffected.[33]

2.5. Cholesterol transport in specialized cells

Hepatocytes collect chylomicrons from the digestive system and other lipoproteins from peripheral tissues. The membrane domains of hepatocytes that are in contact with bile capillaries (biliary canaliculi) are called canalicular membranes. Cholesteryl esters from lipoproteins are hydrolyzed and transported to the canalicular membrane where they are either secreted into the bile (see 2.6 Bile acids and bile salts) or re-esterified into very low-density lipoproteins (VLDLs). Hepatocytes are polarized cells and maintain distinct steady-state lipid compositions in their apical and basolateral membranes.[2] At least two

specific LTPs are known to regulate cholesterol transport in the liver. Niemann Pick C1-Like 1 (NPC1L1) protein is localized in the canalicular domains. The main function of NPC1L1 is to facilitate intestinal cholesterol uptake and it is the target protein of ezetimibe, a cholesterol absorption inhibitor used in treating hypercholesterolemia.[37] SR-B1 protein mediates the uptake of HDL-cholesterol into hepatocytes which is necessary for the healthy function of reverse cholesterol transport. Overexpression of SR-B1 in mice increases hepatic cholesterol uptake and cholesterol efflux rate from macrophages, indirectly decreasing the degree of atherosclerosis, despite also decreasing plasma HDL levels.[38,39]

Cholesteryl ester accumulation in macrophages is one of the first steps in the formation of atherosclerosis, and thus the transport of lipids in macrophages is of great interest. One observation is that VLDL, not LDL, derived cholesteryl esters are stored in lipid droplets due to receptor downregulation. This is also due to the larger size and heavier cholesterol load of VLDLs. In addition, over a certain threshold level of free cellular cholesterol, esterification is increased greatly. ABCA1 and ABCG1 transporters are the main promoters of reverse cholesterol transport in macrophages. SR-B1 is expressed by macrophages but does not appear to greatly contribute to cholesterol efflux *in vivo*.[40]

In mitochondria of gonadal and adrenal cells, cholesterol is the precursor for steroid hormone synthesis (Figure 13). Steroidogenic cells receive cholesteryl esters from both LDL and HDL, which are transported into lipid droplets and subsequently hydrolyzed in an extralysosomal process that is distinct to steroidogenic tissues. Free cholesterol is then either stored or transported to mitochondria. The inner leaflet of the mitochondrial membrane contains an enzyme, C27 side chain cleavage cytochrome P450, which initiates hormone synthesis by converting cholesterol to pregnenolone. The transmembrane movement of cholesterol in mitochondria is thought to be the rate limiting step in steroid hormone synthesis. StAR proteins on the mitochondrial membrane have been studied intensively and recent work on the topic has demonstrated a transport system dependent on the interaction of StAR proteins, peripheral-type benzodiazepine receptor and cAMP-dependent protein kinase.[3,41,42]

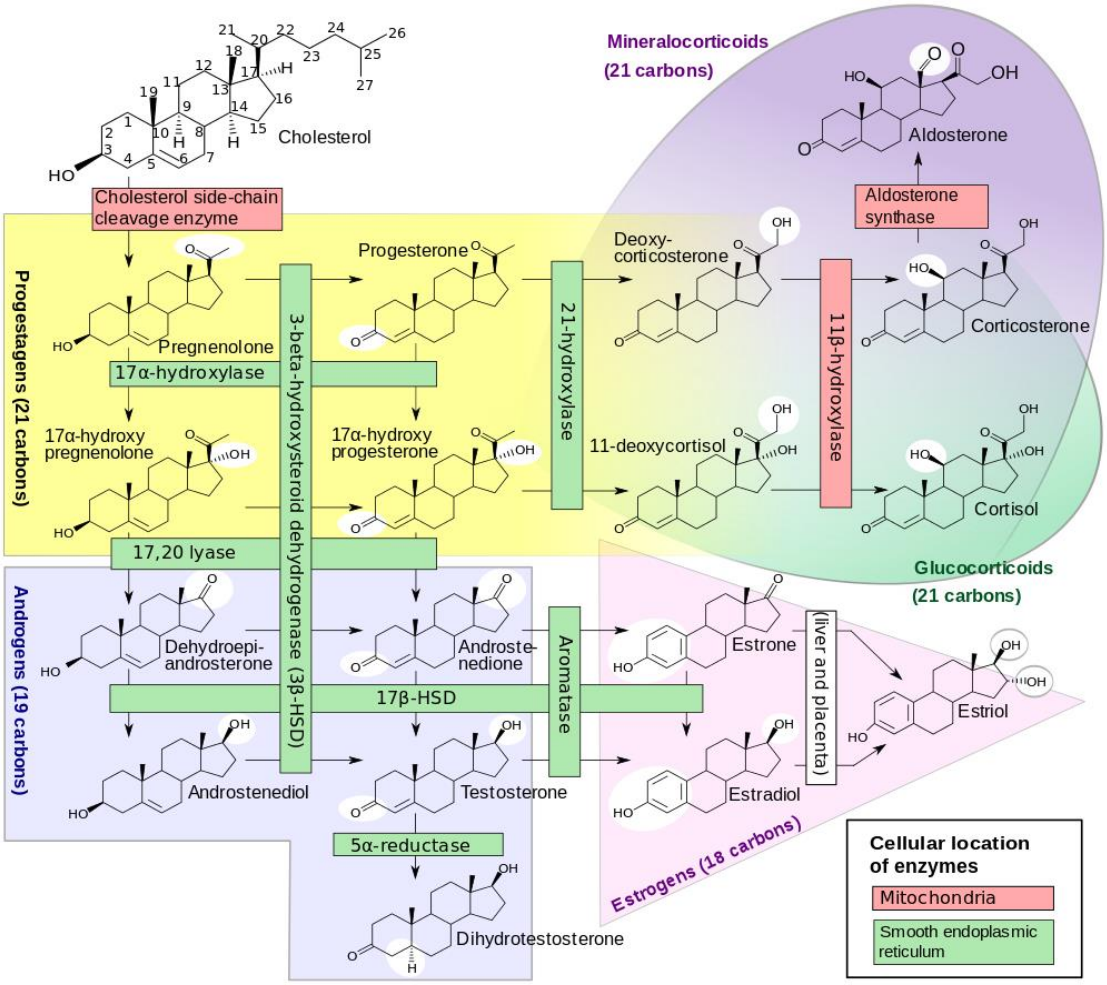

Figure 13. Overview of human steroidogenesis.[43]

2.6. Bile acids and bile salts

Excess cholesterol is transported to hepatic cells by HDL in reverse cholesterol transport. Cholesteryl esters not to be recycled are enzymatically converted in the liver into primary bile acids, cholic acid and chenodeoxycholic acid (Figure 14). These conversions include multiple different cellular organs and enzymes. Modifications into the steroid skeleton are epimerization of the 3β-OH group, saturation of the double bond and hydroxylation of position 7α and also position 12α if cholic acid is synthesized. These processes are cytochrome P450-dependent and the first in the conversion of cholesterol into bile acids. The cleavage and oxidation of the side chain is achieved through multiple acyl coenzyme-A intermediates. Primary bile acids are conjugated with glycine and taurine into bile salts, amide conjugates of bile acids, before being excreted into the gall bladder. Microbes in the

intestinal tract subsequently convert part of the salts into secondary bile acids deoxycholic acid and lithocholic acid (Figure 14). Most of the bile acids in the intestinal tract are absorbed and returned to the liver to be reconjugated and reexcreted into the bile. Bile acid synthesis and conjugation is an efficient way of removing excess cholesterol and simultaneously nitrogen in the form of taurine and glycine conjugates.[44] In addition, bile acids seem to play a role in regulating intracellular cholesterol levels in hepatic cells. Bile acids are known to regulate at least two genes: cholesterol 7α-hydroxylase, a rate-limiting enzyme in bile acid biosynthesis, and the intestinal bile acid–binding protein, a cytosolic protein involved in bile acid transport.[45]

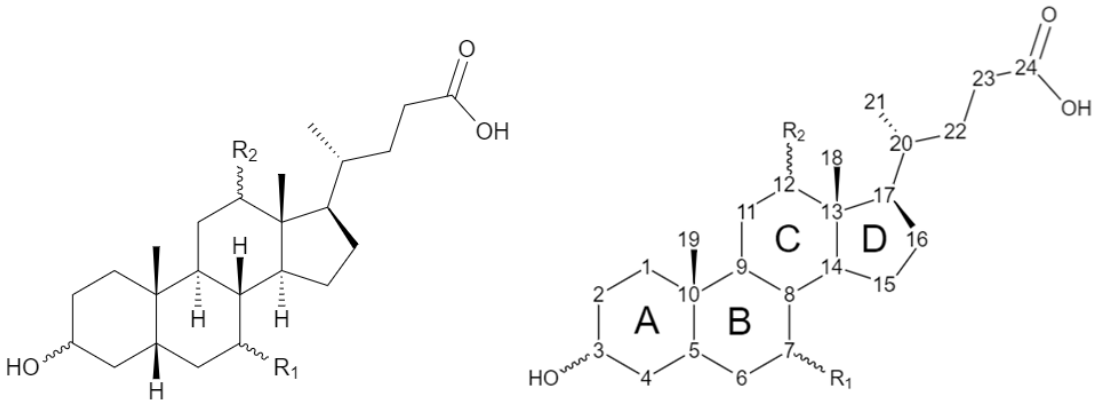

Figure 14. General structure of bile acids. Without (left) and with (right) carbon atom numbering and ring assignment. Cholic acid: $R_1 = R_2 = \alpha$-OH. Chenodeoxycholic acid: $R_1 = \alpha$-OH, R_2 = H. Deoxycholic acid: R_1 = H, $R_2 = \alpha$-OH. Lithocholic acid: $R_1 = R_2$ = H.[46]

2.7. Overview of methods for studying cholesterol metabolism

Density fractionation is one the more traditional methods of characterizing lipid distribution in cells. In this method, organelles are isolated by their density in a centrifuge or by other physical separation. This poses practical problems because PM density is similar to ER, Golgi apparatus and endosomes. In addition, lo and ld phases of the PM might possibly separate. One particularly usable application of subcellular fractionation has been magnetic affinity chromatography, which has been used to separate intact PM in animal cells. This method relies on magnetic interactions between the stationary phase and specific proteins in the PM.[47,48]

Cholesterol oxidase treatment can give a reproducible and rapid estimate of cholesterol content in PM when combined with a simultaneous test to determine which cholesterol pool has been oxidized. Cholesterol oxidase access to intramembrane cholesterol can be increased by incubation in hypotonic environment i.e. inducing particle diffusion towards the extracellular environment. Sphingomyelinase treatment also renders cholesterol more sensitive to oxidation by digesting SM and revealing the 3β-OH group of cholesterol. As mentioned before, various pharmacological agents are useful when evaluating the role of different cellular compartments in cholesterol diffusion. Brefeldin A, for example, disrupts the function of the Golgi apparatus. Energy poisons inhibit normal function of ATP and can be used to recognize energy-dependent mechanisms. Hydrophobic amines and sterols, such as progesterone, can be used to occupy vesicular transport space and distinguish the role of vesicular transport.[15]

Fluorescence analyses have been go-to methods in analysis of cellular lipid transport for several decades. In optimal circumstances, fluorescent probes and cholesterol analogues can be used simultaneously with all of the aforementioned methods to yield reproducible steady-state data or real-time kinetic data *in vivo*. However, methods not involving fluorescent labeling of cellular organs are also being developed. Secondary ion mass spectrometry (SIMS) can be used to detect membrane constituents by their fragmentation. Altelaar *et al.*[49] used gold coating on tissue sections and matrix assisted SIMS to gain high-resolution mapping of PM of rat brain cells. Nygren *et al.*[50] on the other hand utilized time-of-flight SIMS to detect cholesterol in freeze dried white blood cells bound to glass surfaces. Microscopy techniques utilizing Raman scattering, especially when combined with fluorescence microscopy, have presented some promising applications for visualizations of lipids. Coherent anti-Stokes Raman scattering (CARS), where the sample is irradiated with two coherent light beams to produce a substantially stronger scattering signal, has been utilized in detection of cholesterol and triacylglycerol esters in human, nematode and *Drosophila* (common fruit fly) tissues.[51–53] The sensitivity and reproducibility of non-labeling methods requires additional research and, in the case of mass spectrometry, cannot be used in live cells. Cellular lipids can also be tracked using their radiolabeled analogs, but this requires purification of cell organelles under harsh conditions, which would perturb intracellular transport.

3. Fluorescent probes in the study of cholesterol transport

The development of probes for the study of cholesterol must address two main aspects. First being how to introduce properties to the probe that minimally perturb cellular structures and the second being how to introduce maximal fluorescent properties. A perfect probe, in this sense, is one that behaves and distributes identically to cholesterol in living cells, has minimal cytotoxicity, and has fluorescent properties that allow it to be used in trace amounts. Understandably, a probe that fills all the criteria has not been developed yet. Three broadly defined categories of probes can be used. External fluorescent groups can be added to cholesterol or cholesteryl esters to retain the binding properties of the steroid backbone. Such probes include boron dipyrromethene difluoride (BODIPY) -cholesterol, 5-dimethylamino-1-napthalenesulfonyl (dansyl) -cholesterol and nitrobenzodiazole (NBD) -cholesterol. Another approach is to use intrinsically fluorescent sterols that tend to modify the composition and stereochemistry of the steroid frame but retain the functions of the peripheral groups (3β-OH group and hydrocarbon side chain) and occupy the same conformational space as cholesterol. These include dehydroergosterol (DHE) and cholestatrienol (CTL). The third approach is to use fluorescent molecules that bind to cholesterol selectively, such as fluorophore-tagged bacterial toxins or the intrinsically fluorescent antibiotic filipin. These have been shown to work well on fixed cells but have limited usage *in vivo*.[15,54,55]

Optimal fluorescent probes should have narrow excitation and emission maxima within the visible spectrum. This is essential in particular with specimens that show significant autofluorescence, such as many nematodes. Photobleaching is a phenomenon where certain excitation wavelengths induce irreversible changes to the fluorophore and consequently cause them to lose their fluorescent properties. Certain fluorophores are more susceptible to photobleaching and special care must be taken in imaging. Several physical and chemical parameters can be used to assess the fluorescent properties of a probe. Fluorescence lifetime (τ) is relative to the delay which an excited molecule takes to return to ground state and determines the lifetime of a fluorescence signal. Fluorescence lifetime imaging microscopy relies on the lifetime, rather than intensity, of the signal to create an image. Quantum yield (Φ_f) means the efficiency of the fluorescence process and is defined as the ratio of the number of photons emitted to the number of photons absorbed. The molar extinction coefficient (ε) of a probe assesses the efficiency of excitation light

absorbance.[15,54,55] The fluorescent properties of a probe may go through changes in cytosolic environment due to factors such as protein interactions and pH. Environmental sensitivity of a probe is a semiquantitative parameter used to assess this propensity and is usually assessed by comparing to a known environmentally insensitive fluorescent dye.[56] Klymchenko[57] and Demchenko *et al*.[58] have developed novel methods, where the sensitivity to specific intracellular elements is used to advantage in cellular imaging using fluorescence.

An optimal fluorescent cholesterol analog should reproduce the interactions of cholesterol in bilayers as closely as possible (see 2.2 Plasma membrane and lipid asymmetry). They should be able to partition into lo phases and induce the formation of these phases in model and biological membranes and show preferred binding with choline-containing lipids such as SM. Optimal fluorescent cholesterol and cholesteryl ester analogs would work as substrates for ACAT and bind to specific LTPs, although the latter mechanisms have not been studied extensively. Cholesterol imaging techniques using fluorescent probes are susceptible to several drawbacks, depending on the probe used and, based on the current knowledge, the best methods usually employ two or more different probes with differing emission maxima.[15,55,59]

3.1. Tools in fluorescence analysis

Sterol tracking within live and fixed cells is the focal point of study of cholesterol transport. Data from live cells can be most easily extrapolated to living organisms. Besides human fibroblasts, hamster and mouse cells have been particularly studied.[31,48] Valuable information on sterol transport from LEs and Lys has been gained from NPC-fibroblasts.[32,37] Regardless of the advantages of using isolated and cultured cells, use of model membranes can provide reproducible and precise information on cholesterol distribution, particularly on partitioning into lo and ld phases. Artificial PtdCho or SM bilayers are some of such model matrices.[24–26] They can be incorporated into supported lipid bilayers or giant unilamellar vesicles (GUVs).

Cholesterol is effluxed and delivered to cells by lipoproteins in living organisms. When dealing with model matrices, sterol probes require a carrier that can efficiently deliver the probes to intracellular environment. Cyclodextrins are cylindrical, crown-shaped

oligosaccharides typically consisting of 6-8 glucose units linked by 1,4-glycosidic bonds. They enhance the solubility of aliphatic and nonpolar substances, thanks to a hydrophobic host cavity, which can include nonpolar guest molecules, and protruding hydroxyl groups, which can be derivatized. Cyclodextrins and cyclodextrin derivatives, such as methyl-β-cyclodextrin (MβCD) readily form water soluble inclusion complexes with cholesterol and other steroids and can function either as cholesterol donors or acceptors. Cyclodextrin-catalyzed manipulation of membranes has been a standard method in the study of cholesterol rich microdomains.[60,61] In addition, cyclodextrins have therapeutic potential as shown by studies, where their administration could reverse dysfunctional lysosome to ER cholesterol transport in NPC cells[62] (Figure 15).

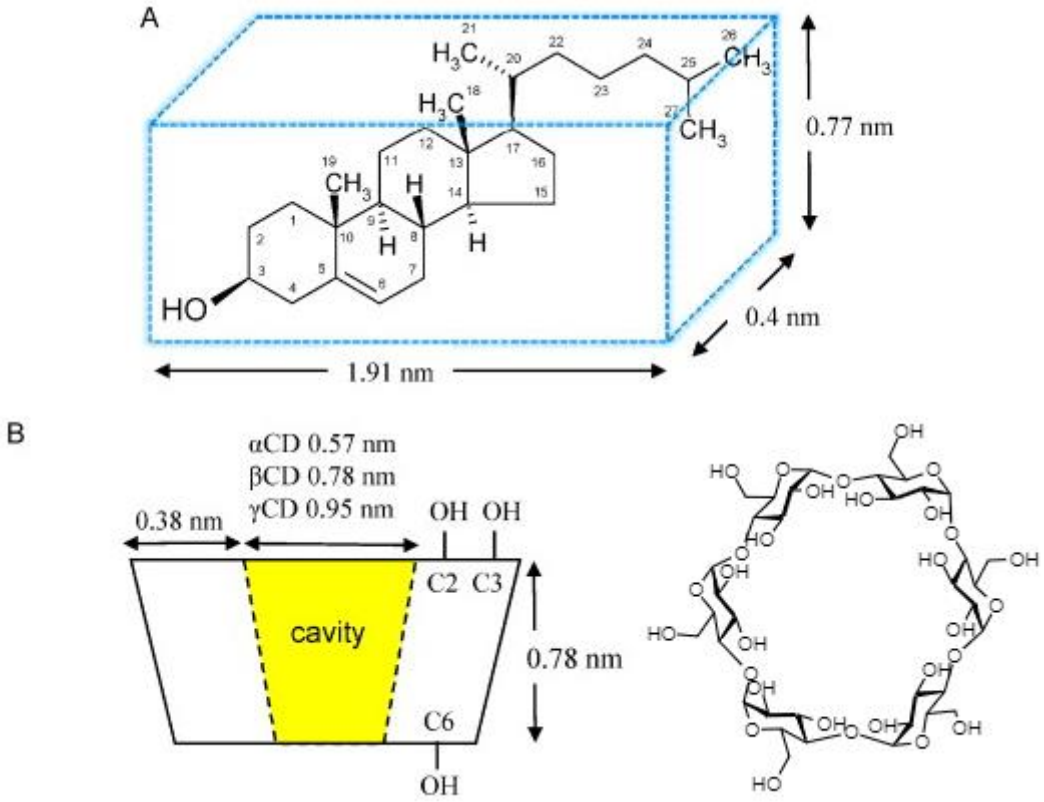

Figure 15. Structure and dimensions of cholesterol (A) and cyclodextrins (B). The cyclodextrin molecules α, β and γ contain either 6, 7 or 8 D-glucose monomers, respectively. The hydroxyl groups in cyclodextrin can be derivatized with less polar groups to modify biophysical properties. Cholesterol can be either partly complexed in a single cyclodextrin units or completely in two stacked unit. Adapted with permission from Gimpl and Gehrig-Burger.[60] Copyright (2010) Elsevier Inc.

Fluorescence microscopy (Figure 16) for the imaging of sterols may require modifications to a regular confocal microscope equipment, particularly in the case of DHE and CTL. A usual necessity is an excitation light source capable of high UV transmittance. Standard collection lenses block transmission around the UV-spectrum and single element collection lenses cannot obtain decent simultaneous UV and visible illumination. Commercially available multi-lens collectors can solve this issue. Other glass elements in the optical path will also need to be checked for UV-transmittance. In the case of very weak fluorophores, near-UV sensitive electron multiplying charge-coupled device (CCD) cameras work best as detectors.[15,63,64]

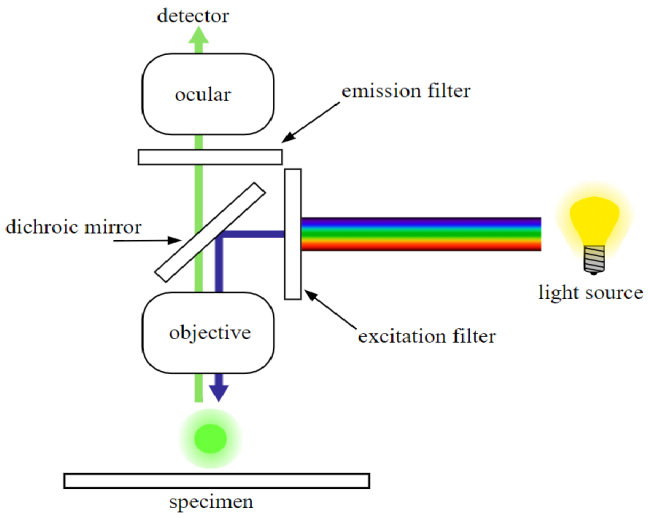

Figure 16. Schematic representation of a fluorescence microscope.[65]

Fluorescence correlation spectroscopy (FCS) is powerful tool that utilizes quantified fluorescence data from a sample. FCS is usually combined with fluorescence microscopy. FCS measurements are based on the statistical analysis of small fluctuations in emission intensity, primarily arising from fluorescent molecules diffusing through a sub femtoliter detection volume. This minute volume is created by focusing an excitation laser to a diffraction limited spot and by confining the detection with a pinhole in the emission path. Behind the pinhole is a high sensitivity light detector, such as a UV-sensitive avalanche photodiode. The raw data, derived from single photon arrival times, is used to construct an autocorrelation curve, which reflects the lifetime of a single molecular event within the detection volume. FCS can also be used as a dual color setup which includes two excitation and detection channels.[66,67] Combined with fluorescence imaging, FCS can provide both dynamic and steady-state data on localized cholesterol content.

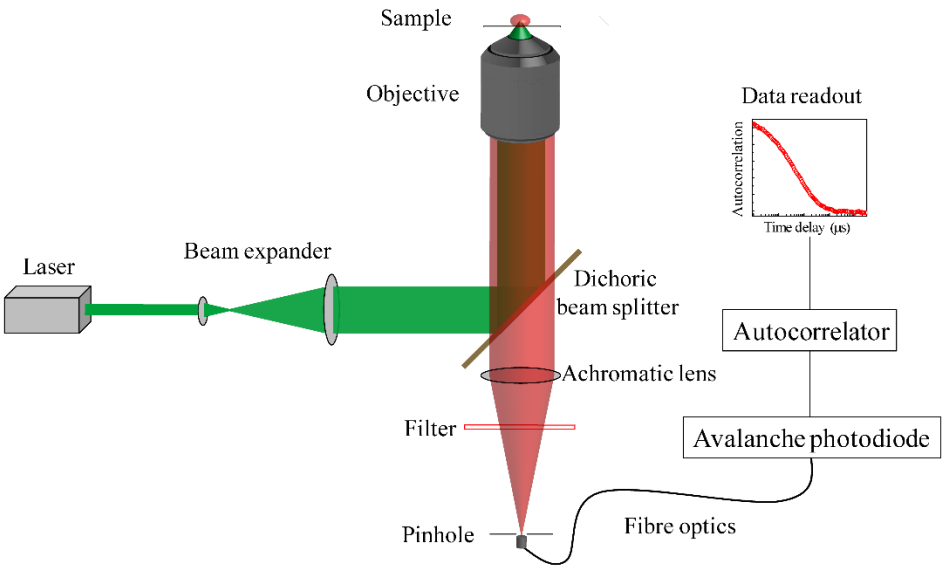

Figure 17. Schematic representation of a monochromatic FCS setup.[68]

Although photobleaching is an undesired effect when several frames of the same field need to be visualized, it can be used to advantage for kinetic measurements of cholesterol transport. Fluorescence loss in photobleaching (FLIP) and fluorescence recovery after photobleaching (FRAP) studies take advantage of this phenomenon with suitable probes. In FLIP, a sample is labeled with a fluorescent probe and a region of interest is defined. This region is imaged on a fluorescence microscope using low intensity excitation and, simultaneously, an adjacent region is imaged using high intensity which causes this region to be photobleached. By tracking the loss of fluorescence in the region of interest over time, sterol flux to the photobleached region can be quantified. Free diffusion causes complete loss of fluorescence whereas, if the regions are non-continuous, no fluorescence loss takes place. In FRAP, the region of interest is visualized with high-intensity excitation, causing photobleaching, and flux of sterol probes causes fluorescence to recover to the imaged area. For example, in a typical FRAP application, DHE fluorescence can be selectively destroyed by illuminating a distinct region with a closed field aperture on a wide field microscope. Fluorescence recovery to the selected region is then measured over time with the field aperture open.[54,69]

3.2. Intrinsically fluorescent sterols

Intrinsically fluorescent sterol probes have several conjugated double bonds in their steroid backbone or in the fatty acyl moiety in the case of sterol esters. First instances of fluorescent sterol probes were sterophenol and steroid hormones with aromatic A rings. The planar A-ring of these molecules was found not to be compatible with the biophysics of cholesterol. The polyene sterols, or P-sterols, DHE and CTL, which are most commonly used as probes, have conjugated double bonds between the B and C rings and no planar rings in the steroid system (Figure 18).[15,54]

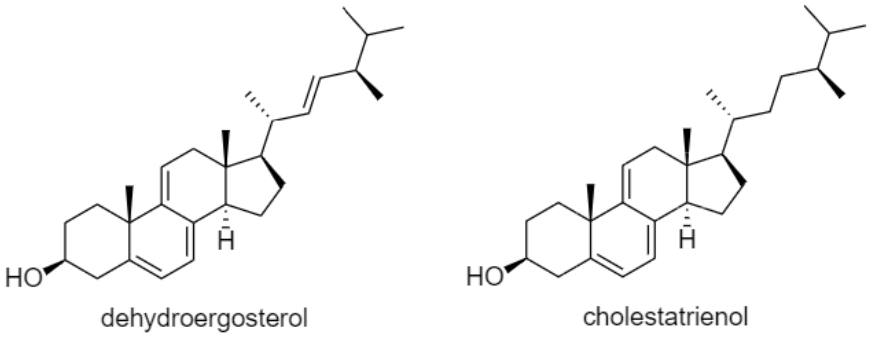

Figure 18. Structures of intrinsically fluorescent sterols dehydroergosterol (DHE) and cholestatrienol (CTL).

Photophysical properties of these sterols are very similar due to the identical fluorophore moiety. In bilayer membranes, both sterols have emission and excitation maxima of λ_{ex} = 320 nm and λ_{em} = 370-400 nm. Fluorescence lifetime of both sterols is short, 0,3 – 0,8 ns, when measured in different solvents and model membranes. Low quantum yield (Φ_f = 0,04 in ethanol) leads to very low fluorescence brightness even with high excitation intensities. Imaging of these sterols requires UV-optimized high sensitivity CCD cameras. In addition, both sterols are very susceptible to photobleaching.[70–72] Incorporation of DHE and CTL into cells can be achieved by several methods. The probes can be injected into the cell medium in an ethanolic stock solution. Their hydrophobicity results in binding into proteins but also in the formation of microcrystals, which can be digested and processed by cells. Another route, which gives a more efficient and homogenous probe distribution, involves incubation of DHE or CTL with MβCD. The newly formed cyclodextrin-sterol complexes are readily taken into cells and the sterol probes are dissociated from their carriers.[15]

DHE is a close analog to ergosterol, the naturally occurring sterol in yeast, differing only by the additional double bond in position 9-11. This makes DHE an optimal analog, in terms of biophysics, when ergosterol transport in yeast cells is investigated. DHE is esterified in mammalian cells to a limited extent when taken in through nonlipoprotein pathways and in *in vitro* studies it has been a less efficient substrate for ACAT. DHE cannot activate the cleavage of SREBP-Scap complex, which indicates reduced affinity for cholesterol metabolizing proteins. DHE partitions preferably into lo phase in bilayers and is able to induce lo domains in model membranes as demonstrated by Garvik *et al*.[73] Up to concentrations of 10 molar-%, DHE can reorder phospholipid acyl chains. An efficient synthesis route for DHE from ergosterol has been utilized by Solanko *et al.*[54] with yields up to 70%. The 3-OH group of ergosterol is protected with acetic acid anhydride and the resulting ester is dehydrogenated with mercury acetate. Finally, the ester group is hydrolyzed with sodium hydroxide. The reaction is carried out in boiling ethanol. The crude product is washed with water, mixed with active carbon and recrystallized from mixture of acetone and ethanol.

CTL is the closest fluorescent analog of cholesterol having two additional double bonds. Akin to DHE, CTL partitions preferably to lo phase in membranes. It can induce lo phases in model membranes but not in live cells. Contrary to DHE, in PtdCho bilayers CTL can order acyl chains with a linear relationship between CTL concentration and ordering capacity. This behavior in model membranes suggests that CTL is more compatible with biophysical properties of cholesterol. However, when injected to PM of live macrophages, adipocytes and fibroblasts, neither DHE nor CTL would partition into microscopically apparent domains.[74] CTL can be synthesized from 7-dehydrocholesterol by dehydrogenation with mercury acetate in a process identical with the synthesis of DHE above. Instead of recrystallization, reverse phase HPLC yields the most stable product in the case of CTL.[75,76]

The photobleaching propensity and low fluorescence brightness of intrinsically fluorescent sterols can be compensated by using multiphoton excitation (Figure 19). In this method, the almost simultaneous absorption of several photons by a molecule causes an electronic transition from the ground to the first excited state. Triphoton excitation has been used advantageously in the imaging of DHE but, in theory, the same principle can be applied to CTL due to the similar photophysical properties. The photons in triphoton excitation have

approximately one-third of the energy compared to conventional single photon excitation, the net energy input being approximately the energy of the transition. This allows the use of longer wavelengths: For triphoton excitation approximately three times longer wavelength compared to single photon excitation can be used. For example, McIntosh *et al.*[77] used multiphoton laser scanning microscopy with an excitation range of 900-920 nm to visualize monomeric and crystalline forms of DHE in model membranes and lipid rafts purified from PMs. The longer excitation wavelengths contribute to less cytotoxicity and photobleaching, less light scattering and deeper penetration. Multiphoton events occur only in the focal plane, which allows sectioned imaging of larger spherical objects, namely intact cells and GUVs. A drawback of multiphoton excitation is the need for several frame averages to produce a quality image. Longer acquisition times decrease the signal-to-noise ratio and make time-resolved imaging challenging.[15,78,79]

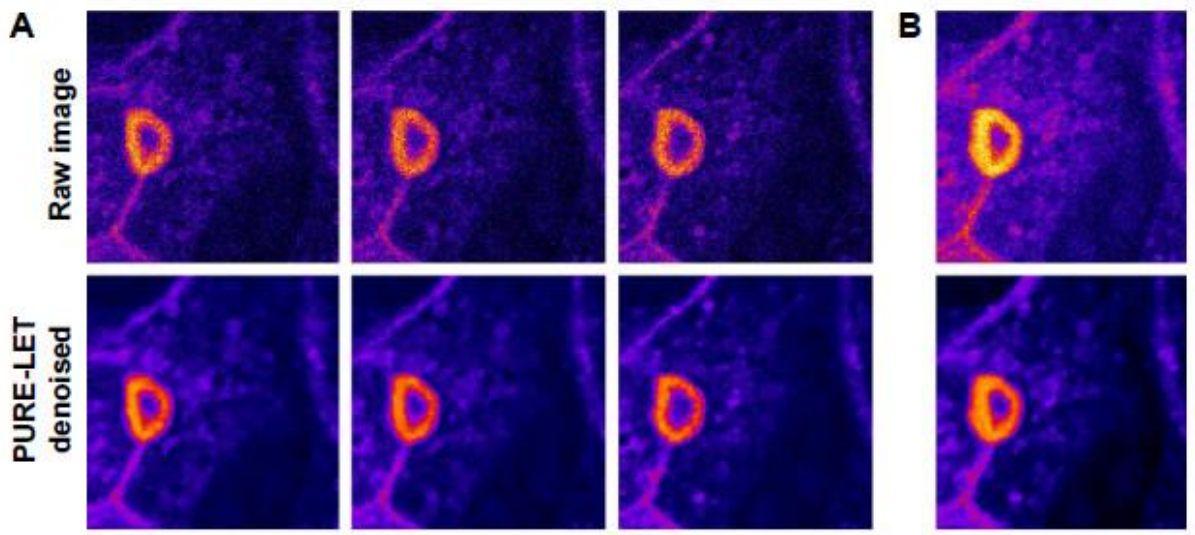

Figure 19. Triphoton excitation of DHE in polarized hepatocyte-like HepG2 cells. After labeling cells with DHE/cyclodextrin complex and fluorescence chasing for 30 minutes, an intercellular biliary canaliculus can be made out. (A) Selected intensity-averaged frames acquired along the optical axis and (B) corresponding maximum intensity projection of all six intensity-averaged images from 10 acquisitions each, either prior to or after denoising. Reprinted with permission from Solanko *et al.*[54] Copyright (2015) SAGE Publications.

3.3. Fluorophore-labeled sterols

Linking naturally occurring sterols and fluorophores presents, in theory, limitless sterol-fluorophore combinations. In addition, much better fluorescent properties, compared to

DHE and CTL, can be achieved with extrinsic groups. This precedes that probes, such as BODIPY-cholesterol can be used in time-resolved fluorescence analyses, thanks to shorter acquisition times (Figure 20). However, only a handful of these probes have been shown to have minimal cytotoxicity along with decent fluorescence, and to mimic cholesterol in cells adequately. In most cases, the aliphatic side chain is used as the link for the fluorophore. Considering the orientation of cholesterol molecules in lipid bilayers (see 2.2 Plasma membrane and lipid asymmetry) this is the most natural approach, with the purpose of pointing the fluorophore towards the hydrophobic bilayer interior and least disturbing the interactions between the steroid frame and phospholipid acyl chains. This sets certain requirements for the fluorescent moiety as well, as ionic or strongly dipolar fluorophores cannot be used. A major drawback that seems to characterize all extrinsically labeled sterols is that they cannot order acyl chains in model PtdCho membranes. This would suggest that such probes cannot fully mimic the important condensing ability of cholesterol.[55]

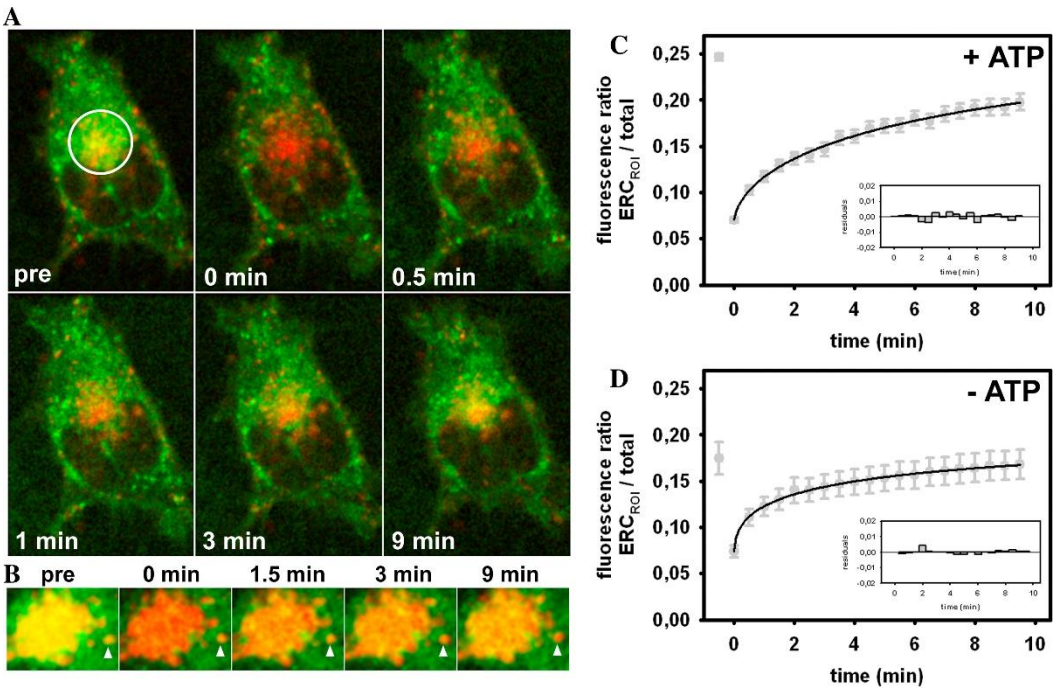

Figure 20. Kinetic analysis of transport of BODIPY-cholesterol by FRAP. Baby hamster kidney were labeled with cyclodextrin-Bchol. After selective photobleaching of ERC (white circle) and recovery of Bchol fluorescence (in green) was monitored. Reprinted with permission from Wüstner et al.[69] Copyright (2015) Elsevier Ireland Ltd.

BODIPY-linked cholesterol, also known as B-chol, was originally introduced by Li *et al.* in 2006[80] and has been widely experimented on. Two BODIPY-derivatives of cholesterol

(Figure 21) have demonstrated similar membrane dynamics with cholesterol. In model membranes, they show a slightly lower partitioning preference towards lo phases, although they have similar transport kinetics with DHE and CTL.[81] However, studies using B-chol esters have demonstrated that the rate of ester hydrolysis in LEs and Lys is substantially decreased by the presence of the fluorophore.[82] BODIPY has major advantages as a fluorophore, however, having excitation and emission maxima of λ_{ex} = 505 nm and λ_{em} = 515 nm, quantum yield of Φ_f = 0,04 and high extinction coefficient.[83] This precedes that BODIPY-probes can be visualized with most conventional fluorescence microscopes and very small concentrations of the probes are needed. Incorporation of B-chol and B-P-chol into cells can be achieved with cyclodextrin carriers, as explained for DHE and CTL. In their 2006 paper, Li *et al.* prepared B-chol from cholenic acid 3β-acetate, which was worked into acid chloride by treating with oxalyl chloride. The BODIPY-moiety was constructed *in situ* via a condensation reaction with 2,4-dimethylpyrrole and $BF_3 \cdot OEt_2$. A more efficient synthesis route for B-chol and B-P-chol has been reported by Liu *et al.*[84] Their method relies on Suzuki and Liebeskind-Srogl cross-coupling of phenyl cholesteryl with different BODIPY-moiety containing compounds.

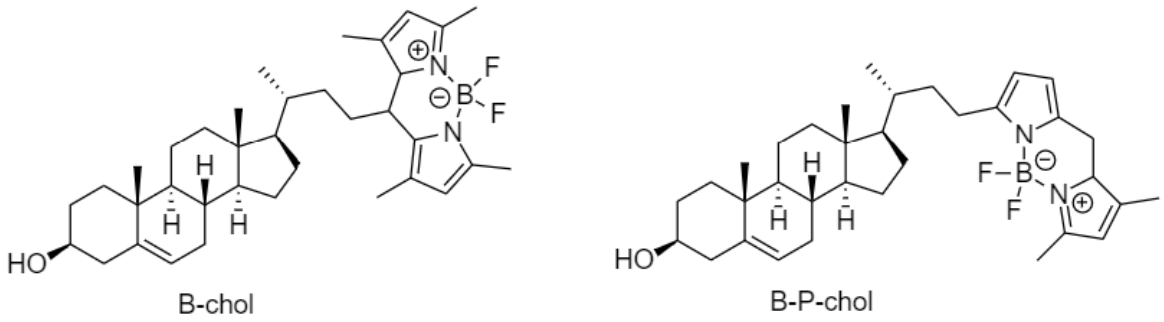

Figure 21. Structures two BODIPY derivatives of cholesterol, BODIPY-cholesterol (B-chol, also sold commercially as TopFluor®) and BODIPY-P-cholesterol (B-P-chol).[15]

Dansyl is a common fluorophore that has been applied to tag proteins and lipids and widely used in chromatography to form fluorescent derivatives. Dansyl has excitation and emission maxima of λ_{ex} = 336 nm and λ_{em} = 515 nm, long fluorescence lifetime and high quantum yield but also a high propensity for photobleaching. A dansyl-tagged analog of cholesterol, D-chol (Figure 22), was originally synthesized by condensing 6-ketocholestanol with dansyl hydrazine in acidic conditions.[85] Notably, this probe had the dansyl-moiety linked to position C6 of the sterol, as opposed to other probes with the

fluorophore in the hydroxyl group or the side chain. Although in the same study D-chol was esterified and hydrolyzed by ACAT with same kinetics as cholesterol, a trait not shown by DHE or B-chol, D-chol does not appear to partition into cholesterol-rich lo phases in model membranes or accumulate into LE-like particles in NPC-cells. This affirms that membrane functions are disturbed by radical modifications in the steroid backbone of cholesterol, including laterally protruding groups such as the 6-dansyl-moiety in D-chol. D-chol is also unsuitable for FCS due to low photostability.[55] NBD-tagged probes (Figure 22) share the same photophysical properties with D-chol, being environmentally sensitive and prone to photobleaching. Nevertheless, they have been used for cellular imaging for several decades. NBD-cholesterol derivatives are relatively water soluble and are exchanged rapidly between cells and the extracellular environment in the presence of protein or cyclodextrin carriers. This also causes their upside-down orientation in bilayers, having the fluorophore moiety oriented towards the phospholipid head groups. Similarly, with D-chol, they cannot order fatty acyl chains in model membranes and partition preferably into cholesterol-poor ld phases. Pyrene-cholesterol is one the newer fluorescent sterols. Pyrene groups form excimers in close proximity to each other, resulting in a characteristic red shifted emission. Cholesterol esters with pyrene group in the acyl chain have been previously used with decent results to track cholesteryl ester in lipoprotein particles. Pyr-met-chol (Figure 22) on the other hand wasn't introduced until 2007. Le Guyader *et al.*[86] synthesized this probe by a condensation reaction between pregnenolone and 1-pyrenecarboxaldehyde. So far there is limited evidence for the suitability of pyrene-tagged probes for study of cholesterol distribution. Pyr-met-chol does not function as a substrate for ACAT and accumulates mainly in intracellular compartments instead of the PM.[54,59]

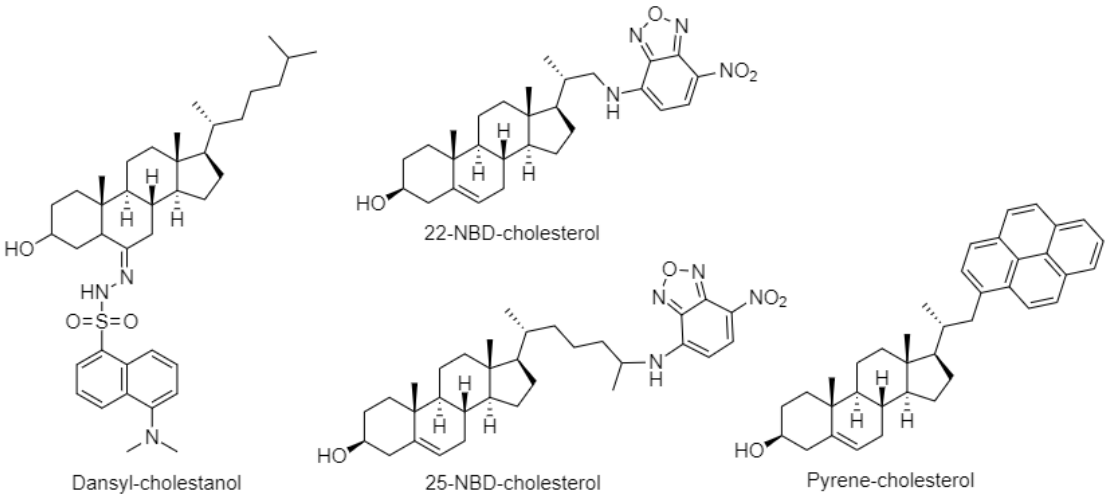

Figure 22. Structures of extrinsically labeled sterol probes dansyl-cholestanol (D-chol), 22-NBD-cholesterol, 25-NBD-cholesterol and 22-methylpyrenyl-cholesterol (pyrene-cholesterol or pyr-met-chol).[15,54]

Click chemistry is a novel strategy that aims to combine the benefits of intrinsically and extrinsically fluorescent sterols. This concept relies on using quick, high-yield reactions to join lipid and fluorophore moieties, usually achieved *in situ.* Peyrot *et al*.[87] found that 20(S)-hydroxycholesterol selectively accumulates in Golgi membranes, using a Huisgen dipolar 1,3-cycloaddition between an oxysterol alkyne derivative and an azide fluorophore (Figure 23). In this method, cells were incubated with an alkyne derivative of 20(S)-OH-cholesterol and fixed. A coverslip containing the azide fluorophore was mounted. After the reaction, the fixed cells were washed off the excess unconjugated fluorophore and imaged with a confocal microscope. In another study focusing on cholesterol instead of oxysterols, Hofmann *et al.*[88] used a similar click reaction between 27-alkyne-cholesterol and azido-sulfo-BODIPY. Although providing promising results and decent fluorescent properties in fixed cultures, click chemistry methods have not yet been successful on live cells. In addition, it is uncertain how the unsaturated side chain affects membrane properties of cholesterol.

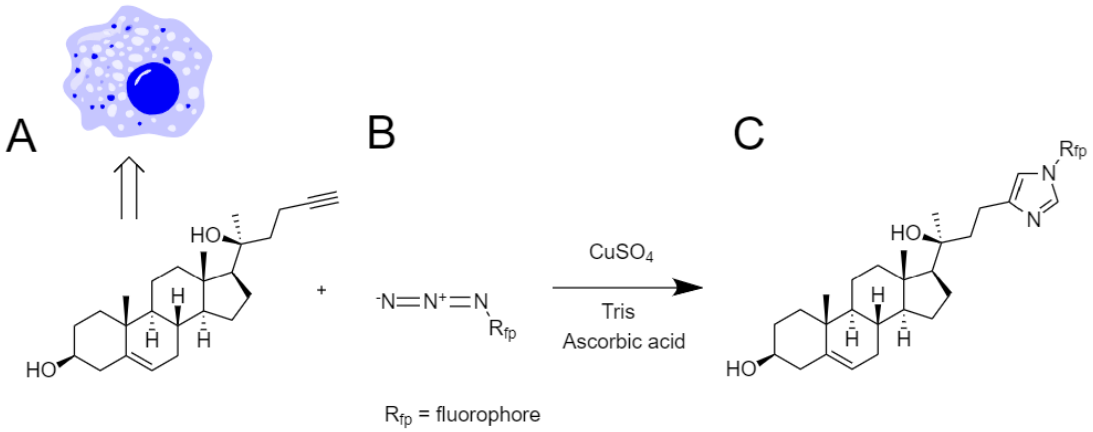

Figure 23. Huisgen cycloaddition in fluorescent cellular imaging of oxysterols. Cells containing 20(S)-OH-24-alkyne-cholesterol (A) are incubated with an azide fluorophore (B) with a copper catalyst. The remaining fluorophore is washed and the fluorescent oxysterol (C) is imaged.[88]

3.4. Cholesterol binding fluorescent probes

Another technique of fluorescent sterol imaging is to use probes that selectively bind cholesterol, such as filipin, nystatin, lagosin and cholesterol-dependent cytolysins. Filipin, commercially known as filipin III (Figure 24), is the most tested of such probes. Filipin is polyene antibiotic that contains a lengthy conjugated hydrocarbon moiety, which gives rise to its fluorescent property. Filipin has excitation and emission maxima of λ_{ex} = 360 nm and λ_{em} = 480 nm, requiring UV-sensitive confocal microscopy equipment. It has low photostability and high propensity for photobleaching. Due to low brightness it cannot be used in FCS applications. Moderate cytotoxicity and ability to disturb bilayers also makes filipin unusable in live cells. Despite these drawbacks, filipin can deliver reproducible and quantifiable results on cholesterol distribution when used in adequate concentrations and with suitable imaging equipment. It shows a clear preference for lo phases in model membranes and has been particularly useful in the imaging of LE- and Ly-like particles of NPC-diseased cells[15,55] (Figure 25).

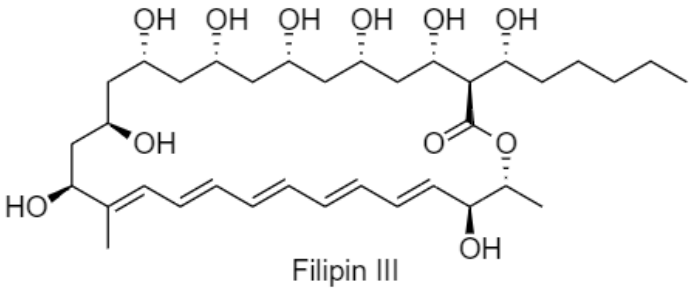

Figure 24. Structure of filipin III, a fluorescent cholesterol-binding antibiotic.

The first quantitative measures of interactions between cholesterol in membranes and polyene antibiotics were obtained in the 70's, showing filipin to exhibit binding selectivity to cholesterol.[89] More specifically, filipin shows selectivity to the 3-OH group of cholesterol, binding only free cholesterol and not esterified forms. The supramolecular chemistry behind this selectivity is not well characterized, as is not the formation of complexes between filipin and PM cholesterol. However, a space filling model suggests that the complexes are 150-250 Å in diameter and include two stacked filipin molecules.[90] In addition to cholesterol, filipin seems to prominently bind GM1 gangliosides, important regulators of neuronal growth. Other interfering substrates cannot be ruled out on this basis. Filipin is toxic to cells which presents problems but can also be considered an advantage. Inoculation of cells with filipin causes a distinct dimpling of the PM that can be clearly observed by electron microscopy.

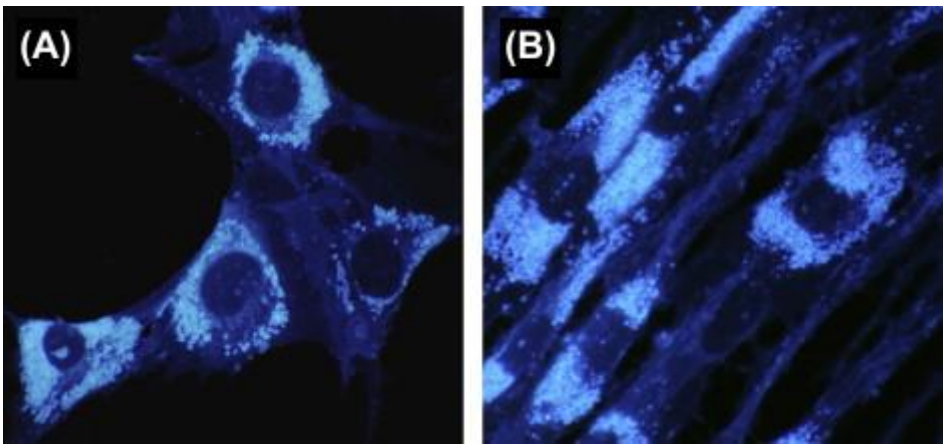

Figure 25. Visualization of free cholesterol by filipin fluorescence in fibroblasts from an individual with NPC1 mutations (A) and an individual with NPC2 mutations (B). Reprinted with permission from Vanier and Latour.[91] Copyright (2015) Elsevier Inc.

Fluorophore-labeled bacterial toxins that bind to cholesterol in bilayers and self-assemble to form pores share many of the same pros and cons with filipin, including that they cannot be used in live cells. However, superior fluorescent properties compared to filipin can be achieved by careful selection of the fluorescent dye. Perifringolysin O (PFO), a soluble bacterial cytolysin obtained from *Clostridium Perfringens*, is one of such probes. PFO can be labeled with a dye directly or the biotinylated form of PFO can be used adjacently with labeled avidin. Sokolov and Radhakrishnan[92] used PFO to bind cholesterol in PMs isolated from cells, whose cholesterol content had been manipulated with cyclodextrin extraction or SREBP-Scap activation. In their novel approach, they used the intrinsic fluorescence of the tryptophan residues in PFO to analyze PM cholesterol content. A general drawback of PFO is that it does not bind to bilayers below cholesterol concentration of 20 mol-%. The structure of PFO entails four polypeptide domains that are dominated by β-strands. The cytolytic activity of PFO depends on access to cholesterol in cell membranes, particularly membrane domains enriched in cholesterol (Figure 26). The binding site for cholesterol has been identified to one of the loops in domain 4 of PFO, and more specifically residues threonine-490 and leucine-491. Although PFO binding is not entirely confined to lo domains or lipid rafts, it seems to be greatly enhanced within the edges of lo and ld domains, which would suggest that PM cholesterol is less hindered in these locations.[93]

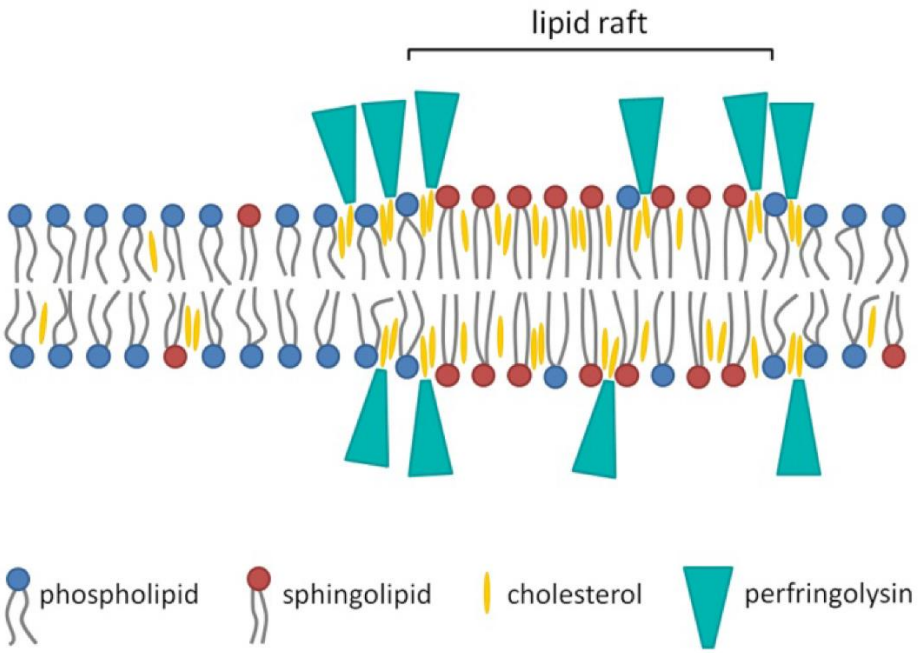

Figure 26. Schematic representation of PFO binding with bilayers. PFO binding is mainly confined to the outer edges of lipid rafts, where cholesterol seems to be most accessible. Reprinted from Verherstraeten *et al.*[93] under Creative Commons (CC BY) license.

3.5. Bile acid derivatives as fluorescent probes

A rather natural extension of fluorescent cholesterol analogs are fluorescent bile acid analogs. The use of such probes is not limited to the study of bile excretion and reabsorption, but they can also provide quantifiable information about the intracellular transport and distribution of bile acids, considering that they are involved in regulating cholesterol homeostasis (see 2.6 Bile acids and bile salts). In addition, unpublished preliminary observations from NMR spectroscopy by a research group in the University of Jyväskylä indicate that bile acids have an ability to bind cholesterol in solution, with cholic acid having the highest observed cholesterol affinity of naturally occurring bile acids.[94] This presents possibilities for their utilization as cholesterol binding fluorescent probes. Bile acids occur in cells naturally and thus are not cytotoxic, however, there is no literature on whether they can partition into bilayers or bind to cholesterol in membranes.

Besides the shorter side chain containing a carboxylic acid head, a prominent distinction between unsaturated sterols and bile acids is the concave α-face, which forms when position 5β is hydrogenated in bile acid synthesis (Figure 27). Binding to cholesterol is supposedly facilitated by the less polar β-face.[94] The saturated and bent steroid frame, different orientation of the 3α-OH group, presence of additional OH groups unless using lithocholic acid, and different side chain can have an impact on the biophysical properties of sterols as discussed previously. These and other properties need to be evaluated when designing fluorescent bile acid analogues. The bile acids occurring in mammalian cells have two functional groups, 3α-hydroxyl and 24-carbonyl groups, which, in theory, could facilitate rather effortless and quick insertion of fluorescent moieties. Both ligation sites present pros and cons as with cholesterol analogs.

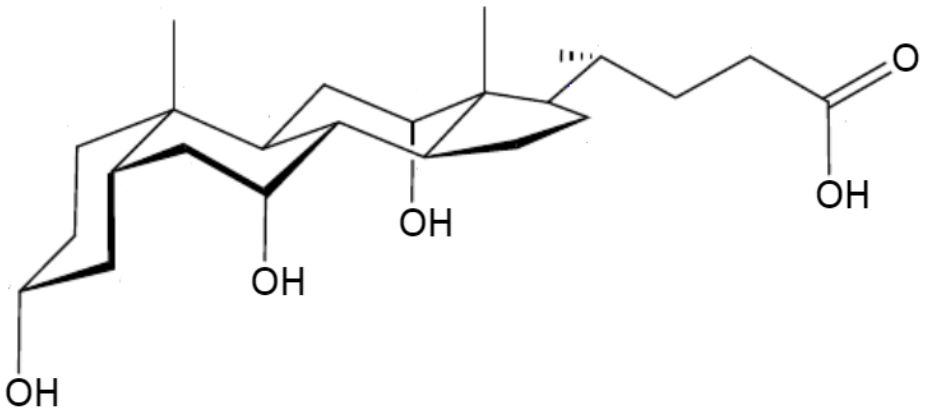

Figure 27. Conformational structure of cholic acid. The three OH groups are oriented unilaterally, distinguishing between the α-face capable of hydrogen bonding and the non-polar β-face.

NBD and fluorescein linked bile acids and bile salts (Figure 28) have been used in the study of hepatic and intestinal bile acid transport in a handful of studies.[95–97] Fluorescein is a commercially available fluorescent dye with excitation and emission maxima of around λ_{ex} = 490 nm and λ_{em} = 510 nm. Fluorescein and its derivatives have common applications in serology, flow cytometry and forensics. As a probe it suffers from the same drawback as NBD having low photostability and high propensity for photobleaching. Weinman *et al.*[95] traced the function of a sodium-bile acid cotransporter in ileal epithelial cells using cholylglycylamidofluorescein, cholyl-(*N*-NBD)-lysine and chenodeoxycholyl-(*N*-NBD)-lysine. Of the three probes, the fluorescein derivative failed to work as a substrate, but the NBD-derivatives were exchanged with sodium with similar kinetics as taurocholate, the other of the natural bile salts. Holzinger *et al.*[97] reported similar results on the biocompatibility of fluorescein versus NBD when following their absorption from the intestine. Although all NBD derivatives of bile acids were absorbed more slowly than taurine or glycine conjugates, fluorescein tagged bile acids underwent little to no absorption. This would discourage the use of fluorescein or similar moieties as fluorescent dyes.

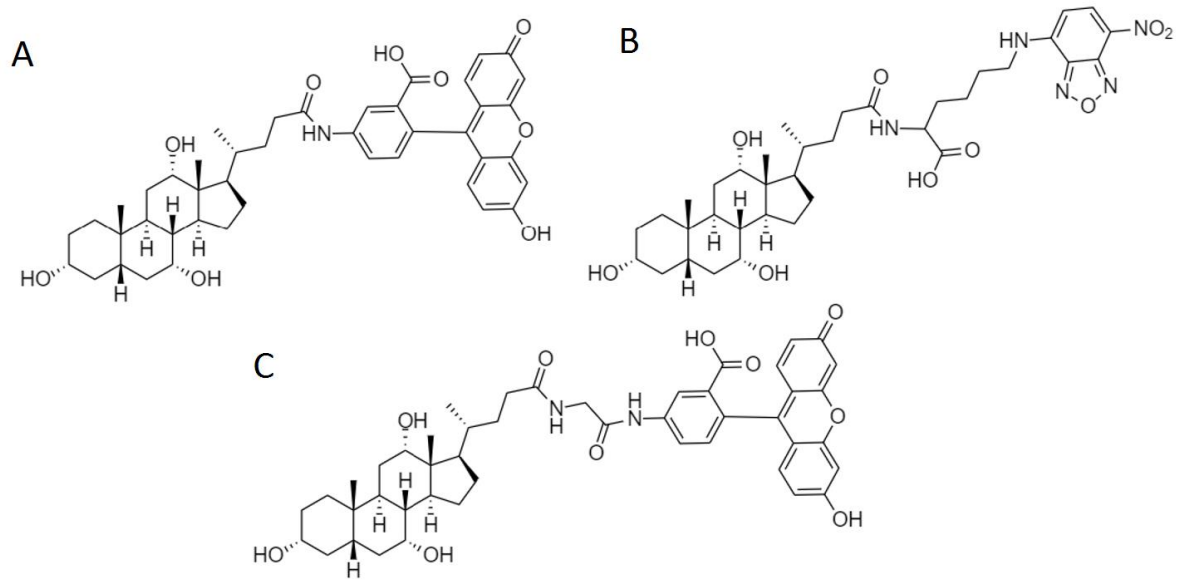

Figure 28. Three fluorescent derivatives of cholic acid and glycocholic acid: Cholylamidofluorescein (A), cholyl-(*N*-NBD)-lysine (B) and cholylglycylamidofluorescein (C).[95,97]

4. Summary of the review of literature

Cells gain cholesterol by *de novo* synthesis in the ER, or lipoprotein-mediated uptake from the extracellular environment. Reverse cholesterol transport relies on HDL-molecules to carry excessive cholesterol into the liver to be recycled or excreted as bile salts. Intracellular cholesterol content is tightly regulated by several homeostatic processes. The components of this homeostasis react, either directly or indirectly, to changes in the levels of intracellular cholesterol by regulating the synthesis, uptake and efflux of cholesterol. The two leaflets of the PM mainly consist of phospholipids and cholesterol with the latter comprising up to 40 % of the membrane lipid content. In steady state, the PM contains also over half of total intracellular cholesterol. The hydrogen bonds between cholesterol and phospholipids, SM in particular, precede the formation of tights lateral domains in membrane leaflets. In literature, these domains are called either lipid rafts or DRMs, depending on the context. This condensing effect of cholesterol decreases the surface area of the membrane and fluctuations in membrane fluidity and, thus, is necessary for healthy membrane function. Transport of cholesterol between the PM and various intracellular organelles employs either vesicles or a variety of different carrier proteins. In some cases, cholesterol can also freely diffuse in close contact of two membrane leaflets. Not all of the

molecules involved in cholesterol transport have been identified and many details of their function are still to be uncovered.

To study the distribution of intracellular cholesterol, density fractionation has been traditionally used. This includes the breaking of cells and separation of the cell components along with proper analysis methods for the different cell phases. However, perfect separation of cell organelles cannot be achieved with any current fractionation methods. Intact cells can be studied with a number of different methods, with fluorescent probes presenting a wide range of possibilities. Many of the probes mentioned above have been useful in the analysis of fixed cells. Filipin, for example, has been used in the study and diagnosis of NPC, a disease that causes cholesterol accumulation into storage organelles.[15]

Investigating the many facets of cholesterol transport thoroughly requires kinetic information and, thus, the use of living cells or *in vivo*-studies. For these purposes, a probe must mimic the functions of intracellular cholesterol as close as possible and yet, at the same time, possess adequate fluorescent properties. A variety of fluorescent cholesterol analogs have been developed for this purpose and, so far, all have been lacking in either of these attributes. In many cases, the probe does not partition the plasma membrane akin to cholesterol or lacks the ability to order phospholipid acyl chains. Click chemistry methods are a promising modern field that might present solutions to many of these challenges. In addition, with the accumulating data on different steroid species and PM lipids, MD simulations might provide means to study the membrane dynamics of fluorescent probes. Development of fluorescent, or otherwise trackable, sterol analogues will present many challenges for synthetic chemists in the future.

II Experimental Part

5. Introduction to the experimental part

The purpose of this study was to investigate the applicability of three novel synthetic fluorophores, provided by Institute of Biotechnology of the Czech Academy of Sciences, in the labeling of bile acids with fluorescent groups. The steroid-binding properties of bile acids combined with the fluorescent properties of the synthetic moieties presented a possibility for the functionalized bile acids to be used as indicators of cholesterol transport and metabolism in live cells. Further studies with cholesterol binding, cytotoxicity and cellular reporting not within the scope of this thesis are to be carried out with at least one of the reaction products.

6. Background

Three stable fluorescent compounds, each with distinct structure and functional groups, were used for the study (Figure 29 - Figure 31. Original compound labels, as written in the containers, are shown in parentheses.) For the sake of convenience, these are referred to as Fp1, Fp2 and Fp3.

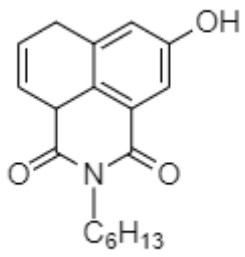

Figure 29. Fluorophore 1 (MHB-90). Molecular weight 297,35 g/mol.

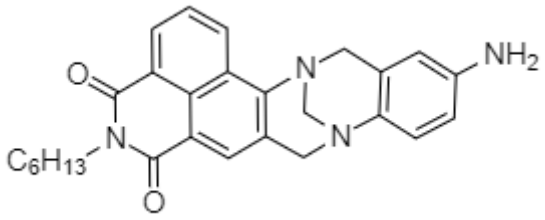

Figure 30. Fluorophore 2 (MHB-127). Molecular weight 440,54 g/mol.

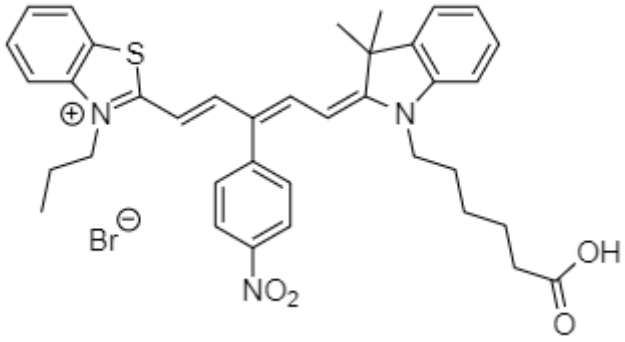

Figure 31. Fluorophore 3 (TBMS-409). Molecular weight 702,71 g/mol.

Due to the minuscule amounts of the fluorophores available, the syntheses had to be carried out in a one-shot fashion using all the starting material at once. Thus, best-proven reaction pathways had to be considered when planning the syntheses. Activation of the 24-carboxylic acid moieties of bile acids with ethyl chloroformate and subsequent derivatization or reduction has been utilized in several studies before[98–105] and also recently in the institute of the author. Thus, the procedures used in this work rely on previous studies by Noponen *et al.* where bile acids were similarly linked with amino acid derivatives.[46,106–108] Ethyl chloroformate is highly reactive with carboxylic acids and the reactions can usually be carried out in mild reaction conditions (Figure 32).

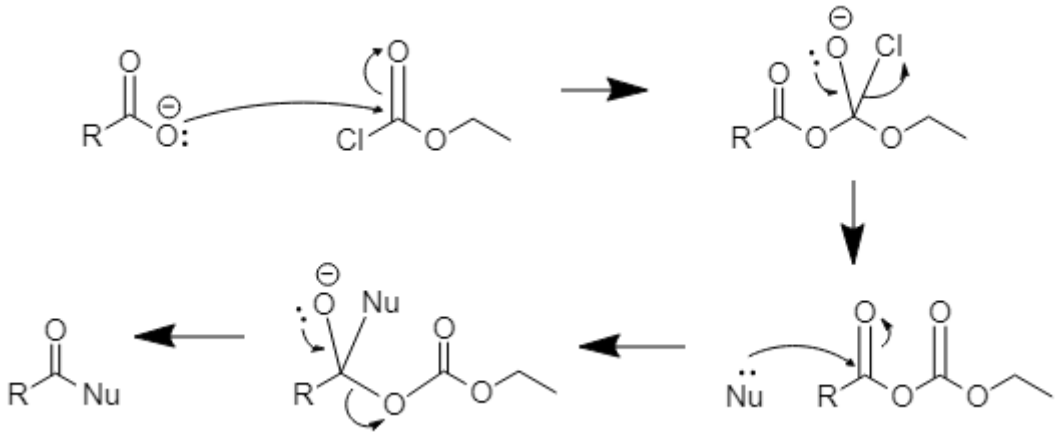

Figure 32. Reaction mechanism: Base-catalyzed activation of carboxylic acid with ethyl chloroformate. Cleavage of chloride forms a reactive anhydride, which can subsequently be cleaved with a nucleophile, such as alcohol or amine.[109]

The synthesis schemes are illustrated in the appendices (Appendix 1 - Appendix 2). The syntheses and products are numbered 1-3 respective to the fluorophores used. Two of the fluorophores (Fp1 and Fp2) contain a nucleophilic group, either a hydroxyl or an amino group. In the first two syntheses, the bile acid was activated with ethyl chloroformate and the resulting anhydride was allowed to react with either Fp1 or Fp2. Fluorophore 3, however, has no explicit nucleophilic groups but, instead, a rather sterically unhindered carboxylic acid moiety. Thus, in the third synthesis the carboxylic acid of the fluorophore was activated with ethyl chloroformate, with the assumption that the 3-OH group of the bile acid would function as a nucleophile.

In the case of syntheses 1 and 2, cholic acid was selected as the bile acid component as per recommendations by a senior researcher. Previous tests by the research group had compared the cholesterol affinity of lithocholic acid, deoxycholic acid and cholic acid. The group demonstrated the third to have the best cholesterol-binding properties.[94] Cholic acid contains three axial OH-groups in positions 3α, 7α and 12α unilaterally, which give rise to its interesting amphiphilic properties.[110] For the third reaction, lithocholic acid was used in its methyl ester form to ensure that the fluorophore would exclusively attach to the 3α-position.

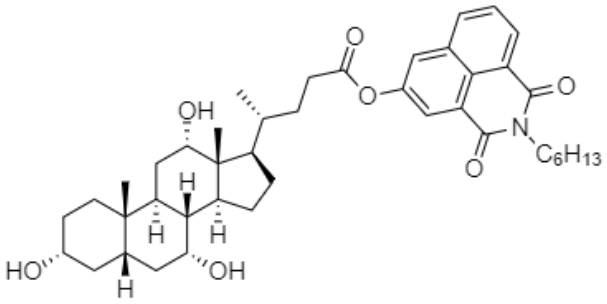

Figure 33. Structure of planned product 1. Chemical Formula: $C_{42}H_{57}NO_7$. Molecular Weight: 687,92 g/mol.

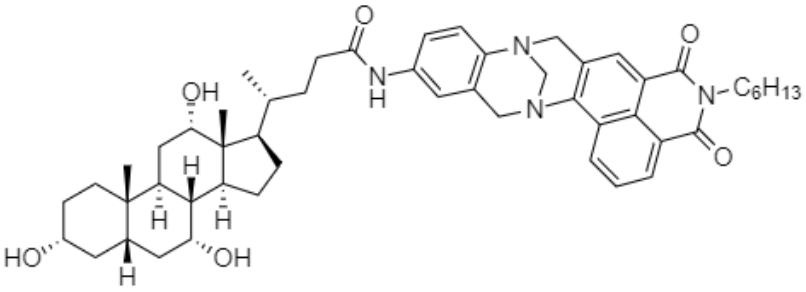

Figure 34. Structure of planned product 2. Chemical Formula: $C_{51}H_{66}N_4O_6$. Molecular Weight: 831,11 g/mol.

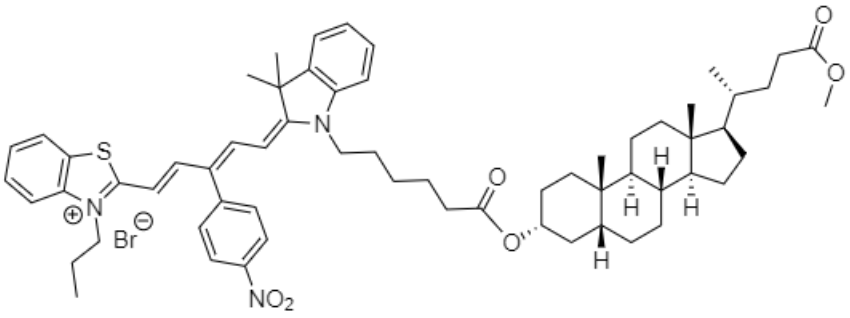

Figure 35. Structure of planned product 3. Chemical Formula: $C_{62}H_{80}BrN_3O_6S$. Molecular Weight: 1075,30 g/mol.

7. Experimental

Fluorophores 1-3 were obtained as a gift from the Institute of Biotechnology of the Czech Academy of Sciences. Cholic acid (purity 98 %) and lithocholic acid (97 %) were purchased from Sigma. Ethyl chloroformate (97 %) and triethylamine were purchased from

Merck and distilled before use. Silica gel 60 (0,063-0,200 mm) was purchased from Merck. All solvents were analytic or HPLC grade.

Methyl lithocholate was prepared with a simple Fischer esterification.[111] An amount of 370 mg of lithocholic acid, 10 ml of MeOH and a small amount of sulfuric acid were added to a flask. The mixture was refluxed for 2,5 hours. MeOH was evaporated, and the residue was reconstituted in 10 ml of chloroform. The product was washed with water (1 x 10 ml), $NaHCO_3$ solution (2 x 10 ml) and once more with 10 ml of water. The product was dried and filtered, and the solvent was evaporated under reduced pressure.

^1H and ^{13}C NMR spectra were recorded on a Bruker Avance III HD Nanobay 300 MHz spectrometer, except for the final spectra of product 1, which were recorded on a Bruker Avance III 500 MHz spectrometer. The ppm scale was calibrated by referencing the resonant frequencies of residual chloroform (^1H NMR δ 7,26 (C**H**Cl_3). ^{13}C NMR δ 77,00 (**C**HCl_3).) Mass spectra were recorded on a Micromass LCT ESI-TOF spectrometer. Previous literature on the subject[106,112,113] and online resources[114–116] were used as references when assigning the NMR signals.

8. Procedures

8.1. Synthesis of the conjugate between cholic acid and Fp1

An amount of 118 mg of cholic acid was dissolved in 4 ml of dry dioxane and cooled to 10 °C in a 50 ml flask. 50 µl of triethylamine and 50 µl of ethyl chloroformate in 0,5 ml of dioxane were added to the flask through a dropping funnel. The mixture was incubated for 30 minutes at room temperature, stirring constantly. All the Fp1, 90 mg, was dissolved in 2,5 ml of dioxane and added dropwise to the flask. The flask was fitted with a reflux condenser and heated in an oil bath set to 80 °C. Progress of the reaction was monitored using ^1H NMR observing the integrals of two singlet peaks at frequencies 0,66 and 0,71 ppm, presumably belonging to the 18-methyl groups of cholic acid and the derivative, respectively (Figure 36). After 6 days the reaction was deemed complete with approximately 60% of cholic acid consumed in the reaction. The mixture was cooled, and the solvent was evaporated under reduced pressure. The crude product was dissolved in

chloroform (10 ml) and washed with water (2 x 7 ml), 0,1 M HCl solution (2 x 7 ml), again with water (2 x 7 ml) and brine (2 x 7 ml). The organic layer was dried with Na_2SO_4, filtered and the solvent was evaporated. ^{1}H NMR screen still showed substantial impurities at this point, which is why the crude product was purified by column chromatography (silica gel, DCM:EtOAc:MeOH 82:9:9). A total of 120 fractions were collected with fractions 81 to 100 containing a small amount of colored solid **1**. The solid was analyzed by ^{1}H and ^{13}C NMR and mass spectrometry.

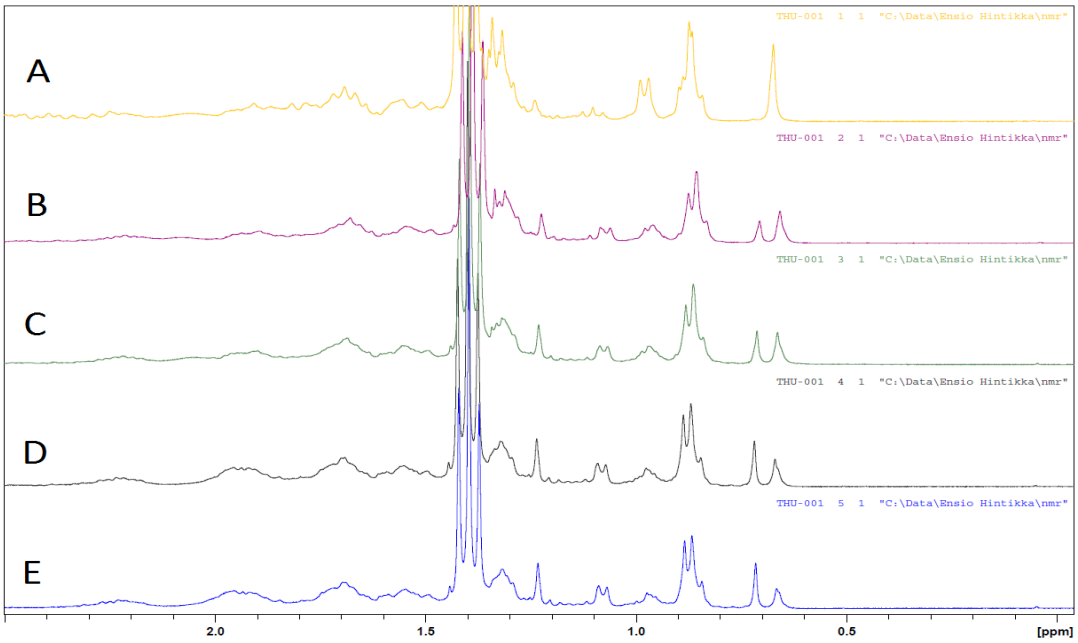

Figure 36. ^{1}H NMR spectra of reaction mixtures containing Fp1 and cholic acid, magnified to 0-3 ppm (A) In the beginning (B) Overnight (C) After 48 hours (D) After 72 hours (E) After 6 days.

1: ^{1}H NMR ($CDCl_3$, 500 MHz, ppm) δ 8,58 (d); 8,34 (s); 8,18 (d); 7,96 (s); 7,79 (t); 7,48 (d); 7,36 (m); 6,3 (s); 4,19 (t); 4,05 (s); 4 (s); 3,88 (s, 12β-H); 3,67 (s, 7β-H); 3,51 (s, 3β-H); 2,75 (m); 2,62 (m); 2,22 (m, 3-OH, 7-OH and 12-OH); 1,95 (m); 1,75 (m); 1,56 (m); 1,44 (m); 1,37 (m); 1,28 (s); 1,12 (d); 1,01 (m); 0,93 (m, 21-CH_3 and 19-CH_3); 0,77 (s); 0,71 (d, 18-CH_3). ^{13}C NMR ($CDCl_3$, 125 MHz, ppm): δ 180,2; 174,7; 174,0; 172,5 (C24); 163,9; 163,4; 149,2; 141,1; 133,4; 132,5; 130,8; 130,0; 128,5; 128,4; 128,1; 127,8; 127,7; 127,3; 126,5; 126,1; 124,8; 124,4; 122,8; 74,0; 73,0 (C12); 72,1 (C3); 68,4 (C7); 68,3; 68,2; 55,4; 47,1; 46,9 (C17); 46,6 (C13); 42,0 (C14); 41,5 (C5); 41,2; 40,6; 39,6 (C8, C4); 35,2; 35,1 (C20); 34,9 (C1); 34,7 (C10); 34,5 (C6); 31,9 (C23); 31,5; 31,2 (C22); 30,8; 30,5 (C2); 29,7¸29,3; 28,5; 28,2 (C11); 28,0; 27,4 (C16); 26,8 (C9); 23,2 (C15); 22,7 (C19);

22,6; 17,4 (C21); 14,0; 12,6; 12,5 (C18). ESI-TOF MS: *m/z* 635, *m/z* 693, *m/z* 836, *m/z* 1102.

8.2. Synthesis of the conjugate between cholic acid and Fp2

An amount of 55 mg of cholic acid was dissolved in 4 ml of dioxane and cooled to 10 °C in a 50 ml flask. 19 µl of triethylamine and 13 µl of ethyl chloroformate in 0,5 ml of dioxane were added to the flask through a dropping funnel. The mixture was incubated for 30 minutes at room temperature, stirring constantly. All of the Fp2, 60 mg, was dissolved in 2,5 ml of MeOH:dioxane (50:50) and added dropwise to the flask. The flask was fitted with a reflux condenser and heated in an oil bath set to 80 °C. After 7 days the reaction was halted, the mixture was cooled, and solvent was evaporated under reduced pressure. The crude product was dissolved in chloroform (10 ml) and washed with water (2 x 10 ml), 0,1 M HCl solution (2 x 10 ml), again with water (2 x 10 ml) and brine (2 x 10 ml). The organic layer was dried with Na_2SO_4 and filtered. ^{1}H NMR showed impurities, which is why the layer was washed anew with 1M NaOH (4 x 10 ml), 1 M HCl (2 x 10 ml) and water (1 x 10 ml). The organic layer was dried and filtered, and volatiles were evaporated under reduced pressure. The crude product was recrystallized in ACN. At this point small amount of impurities crystallized, which were filtered out. The crude product was dissolved in equal parts of MeOH and hexane. Small amount of water was added until the compound crystallized as brown solid **2**. The brown solid was analyzed by NMR and mass spectrometry. MeOH, hexane and water were evaporated under reduced pressure, which yielded another yellow solid **2b**. This was also analyzed by NMR.

2: ^{1}H NMR ($CDCl_3$, 300 MHz, ppm) δ 8,52 (d, 2H, 39-H and 42-H); 8,10(s, 1H, 40-H); 7,53 (t, 2H, N-H, 41-H); 7,3 (s, 1H, 26-H); 7,11 (s, 2H, 29-H and 30-H); 4,83 (d, 2H, 32-H); 4,38 (m, 4H, 31-H and 33-H); 4,11 (t, 2H, 46-H); 3,88 (s, 1H, 12β-H); 3,78 (s, 1H, 7β-H); 3,4 (s, 1H, 3β-H); 2,15 (m, 3H, 3-OH, 7-OH and 12-OH); 1,95 - 1,1 (br. m, 32H); 0,86 (m, 9H, 21-CH_3, 19-CH_3 and 51-CH_3); 0,59 (s, 3H, 18-CH_3). ^{13}C NMR ($CDCl_3$, 75 MHz, ppm): δ 172,2 (C24); 164,2 (C44); 163,8 (C45); 149,9 (C28); 143,1 (C43); 134,8 (C35); 130,7 (C37); 130,6 (C36); 128,8 (C39); 128,2 (C42); 127,7 (C25); 127,2 (C41); 126,6 (C27); 125,6 (C40); 125,4 (C38); 123,1 (C34); 119,7 (C30); 118,4 (C26); 118,0 (C29); 73,1 (C12); 71,9 (C3); 68,4 (C7); 67,1 (C32); 61,2 (methanol); 58,6 (C33); 57,4 (C31); 46,3 (C17, C13); 41,8 (C14); 41,4 (C5); 40,3 (C46); 39,7 (C4); 39,4 (C8); 35,2 (C20); 35,0

(C1); 34,7 (C10, C6); 31,9 (C23); 31,5 (C47); 31,3 (C22); 30,5 (C2); 29,7 (C48); 29,3 (hexane); 28,2 (C11); 28,1 (C29); 27,4 (C16); 26,7 (C49); 26,5 (C9); 23,2 (C15); 22,5 (C19); 22,4 (C50); 17,4 (C21); 14,6 (hexanes); 14 (C51); 12,4 (C18). ESI-TOF MS: $[M + Na]^+$ *m/z* 854, $[M + K]^+$ *m/z* 870. Yield 14%.

2b: ^{1}H NMR ($CDCl_3$, 300 MHz, ppm) δ 8,53 (m, 2H); 8,10 (s, 1H); 7,75 (m, 2H); 7,31 (s, 1H); 7,12 (s, 2H); 4,83 (d, 2H); 4,35 (m, 3H); 4,11 (t, 2H); 3,89 (s, 1H); 3,72 (m, triethylamine); 3,4 (s, 1H,); 2,14 (m, 3H); 1,95 - 1,1 (br. m); 1,24 (m, triethylamine); 0,85 (m, 16H); 0,7 (s, 1H); 0,6 (s, 3H).

8.3. Synthesis of the conjugate between methyl lithocholate and Fp3

All the Fp3, 60 mg, was dissolved in 4 ml of dioxane and cooled to 10 °C in a 50 ml flask. 16 µl of triethylamine and 11 µl of ethyl chloroformate in 0,5 ml of dioxane were added to the flask through a dropping funnel. The mixture was incubated for 30 minutes at room temperature, stirring constantly. 43 mg of methyl lithocholate was dissolved in 1 ml of dioxane and added dropwise to the flask. The flask was fitted with a reflux condenser and heated in an oil bath set to 80 °C. After 7 days the reaction was halted, the mixture was cooled, and solvent was evaporated under reduced pressure. The crude product was dissolved in chloroform (10 ml) and washed with water (2 x 10 ml), 0,1 M HCl solution (2 x 10 ml), again with water (2 x 10 ml) and brine (2 x 10 ml). The organic layer was dried with anhydrous $CaCl_2$ and filtered, and the volatiles were evaporated under reduced pressure. As in synthesis 2, phase separation was achieved by dissolving the solids in equal parts MeOH, hexane and water. The phases were separated and, after evaporation of the solvent, the aqueous/MeOH phase yielded a blue solid (**3**) and the hexane/MeOH phase a red solid (**3b**). Both products were analyzed by NMR and product **3** also by mass spectrometry.

3: ^{1}H NMR ($CDCl_3$, 300 MHz, ppm) δ 3,66 (s, 24-O-CH3); 3,61 (m, 3b-H); 2,36 (m, 23-H); 2,21 (m, 23-H); 1,9 - 0,99 (br. m); 0,88 (m, 21-CH3, 19-CH3); 0,65 (s, 18-CH3); ^{13}C NMR ($CDCl_3$, 75 MHz, ppm): δ 174,8 (C24); 71,9 (C3); 56,5 (C14); 56 (C17); 51,5 (C24-O-Me); 42,8 (C13); 42,1 (C5); 41,4; 40,5 (C23); 40,2 (C9); 36,5 (C12); 35,9 (C11); 35,4 (C1, C20); 34,6 (C8); 31,1 (C10); 31 (C7); 30,6 (C15); 29,7; 29,1; 28,9; 28,2 (C16); 27,2

(C6); 26,4 (C4); 24,2 (C2); 23,4 (C19); 22,6; 20,8 (C22); 20,4; 19,4; 18,3 (C21); 14,3; 12 (C18); 11,4. ESI-TOF MS: *m/z* 608, *m/z* 623, *m/z* 679, *m/z* 995.

3b: ^{1}H NMR ($CDCl_3$, 300 MHz, ppm) δ 3,71 (m, triethylamine); 3,64 (m); 2,36 (m); 2,21 (m); 1,8 (br. m); 1,7 (s); 1,34 (br. s); 1,24 (t, triethylamine); 0,89 (m); 0,63 (s).

9. Results

The first synthesis yielded a microgram-scale amount of brown colored solid **1**. This was readily soluble in chloroform and acetone but not in aqueous solvents. Multitude of aromatic carbon peaks in NMR (Appendix 4) and several varying peaks in mass spectrum (Appendix 5) revealed, in this case, a mixture of cholic acid derivatives. The mass spectrum along with estimated correlating structures is shown below (Figure 37).

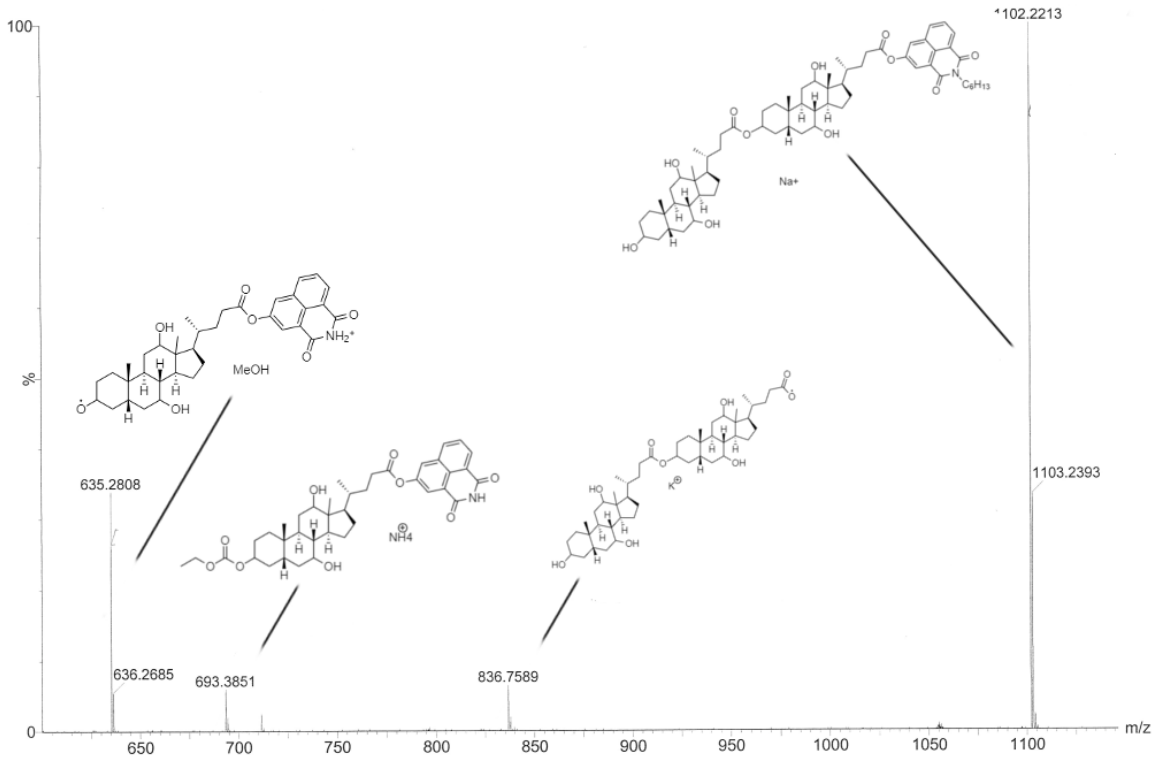

Figure 37. Mass spectrum of product **1** (mixture) with correlating structures.

Regrettably, after pooling fractions 64-83 of the column chromatography their contents were lost due to faulty glassware. The chemical content of these fractions could not be

analyzed, but they possibly contained some, if not most, of the desired product. Modest excess of ethyl chloroformate was used in the first synthesis, which explains the presence of the anhydride analogues of Fp1 and cholic acid-fluorophore. Thus, the amount of ethyl chloroformate was adjusted to stoichiometric values in the following syntheses.

Product from the second synthesis was a brownish solid (**2**) with a yield of 16 mg (Figure 38). The structure derived from the NMR and MS spectra (Appendix 6 - Appendix 8) for this compound corresponded to the planned one. The compound was readily soluble in organic solvents but demonstrated extreme hydrophobicity, crystallizing with the slightest addition of water. Based on the NMR spectra, small hexane and methanol residues were present in product **2** due to the solids being slightly damp. The compound was allowed to properly desiccate before storage. Curiously, the secondary yellow solid **2b** had the same chemical structure according to ^{1}H NMR but with the presence of triethylamine. Because of the small amount of this compound, no further purifications were attempted for **2b**.

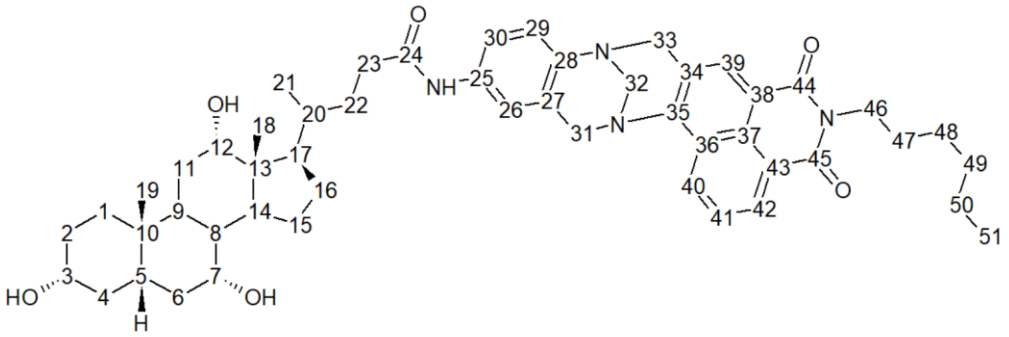

Figure 38. The structure of product **2** with carbon atoms numbered

Evaporation of solvents from the phase separation yielded 30 mg of blue solid **3** (MeOH and water phase) and a diminutive amount of red solid **3b** (hexane and MeOH phase), which were both concluded to contain methyl lithocholate and impurities based on the NMR analysis. Appearance of solid **3** was much like that of Fp3, being a crystalline substance with a bright blue color, however, NMR showed only the distinct spectrum of methyl lithocholate with nonconforming signals within the aliphatic frequencies. Peaks in mass spectrum could not be associated with any probable methyl lithocholate analogues, which would indicate not a successful ligation with the fluorophore, but rather a complexation or salt formation with Fp3 or a chromogenic fragment of the molecule.

10. Discussion

As mentioned above, a part of the product of the first synthesis was lost in the column chromatographic process and therefore the success of the synthesis cannot be fully evaluated. However, the desired compound was not present in quantitative amounts in the fractions isolated. A major aspect to consider with base-catalyzed substitution reaction involving the cholic acid anhydride and a hydroxyl group from another molecule is to steer selectivity away from the hydroxyl groups at positions 3α, 7α and 12α of the cholic acid. If structural analogues of the hydroxyl groups are compared (Figure 39), the phenolic group in Fp1 is more basic by a factor of 10^9. Using triethylamine as a base would not risk the formation of competing cholic acid alkoxide anions. While dimerization and polymerization of bile acids, by a linkage of either 3- or 24-carbon extremities, is not unheard of[117–119], they generally require harsher conditions and specific catalysts. Only traces of cholic acid dimers were present in the solids analyzed with mass spectrometry. Examples of synthesis of similar aryl esters of bile acids are rather scarce. Phenyl cholate has been synthesized before using iodosoarenes (ArIO) with trimethoxybenzene[120] and also by arylation of potassium cholate with diaryliodonium salts.[121] More complex aryl esters, which potentially aid healing from oxidative cell damage, have been synthesized in low temperatures using *N*,*N'*-dicyclohexylcarbodiimide and 4-dimethylamino pyridine.[122] Very prominent ultrasound- and microwave-irradiation techniques for the esterification of bile acids have been tested by Cravotto *et al*[123]. This technique involved a *p*-toluenesulfonic acid activation and a subsequent esterification of the carboxylic acid end.

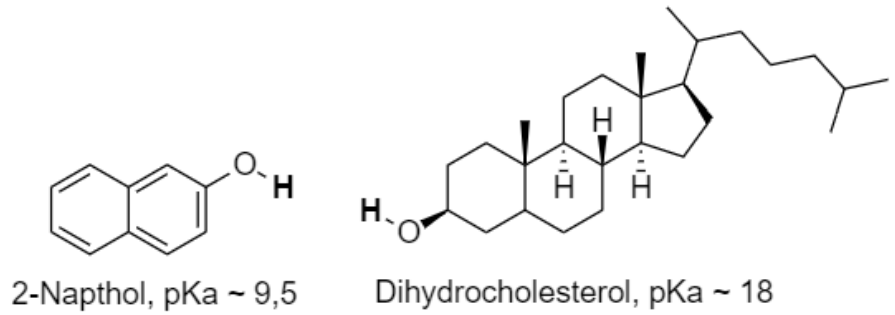

Figure 39. Two structural analogues of Fp1 and cholic acid with the acidity of the hydroxyl groups compared: 2-naphthol and dihydrocholesterol.[124,125]

The second synthesis involved formation of a bile acid amide, so the reaction scheme had most similarities with the experiments that this study was based on. The articles by Noponen *et al.* [46,106,107] and Löfman *et al.*[112,113] studied cysteamine, amino acids and alkylamines as ligands and the reaction scheme was largely replicated from these papers. Different amino acids and taurine have been incorporated into bile acid amides in several studies before. Glycine and taurine are also natural conjugates of bile acids in mammalian cells (see 2.6 Bile acids and bile salts) and have been used to bridge other fluorescent groups to bile acids (3.5 Bile acid derivatives as fluorescent probes). Besides the ethyl chloroformate method utilized here, different ways of conjugating bile acids have been reported: Bile acids can be activated in basic conditions with 2-ethoxy-1-ethoxycarbonyl-1,2-dihydroquinoline, isobutyl chloroformate or 1-ethyl-(3-(3-dimethylamino)-propyl)-carbodiimide hydrochloride, prior to amidation[126–128] Also a method with imidazole and amine under microwave irradiation has been tested.[123] The wide array of methods suggest that amines can be readily incorporated into a bile acid, given that its carbonyl group is functionalized with a good leaving group. The reaction scheme in this experiment posed particular challenges due to the bulky primary amine used as the ligand. Despite the relatively long incubation, yield was very modest compared to yields as high as 90 % with smaller amines. In accordance with methods of Noponen *et al.* and Löfman *et al.*, incubation temperature was also kept under boiling point, so as not to induce damage to the fluorophore. This may have been excessively conservative, and a greater yield could have been potentially achieved by refluxing the reaction mixture.

The third synthesis did not yield the planned product, at least in quantifiable amounts. In this reaction, the ethyl chloroformate-activated carboxylic acid domain of Fp3 was to be linked to the 3α-hydroxyl group of lithocholic acid *via* an ester bond. Considering the pKa value of dihydrocholesterol (approximately 18), it is plausible that the reaction mixture was not basic enough to drive the substitution reaction at the carbonyl group. However, judging from the appearance of the washed and extracted solid, salt or solid-state complex formation is likely. The bright blue color of Fp3 and its analogues is attributable to the conjugated network of the molecule, not unlike those seen in organic blue light emitting materials. [129,130] The crystalline substance isolated most likely contains the conjugated structure, if not the whole fluorophore. A few examples of preparation of lithocholic acid 3-esters can be found. Simple acetyl and formyl derivatives have been synthesized by do Nascimiento *et al*[131]. The group experimented a reaction of lithocholic acid and its 24-

esters with acetic anhydride and 4-(dimethylamino)-pyridine to give acetyl derivatives with yields up to 97%. Formyl derivatives with yields up to 93 % were synthesized with formic acid and perchloric acid catalyst. Chattopadhyay and Pandey[132] have reported a synthesis of slightly more novel methyl lithocholate-uracil derivatives with yields up to 70 % using bromoacetyl bromide as an activating and bridging agent in basic conditions.

11. Conclusions

Three different custom fluorophores Fp1-Fp3 obtained from the Czech Academy of Sciences were under investigation with the view of ligating them with bile acids to form fluorescent cholesterol hosts to be used as cellular reporters. Using a known method of carboxylic acid activation with ethyl chloroformate, synthesis of three bile acid analogues was attempted: cholic acid-Fp1, cholic acid-Fp2 and methyl lithocholate-Fp3. Cholic acid-Fp2 was successfully synthesized and isolated and will be utilized in sequential studies.

Numerous studies, not limited to those cited here, show that bile acids, most prominently cholic acid, deoxycholic acid and lithocholic acid, can be linked with a myriad of different organic and inorganic ligands either utilizing either the 3-hydroxyl group or the terminal carboxylic acid group. They can also form dimers or be incorporated into polymers either via the side chain or the backbone.[133–135] The steroid binding abilities of particularly cholic acid attract attention to usage of bile acids as cellular reporters, when functionalized with optically active or otherwise detectable moieties. This work confirmed the compatibility of the ethyl chloroformate method with functionalization of the terminal carboxylic acid. Reactions can be carried out in mild conditions and yields improved by lengthening the reaction times. If bile acids are to be converted into their esters, modifications to the aforementioned method or overall different reaction scheme would be advised. The activated 24-carbonyl moiety of bile acids can be readily functionalized with an amine ligand as seen in this and other[106,123,127] experiments. This also retains the composition of the steroid frame and the 3-OH group. This experiment was limited by the small amount of starting materials, namely the custom fluorophores. Additional studies derived from this experiment would be experimenting syntheses 1 and 3 with different reaction schemes and experimenting synthesis 2 with a longer reaction time and possibly different purification

methods. Thorough cholesterol-binding and *in vivo* fluorescence tests with the products would also be a topic of interest.

Bibliography

1. The top 10 causes of death, http://www.who.int/news-room/fact-sheets/detail/the-top-10-causes-of-death, World Health Organization (10.10.2018).

2. Maxfield, F. R., Intracellular cholesterol transport, *J. Clin. Invest.*, **2002**, *110*, 891–898.

3. Liscum, L. and Munn, N. J., Intracellular cholesterol transport, *Biochim. Biophys. Acta - Mol. Cell Biol. Lipids*, **1999**, *1438*, 19–37.

4. Hao, M.; Lin, S. X.; Karylowski, O. J.; Wüstner, D.; McGraw, T. E. and Maxfield, F. R., Vesicular and Non-vesicular Sterol Transport in Living Cells, *J. Biol. Chem.*, **2002**, *277*, 609–617.

5. Calkin, A. C. and Tontonoz, P., Transcriptional integration of metabolism by the nuclear sterol-activated receptors LXR and FXR, *Nat. Rev. Mol. Cell Biol.*, **2012**, *13*, 213–224.

6. Brown, M. S. and Goldstein, J. L., A proteolytic pathway that controls the cholesterol content of membranes, cells, and blood, *Proc. Natl. Acad. Sci. U. S. A.*, **1999**, *96*, 11041–11048.

7. Sharpe, L. J.; Cook, E. C. L.; Zelcer, N. and Brown, A. J., The UPS and downs of cholesterol homeostasis, *Trends Biochem. Sci.*, **2014**, *39*, 527–535.

8. Reece, J. B.; Urry, L. A.; Cain, M. L.; Wasserman, S. A.; Minorsky, P. V and Jackson, R. B., Membrane structure and function. In: Reece, J. B. and Campbell, N. A. (eds.), *Campbell biology*, 10th edition, Pearson, San Francisco, 2011, p. 127.

9. Roelofsen, B. and den Kamp, J. A. F., Chapter 1 - Plasma Membrane Phospholipid Asymmetry and Its Maintenance: The Human Erythrocyte as a Model, *Curr. Top. Membr.*, **1994**, *40*, 7–46.

10. Cogan, U. and Schachter, D., Asymmetry of lipid dynamics in human erythrocyte membranes studied with impermeant fluorophores, *Biochemistry*, **1981**, *20*, 6396–6403.

11. Boesze-Battaglia, K.; Clayton, S. T. and Schimmel, R. J., Cholesterol redistribution within human platelet plasma membrane: evidence for a stimulus-dependent event, *Biochemistry*, **1996**, *35*, 6664–6673.

12. Schroeder, F.; Gallegos, A. M.; Atshaves, B. P.; Storey, S. M.; Mcintosh, A. L.; Petrescu, A. D.; Huang, H.; Starodub, O.; Chao, H.; Yang, H.; Frolov, A. and Kier, A. B., Recent Advances in Membrane Microdomains: Rafts, Caveolae, and Intracellular Cholesterol Trafficking, *Exp. Biol. Med.*, **2001**, *226*, 873–890.

13. Schroeder, F.; Frolov, A. A.; Murphy, E. J.; Atshaves, B. P.; Jefferson, J. R.; Pu, L.; Wood, W. G.; Foxworth, W. B. and Kier, A. B., Recent Advances in Membrane Cholesterol Domain Dynamics and Intracellular Cholesterol Trafficking, *Proc. Soc. Exp. Biol. Med.*, **1996**, *213*, 150–177.

14. Singer, S. J. and Nicolson, G. L., The fluid mosaic model of the structure of cell membranes, *Science (80-.).*, **1972**, *175*, 720–731.

15. Maxfield, F. R. and Wüstner, D., Chapter 17 - Analysis of Cholesterol Trafficking with Fluorescent Probes, *Methods Cell Biol.*, **2012**, *108*, 367–393.

16. Maxfield, F. R., Plasma membrane microdomains, *Curr. Opin. Cell Biol.*, **2002**, *14*, 483–487.

17. Simons, K. and Ikonen, E., Functional rafts in cell membranes, *Nature*, **1997**, *387*, 569–572.

18. Lichtenberg, D.; Goñi, F. M. and Heerklotz, H., Detergent-resistant membranes should not be identified with membrane rafts, *Trends Biochem. Sci.*, **2005**, *30*, 430–436.

19. Brown, D. A. and Rose, J. K., Sorting of GPI-anchored proteins to glycolipid-enriched membrane subdomains during transport to the apical cell surface, *Cell*, **1992**, *68*, 533–544.

20. Brown, D. A., Lipid Rafts, Detergent-Resistant Membranes, and Raft Targeting Signals, *Physiology*, **2006**, *21*, 430–439.

21. Fielding, C. J.; Bist, A. and Fielding, P. E., Intracellular cholesterol transport in synchronized human skin fibroblasts, *Biochemistry*, **1999**, *38*, 2506–2513.

22. Fielding, C. J. and Fielding, P. E., Intracellular cholesterol transport, *J. Lipid Res.*, **1997**, *38*, 1503–1521.

23. Aittoniemi, J.; Róg, T.; Niemelä, P.; Pasenkiewicz-Gierula, M.; Karttunen*, M. and Vattulainen, I., Tilt: Major Factor in Sterols' Ordering Capability in Membranes, **2006**.

24. Khelashvili, G.; Pabst, G. and Harries, D., Cholesterol orientation and tilt modulus in DMPC bilayers, *J. Phys. Chem. B*, **2010**, *114*, 7524–7534.

25. Khelashvili, G. and Harries, D., How Cholesterol Tilt Modulates the Mechanical

Properties of Saturated and Unsaturated Lipid Membranes, *J. Phys. Chem. B*, **2013**, *117*, 2411–2421.

26. Bennett, W. F. D.; MacCallum, J. L.; Hinner, M. J.; Marrink, S. J. and Tieleman, D. P., Molecular View of Cholesterol Flip-Flop and Chemical Potential in Different Membrane Environments, *J. Am. Chem. Soc.*, **2009**, *131*, 12714–12720.

27. Wüstner, D. and Solanko, K., How cholesterol interacts with proteins and lipids during its intracellular transport, *Biochim. Biophys. Acta - Biomembr.*, **2015**, *1848*, 1908–1926.

28. Frolov, A.; Woodford, J. K.; Murphy, E. J.; Billheimer, J. T. and Schroeder, F., Spontaneous and Protein-mediated Sterol Transfer between Intracellular Membranes, *J. Biol. Chem.*, **1996**, *271*, 16075–16083.

29. Lev, S., Nonvesicular lipid transfer from the endoplasmic reticulum, *Cold Spring Harb. Perspect. Biol.*, **2012**, *4*.

30. Slotte, J. P., Cholesterol-Sphingomyelin Interactions in Cells—Effects on Lipid Metabolism. In: Bittman, R. (ed.), *Cholesterol*, Springer, Boston, 1997, pp. 277–293.

31. Skiba, P. J.; Zha, X.; Maxfield, F. R.; Schissel, S. L. and Tabas, I., The distal pathway of lipoprotein-induced cholesterol esterification, but not sphingomyelinase-induced cholesterol esterification, is energy-dependent, *J. Biol. Chem.*, **1996**, *271*, 13392–13400.

32. Carstea, E. D.; Morris, J. A.; Coleman, K. G.; Loftus, S. K.; Zhang, D.; Cummings, C.; Gu, J.; Rosenfeld, M. A.; Pavan, W. J.; Krizman, D. B.; Nagle, J.; Polymeropoulos, M. H.; Sturley, S. L.; Ioannou, Y. A.; Higgins, M. E.; Comly, M.; Cooney, A.; Brown, A.; Kaneski, C. R.; Blanchette-Mackie, E. J.; Dwyer, N. K.; Neufeld, E. B.; Chang, T. Y.; Liscum, L.; Strauss, J. F.; Ohno, K.; Zeigler, M.; Carmi, R.; Sokol, J.; Markie, D.; O'Neill, R. R.; van Diggelen, O. P.; Elleder, M.; Patterson, M. C.; Brady, R. O.; Vanier, M. T.; Pentchev, P. G. and Tagle, D. A., Niemann-Pick C1 disease gene: homology to mediators of cholesterol homeostasis, *Science*, **1997**, *277*, 228–231.

33. Ohashi, R.; Mu, H.; Wang, X.; Yao, Q. and Chen, C., Reverse cholesterol transport and cholesterol efflux in atherosclerosis, *QJM An Int. J. Med.*, **2005**, *98*, 845–856.

34. Fielding, C. J. and Fielding, P. E., Molecular physiology of reverse cholesterol transport., *J. Lipid Res.*, **1995**, *36*, 211–228.

35. Smart, E. J.; Ying, Y.; Donzell, W. C. and Anderson, R. G. W., A Role for Caveolin in Transport of Cholesterol from Endoplasmic Reticulum to Plasma Membrane, *J. Biol. Chem.*, **1996**, *271*, 29427–29435.

36. Heinecke, J. W., A new era for quantifying HDL and cardiovascular risk?, *Nat. Med.*, **2012**, *18*, 1346–1347.

37. Jia, L.; Betters, J. L. and Yu, L., Niemann-Pick C1-Like 1 (NPC1L1) Protein in Intestinal and Hepatic Cholesterol Transport, *Annu. Rev. Physiol.*, **2011**, *73*, 239–259.

38. Zhang, Y.; Silva, J. R. Da; Reilly, M.; Billheimer, J. T.; Rothblat, G. H. and Rader, D. J., Hepatic expression of scavenger receptor class B type I (SR-BI) is a positive regulator of macrophage reverse cholesterol transport in vivo, *J. Clin. Invest.*, **2005**, *115*, 2870–2874.

39. Mardones, P.; Quiñones, V.; Amigo, L.; Moreno, M.; Miquel, J. F.; Schwarz, M.; Miettinen, H. E.; Trigatti, B.; Krieger, M.; VanPatten, S.; Cohen, D. E. and Rigotti, A., Hepatic cholesterol and bile acid metabolism and intestinal cholesterol absorption in scavenger receptor class B type I-deficient mice, *J. Lipid Res.*, **2001**, *42*, 170–180.

40. Wang, X.; Collins, H. L.; Ranalletta, M.; Fuki, I. V; Billheimer, J. T.; Rothblat, G. H.; Tall, A. R. and Rader, D. J., Macrophage ABCA1 and ABCG1, but not SR-BI, promote macrophage reverse cholesterol transport in vivo, *J. Clin. Invest.*, **2007**, *117*, 2216–2224.

41. Hauet, T.; Liu, J.; Li, H.; Gazouli, M.; Culty, M. and Papadopoulos, V., PBR, StAR, and PKA: Partners in cholesterol transport in steroidogenic cells, *Endocr. Res.*, **2002**, *28*, 395–401.

42. Lacapère, J.-J. and Papadopoulos, V., Peripheral-type benzodiazepine receptor: structure and function of a cholesterol-binding protein in steroid and bile acid biosynthesis, *Steroids*, **2003**, *68*, 569–585.

43. File:Steroidogenesis.svg, Wikimedia Commons.

44. Kevresan, S.; Kuhajda, K.; Kandrac, J.; Fawcett, J. P. and Mikov, M., Biosynthesis of bile acids in mammalian liver, *Eur. J. Drug Metab. Pharmacokinet.*, **2006**, *31*, 145–156.

45. Parks, D. J.; Blanchard, S. G.; Bledsoe, R. K.; Chandra, G.; Consler, T. G.; Kliewer, S. A.; Stimmel, J. B.; Willson, T. M.; Zavacki, A. M.; Moore, D. D. and Lehmann, J., Bile Acids: Natural Ligands for an Orphan Nuclear Receptor, *Science (80-.).*, **1999**, *284*, 1365.

46. Noponen, V.; Lahtinen, M.; Valkonen, A.; Salo, H.; Kolehmainen, E. and Sievänen, E., Bile acid–amino acid ester conjugates: gelation, structural properties, and thermoreversible solid to solid phase transition, *Soft Matter*, **2010**, *6*, 3789–3796.

47. Overview of Affinity Purification, https://www.thermofisher.com/uk/en/home/life-

science/protein-biology/protein-biology-learning-center/protein-biology-resource-library/pierce-protein-methods/overview-affinity-purification.html, Thermo Fisher (21.10.2018).

48. Warnock, D. E.; Roberts, C.; Lutz, M. S.; Blackburn, W. A.; Young, W. W. and Baenziger, J. U., Determination of plasma membrane lipid mass and composition in cultured Chinese hamster ovary cells using high gradient magnetic affinity chromatography., *J. Biol. Chem.*, **1993**, *268*, 10145–10153.

49. Altelaar, A. F. M.; Klinkert, I.; Jalink, K.; Lange, R. P. J.; Adan, R. A. H.; Heeren, R. M. A. and Piersma, S. R., Gold-enhanced biomolecular surface imaging of cells and tissue by SIMS and MALDI mass spectrometry, *Anal. Chem.*, **2006**, *78*, 734–742.

50. Nygren, H. and Malmberg, P., Silver deposition on freeze-dried cells allows subcellular localization of cholesterol with imaging TOF-SIMS, *J. Microsc.*, **2004**, *215*, 156–161.

51. Nan, X.; Cheng, J.-X. and Xie, X. S., Vibrational imaging of lipid droplets in live fibroblast cells with coherent anti-Stokes Raman scattering microscopy, *J. Lipid Res.*, **2003**, *44*, 2202–2208.

52. Yen, K.; Le, T. T.; Bansal, A.; Narasimhan, S. D.; Cheng, J.-X. and Tissenbaum, H. A., A Comparative Study of Fat Storage Quantitation in Nematode Caenorhabditis elegans Using Label and Label-Free Methods, *PLoS One*, **2010**, *5*, e12810.

53. Chien, C.-H.; Chen, W.-W.; Wu, J.-T. and Chang, T.-C., Label-free imaging of Drosophila in vivo by coherent anti-Stokes Raman scattering and two-photon excitation autofluorescence microscopy, *J. Biomed. Opt.*, **2011**, *16*, 16012.

54. Solanko, K. A.; Modzel, M.; Solanko, L. M. and Wüstner, D., Fluorescent Sterols and Cholesteryl Esters as Probes for Intracellular Cholesterol Transport, *Lipid Insights*, **2015**, *8*, 95–114.

55. Sezgin, E.; Can, F. B.; Schneider, F.; Clausen, M. P.; Galiani, S.; Stanly, T. A.; Waithe, D.; Colaco, A.; Honigmann, A.; Wüstner, D.; Platt, F. and Eggeling, C., A comparative study on fluorescent cholesterol analogs as versatile cellular reporters, *J. Lipid Res.*, **2016**, *57*, 299–309.

56. Chen, A. K.; Cheng, Z.; Behlke, M. A. and Tsourkas, A., Assessing the Sensitivity of Commercially Available Fluorophores to the Intracellular Environment, *Anal. Chem.*, **2008**, *80*, 7437–7444.

57. Klymchenko, A. S., Solvatochromic and Fluorogenic Dyes as Environment-Sensitive Probes: Design and Biological Applications, *Acc. Chem. Res.*, **2017**, *50*, 366–375.

58. Demchenko, A. P.; Mély, Y.; Duportail, G. and Klymchenko, A. S., Monitoring Biophysical Properties of Lipid Membranes by Environment-Sensitive Fluorescent Probes, *Biophys. J.*, **2009**, *96*, 3461–3470.

59. Wüstner, D., Fluorescent sterols as tools in membrane biophysics and cell biology, *Chem. Phys. Lipids*, **2007**, *146*, 1–25.

60. Gimpl, G. and Gehrig-Burger, K., Probes for studying cholesterol binding and cell biology, *Steroids*, **2011**, *76*, 216–231.

61. Ohvo-Rekilä, H.; Åkerlund, B. and Slotte, J. P., Cyclodextrin-catalyzed extraction of fluorescent sterols from monolayer membranes and small unilamellar vesicles, *Chem. Phys. Lipids*, **2000**, *105*, 167–178.

62. Scheek, S.; Brown, M. S.; Goldstein, J. L.; Goldstein, J. L. and Brown, M. S., Sphingomyelin depletion in cultured cells blocks proteolysis of sterol regulatory element binding proteins at site 1, *Proc. Natl. Acad. Sci.*, **1997**, *94*, 11179–11183.

63. Kruth, H. S.; Avigan, J.; Gamble, W. and Vaughan, M., Effect of Cell Density on Binding and Uptake of Low Density Lipoprotein by Human Fibroblasts, *J. Cell Biol.*, **1979**, *83*, 588–594.

64. Korlach, J.; Schwille, P.; Webb, W. W. and Feigenson, G. W., Characterization of lipid bilayer phases by confocal microscopy and fluorescence correlation spectroscopy, *Proc. Natl. Acad. Sci.*, **1999**, *96*, 8461–8466.

65. File:FluorescenceFilters 2008-09-28.svg, https://commons.wikimedia.org/wiki/File:FluorescenceFilters_2008-09-28.svg, Wikimedia Commons (26.1.2019).

66. Ries, J. and Schwille, P., Fluorescence correlation spectroscopy, *BioEssays*, **2012**, *34*, 361–368.

67. Thompson, N. L., Fluorescence Correlation Spectroscopy. In: Lakowicz, J. R. (ed.), *Topics in Fluorescence Spectroscopy*, Springer, Boston, 2002, pp. 337–378.

68. File:Schematic of FCS setup.png, https://commons.wikimedia.org/wiki/File:Schematic_of_FCS_setup.png, Wikimedia Commons (28.12.2018).

69. Wüstner, D.; Lund, F. W.; Röhrl, C. and Stangl, H., Potential of BODIPY-cholesterol for analysis of cholesterol transport and diffusion in living cells, *Chem. Phys. Lipids*, **2016**, 194, 12–28.

70. Rogers, J.; Lee, A. G. and Wilton, D. C., The organisation of cholesterol and ergosterol in lipid bilayers based on studies using non-perturbing fluorescent sterol probes, *Biochim. Biophys. Acta - Biomembr.*, **1979**, *552*, 23–37.

71. Hyslop, P. A.; Morel, B. and Sauerheber, R. D., Organization and interaction of cholesterol and phosphatidylcholine in model bilayer membranes, *Biochemistry*, **1990**, *29*, 1025–1038.

72. Mukherjee, S.; Zha, X.; Tabas, I. and Maxfield, F. R., Cholesterol distribution in living cells: fluorescence imaging using dehydroergosterol as a fluorescent cholesterol analog, *Biophys. J.*, **1998**, *75*, 1915–1925.

73. Garvik, O.; Benediktson, P.; Simonsen, A. C.; Ipsen, J. H. and Wüstner, D., The fluorescent cholesterol analog dehydroergosterol induces liquid-ordered domains in model membranes, *Chem. Phys. Lipids*, **2009**, *159*, 114–118.

74. Wüstner, D. and Færgeman, N. J., Spatiotemporal analysis of endocytosis and membrane distribution of fluorescent sterols in living cells, *Histochem. Cell Biol.*, **2008**, *130*, 891.

75. Fischer, R. T.; Stephenson, F. A.; Shafiee, A. and Schroeder, F., Δ5, 7, 9 (11)-Cholestatrien-3β-ol: A fluorescent cholesterol analogue, *Chem. Phys. Lipids*, **1984**, *36*, 1–14.

76. Windaus, A.; Deppe, M. and Roosen-Runge, C., Über die Pyro-vitamine D3 und ihre Dehydro-derivate, *Justus Liebigs Ann. Chem.*, **1938**, *687*, 1–10.

77. McIntosh, A. L.; Gallegos, A. M.; Atshaves, B. P.; Storey, S. M.; Kannoju, D. and Schroeder, F., Fluorescence and Multiphoton Imaging Resolve Unique Structural Forms of Sterol in Membranes of Living Cells, *J. Biol. Chem.*, **2003**, *278*, 6384–6403.

78. Xu, C.; Zipfel, W.; Shear, J. B.; Williams, R. M. and Webb, W. W., Multiphoton fluorescence excitation: new spectral windows for biological nonlinear microscopy, *Proc. Natl. Acad. Sci.*, **1996**, *93*, 10763–10768.

79. Diaspro, A.; Bianchini, P.; Vicidomini, G.; Faretta, M.; Ramoino, P. and Usai, C., Multi-photon excitation microscopy, *Biomed. Eng. Online*, **2006**, *5*, 36–50.

80. Li, Z.; Mintzer, E. and Bittman, R., First Synthesis of Free Cholesterol−BODIPY Conjugates, *J. Org. Chem.*, **2006**, *71*, 1718–1721.

81. Hölttä-Vuori, M.; Uronen, R.; Repakova, J.; Salonen, E.; Vattulainen, I.; Panula, P.; Li, Z.; Bittman, R. and Ikonen, E., BODIPY-Cholesterol: A New Tool to Visualize Sterol Trafficking in Living Cells and Organisms, *Traffic*, **2008**, *9*, 1839–1849.

82. Kanerva, K.; Uronen, R.-L.; Blom, T.; Li, S.; Bittman, R.; Lappalainen, P.; Peränen, J.; Raposo, G. and Ikonen, E., LDL Cholesterol Recycles to the Plasma Membrane via a Rab8a-Myosin5b-Actin-Dependent Membrane Transport Route, *Dev. Cell*, **2013**, *27*, 249–262.

83. Johnson, I. D.; Kang, H. C. and Haugland, R. P., Fluorescent membrane probes incorporating dipyrrometheneboron difluoride fluorophores, *Anal. Biochem.*, **1991**, *198*, 228–237.

84. Liu, Z.; Thacker, S. G.; Fernandez-Castillejo, S.; Neufeld, E. B.; Remaley, A. T. and Bittman, R., Synthesis of Cholesterol Analogues Bearing BODIPY Fluorophores by Suzuki or Liebeskind–Srogl Cross-Coupling and Evaluation of Their Potential for Visualization of Cholesterol Pools, *ChemBioChem*, **2014**, *15*, 2087–2096.

85. Wiegand, V.; Chang, T.-Y.; Strauss, J. F.; Fahrenholz, F. and Gimpl, G., Transport of plasma membrane-derived cholesterol and the function of Niemann-Pick C1 Protein, *FASEB J.*, **2003**, *17*, 782–784.

86. Le Guyader, L.; Le Roux, C.; Mazères, S.; Gaspard-Iloughmane, H.; Gornitzka, H.; Millot, C.; Mingotaud, C. and Lopez, A., Changes of the Membrane Lipid Organization Characterized by Means of a New Cholesterol-Pyrene Probe, *Biophys. J.*, **2007**, *93*, 4462–4473.

87. Peyrot, S. M.; Nachtergaele, S.; Luchetti, G.; Mydock-McGrane, L. K.; Fujiwara, H.; Scherrer, D. E.; Jallouk, A.; Schlesinger, P. H.; Ory, D. S.; Covey, D. F. and Rohatgi, R., Tracking the subcellular fate of 20(S)-hydroxycholesterol with click chemistry reveals a transport pathway to the golgi, *J. Biol. Chem.*, **2014**, *289*, 11095–11110.

88. Hofmann, K.; Thiele, C.; Schött, H.-F.; Gaebler, A.; Schoene, M.; Kiver, Y.; Friedrichs, S.; Lütjohann, D. and Kuerschner, L., A novel alkyne cholesterol to trace cellular cholesterol metabolism and localization, *J. Lipid Res.*, **2014**, *55*, 583–591.

89. Bittman, R. and Fischkoff, S. A., Fluorescence Studies of the Binding of the Polyene Antibiotics Filipin III, Amphotericin B,. Nystatin, and Lagosin to Cholesterol, 69, 1972.

90. De Kruijff, B. and Demel, R. A., Polyene antibiotic-sterol interactions in membranes of Acholeplasma laidlawii cells and lecithin liposomes. III. Molecular structure of the polyene antibiotic-cholesterol complexes, *Biochim. Biophys. Acta - Biomembr.*, **1974**, *339*, 57–70.

91. Vanier, M. T. and Latour, P., Laboratory diagnosis of Niemann–Pick disease type C: The filipin staining test, *Methods Cell Biol.*, **2015**, *126*, 357–375.

92. Sokolov, A. and Radhakrishnan, A., Accessibility of Cholesterol in Endoplasmic Reticulum Membranes and Activation of SREBP-2 Switch Abruptly at a Common Cholesterol Threshold, *J. Biol. Chem.*, **2010**, *285*, 29480–29490.

93. Verherstraeten, S.; Goossens, E.; Valgaeren, B.; Pardon, B.; Timbermont, L.; Haesebrouck, F.; Ducatelle, R.; Deprez, P.; Wade, K.; Tweten, R.; Van Immerseel, F.; Verherstraeten, S.; Goossens, E.; Valgaeren, B.; Pardon, B.; Timbermont, L.; Haesebrouck, F.; Ducatelle, R.; Deprez, P.; Wade, K. R.; Tweten, R. and Van

Immerseel, F., Perfringolysin O: The Underrated Clostridium perfringens Toxin?, *Toxins (Basel).*, **2015**, *7*, 1702–1721.

94. Sievänen, E., correspondency, **2018**.

95. Weinman, S. A.; Carruth, M. W. and Dawson, P. A., Bile Acid Uptake via the Human Apical Sodium-Bile Acid Cotransporter Is Electrogenic, *J. Biol. Chem.*, **1998**, *273*, 34691–34695.

96. Kitamura, T.; Gatmaitan, Z. and Arias, I. M., Serial quantitative image analysis and confocal microscopy of hepatic uptake, intracellular distribution and biliary secretion of a fluorescent bile acid analog in rat hepatocyte doublets, *Hepatology*, **1990**, *12*, 1358–1364.

97. Holzinger, F.; Schteingart, C. D.; Ton-Nu, H.; Eming, S. A.; Monte, M. J.; Hagey, L. R. and Hofmann, A. F., Fluorescent bile acid derivatives: Relationship between chemical structure and hepatic and intestinal transport in the rat, *Hepatology*, **1997**, *26*, 1263–1271.

98. Hjelmeland, L. M.; Nebert, D. W. and Osborne, J. C., Sulfobetaine derivatives of bile acids: Nondenaturing surfactants for membrane biochemistry, *Anal. Biochem.*, **1983**, *130*, 72–82.

99. Hjelmeland, L. M., A nondenaturing zwitterionic detergent for membrane biochemistry: design and synthesis, *Proc. Natl. Acad. Sci.*, **1980**, *77*, 6368–6370.

100. Lehmann, T. J. and Engels, J. W., Synthesis and Properties of Bile Acid Phosphoramidites 5′-Tethered to Antisense Oligodeoxynucleotides against HCV, *Bioorg. Med. Chem.*, **2001**, *9*, 1827–1835.

101. Mateo-Castro, R.; Gimeno-Adelantado, J. V; Bosch-Reig, F.; Doménech-Carbó, A.; Casas-Catalán, M. J.; Osete-Cortina, L.; la Cruz-Cañizares, J. De and Doménech-Carbó, M. T., Identification by GC-FID and GC-MS of amino acids, fatty and bile acids in binding media used in works of art, *Fresenius. J. Anal. Chem.*, **2001**, *369*, 642–646.

102. Pope, J. L., Crystallization of sodium taurocholate, *J. Lipid Res.*, **1967**, *8*, 146–147.

103. Kihira, K.; Yoshii, M.; Okamoto, A.; Ikawa, S.; Ishii, H. and Hoshita, T., Synthesis of new bile salt analogues, sodium 3 alpha, 7 alpha-dihydroxy-5 beta-cholane-24-sulfonate and sodium 3 alpha, 7 beta-dihydroxy-5 beta-cholane-24-sulfonate, *J. Lipid Res.*, **1990**, *31*, 1323–1326.

104. Ogawa, S.; Mitamura, K.; Ikegawa, S.; Krasowski, M. D.; Hagey, L. R.; Hofmann, A. F. and Iida, T., Chemical synthesis of the (25R)- and (25S)-epimers of 3α,7α,12α-trihydroxy-5α-cholestan-27-oic acid as well as their corresponding glycine and taurine conjugates, *Chem. Phys. Lipids*, **2011**, *164*, 368–377.

105. Bergström, S. and Norman, A., Synthesis of Conjugated Bile Acids. Bile Acids and Steroids 5., *Acta Chem. Scand.*, **1953**, *7*, 1127.

106. Noponen, V.; Belt, H.; Lahtinen, M.; Valkonen, A.; Salo, H.; Ulrichová, J.; Galandáková, A. and Sievänen, E., Bile acid–cysteamine conjugates: Structural properties, gelation, and toxicity evaluation, *Steroids*, **2012**, *77*, 193–203.

107. Noponen, V.; Valkonen, A.; Lahtinen, M.; Salo, H. and Sievänen, E., Self-assembly properties of bile acid derivatives of l-cysteine, l-valine and l-serine alkyl esters, *Supramol. Chem.*, **2013**, *25*, 133.

108. Kuosmanen, R.; Puttreddy, R.; Willman, R.-M.; Äijäläinen, I.; Galandáková, A.; Ulrichová, J.; Salo, H.; Rissanen, K. and Sievänen, E., Biocompatible hydrogelators based on bile acid ethyl amides, *Steroids*, **2016**, 108, 7–16.

109. Kim, S.; Lee, J. I. and Kim, Y. C., A simple and mild esterification method for carboxylic acids using mixed carboxylic-carbonic anhydrides, *J. Org. Chem.*, **1985**, *50*, 560–565.

110. Giammei, C., *Biphosphonate prodrugs utilizing endogenous carriers*, MSc Thesis, Department of Chemistry, University Of Jyväskylä, 2016.

111. Smith, J. G., Organic chemistry. 3rd edition, McGraw-Hill, New York, 2011, pp. 848–850.

112. Löfman, M.; Koivukorpi, J.; Noponen, V.; Salo, H. and Sievänen, E., Bile acid alkylamide derivatives as low molecular weight organogelators: systematic gelation studies and qualitative structural analysis of the systems., *J. Colloid Interface Sci.*, **2011**, *360*, 633–644.

113. Löfman, M., *Bile acid amides as components of microcrystalline organogels*, Dissertation, Department Of Chemistry, University Of Jyväskylä, 2015.

114. Proton Chemical Shifts, https://www.chem.wisc.edu/areas/reich/nmr/h-data/hdata.htm, University of Wisconsin (17.9.2018).

115. C-13 Chemical Shifts, https://www.chem.wisc.edu/areas/reich/nmr/c13-data/cdata.htm, University of Wisconsin (17.9.2018).

116. Biological Magnetic Resonance Data Bank, http://www.bmrb.wisc.edu, University of Wisconsin (18.9.2018).

117. Gouin, S. and Zhu, X. X., Synthesis of 3α- and 3β-dimers from selected bile acids, *Steroids*, **1996**, *61*, 664–669.

118. Meijide, F.; de Frutos, S.; Soto, V.; Jover, A.; Seijas, J.; Vázquez-Tato, M.; Fraga, F. and Tato, J., A Standard Structure for Bile Acids and Derivatives, *Crystals*, **2018**,

8, 86–104.

119. Wess, G.; Kramer, W.; Enhsen, A.; Glombik, H.; Baringhaus, K.-H.; Boeger, G.; Urmann, M.; Bock, K. and Kleine, H., Specific Inhibitors of Ileal Bile Acid Transport, *J. Med. Chem.*, **1994**, *37*, 873–875.

120. Dohi, T.; Koseki, D.; Sumida, K.; Okada, K.; Mizuno, S.; Kato, A.; Morimoto, K. and Kita, Y., Metal-Free O-Arylation of Carboxylic Acid by Active Diaryliodonium(III) Intermediates Generated in situ from Iodosoarenes, *Adv. Synth. Catal.*, **2017**, *359*, 3503–3508.

121. Bhattarai, B.; Tay, J.-H. and Nagorny, P., Thiophosphoramides as cooperative catalysts for copper-catalyzed arylation of carboxylates with diaryliodonium salts, *Chem. Commun.*, **2015**, *51*, 5398–5401.

122. Soldato, P. Del, Steroid Nitrates for the Treatment of Oxidative Injury and Endothelial Dysfunction, 2002.

123. Cravotto, G.; Boffa, L.; Turello, M.; Parenti, M. and Barge, A., Chemical modifications of bile acids under high-intensity ultrasound or microwave irradiation, *Steroids*, **2005**, *70*, 77–83.

124. Betanaphthol, https://pubchem.ncbi.nlm.nih.gov/compound/8663, Pubchem (24.9.2018).

125. 5alpha-Cholestanol (HMDB0000908), http://www.hmdb.ca/metabolites/HMDB0000908, Human Metabolome Database (24.9.2018).

126. Kågedahl, M.; Swaan, P. W.; Redemann, C. T.; Tang, M.; Craik, C. S.; Szoka, F. C. and Øie, S., Use of the Intestinal Bile Acid Transporter for the Uptake of Cholic Acid Conjugates with HIV-1 Protease Inhibitory Activity, *Pharm. Res.*, **1997**, *14*, 176–180.

127. Venturoni, F.; Gioiello, A.; Sardella, R.; Natalini, B. and Pellicciari, R., Continuous flow synthesis and scale-up of glycine- and taurine-conjugated bile salts, *Org. Biomol. Chem.*, **2012**, *10*, 4109–4115.

128. Li, Q.; He, W.; Zhang, L.; Zu, Y.; Zhu, Q.; Deng, X.; Zhao, T.; Zhang, W. G. and Baoyou, Synthesis, Anticancer Activities, Antimicrobial Activities and Bioavailability of Berberine-Bile Acid Analogues, *Lett. Drug Des. Discov.*, **2012**, *9*, 573–580.

129. Jayabharathi, J.; Sathishkumar, R.; Thanikachalam, V. and Jayamoorthy, K., High efficiency, blue emitting materials based on phenanthro[9,10-d]imidazole derivatives, *J. Lumin.*, **2014**, *153*, 343–349.

130. Li, W.; Wang, Z. and Lu, P., Blue organic light emitting materials from π-conjugated compounds, *Opt. Mater. (Amst).*, **2004**, *26*, 243–246.

131. do Nascimento, P. G. G.; Lemos, T. L. G.; Almeida, M. C. S.; de Souza, J. M. O.; Bizerra, A. M. C.; Santiago, G. M. P.; da Costa, J. G. M. and Coutinho, H. D. M., Lithocholic acid and derivatives: Antibacterial activity, *Steroids*, **2015**, *104*, 8–15.

132. Chattopadhyay, P. and Pandey, P. S., Bile acid-based receptors containing 2,6-bis(acylamino)pyridine for recognition of uracil derivatives, *Bioorg. Med. Chem. Lett.*, **2007**, *17*, 1553–1557.

133. Gautrot, J. E. and Zhu, X. X., Main-Chain Bile Acid Based Degradable Elastomers Synthesized by Entropy-Driven Ring-Opening Metathesis Polymerization, *Angew. Chem. Int. Ed.*, **2006**, *45*, 6872–6874.

134. Gautrot, J. E. and Zhu, X. X., High molecular weight bile acid and ricinoleic acid-based copolyesters via entropy-driven ring-opening metathesis polymerisation, *Chem. Commun. (Camb).*, **2008**, *54*, 1674–1676.

135. Strandman, S.; Tsai, I.-H.; Lortie, R. and Zhu, X. X., Ring-opening polymerization of bile acid macrocycles by Candida antarctica lipase B, *Polym. Chem.*, **2013**, *4*, 4312–4316.

List of appendices

Appendix 1. Planned synthetic route to products **1** and **2**.

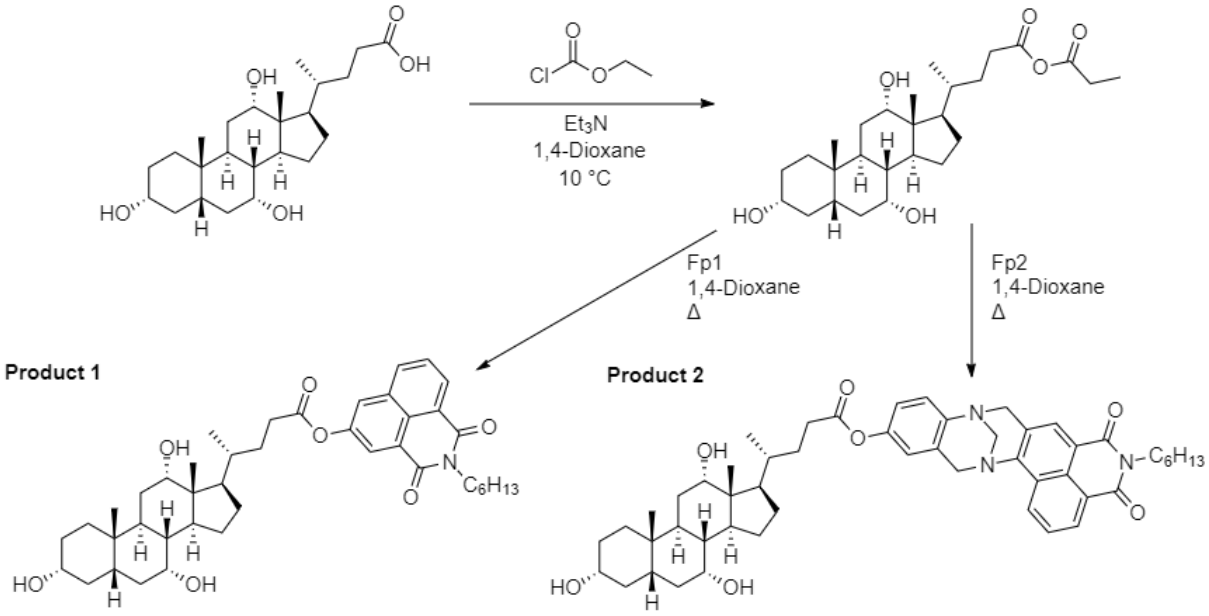

Appendix 2. Planned synthetic route to product **3**.

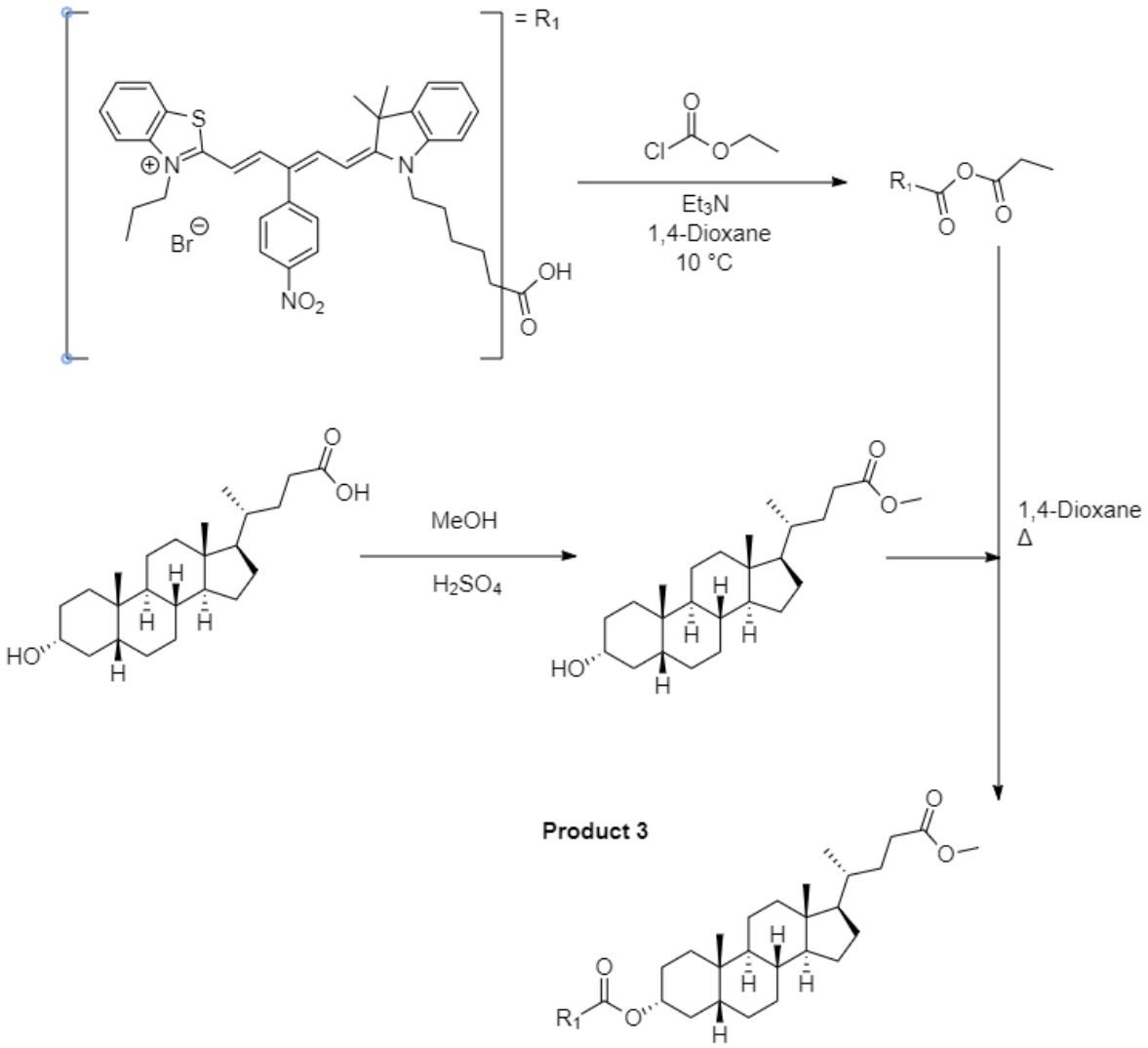

Appendix 3. ^{1}H NMR spectrum of product **1**

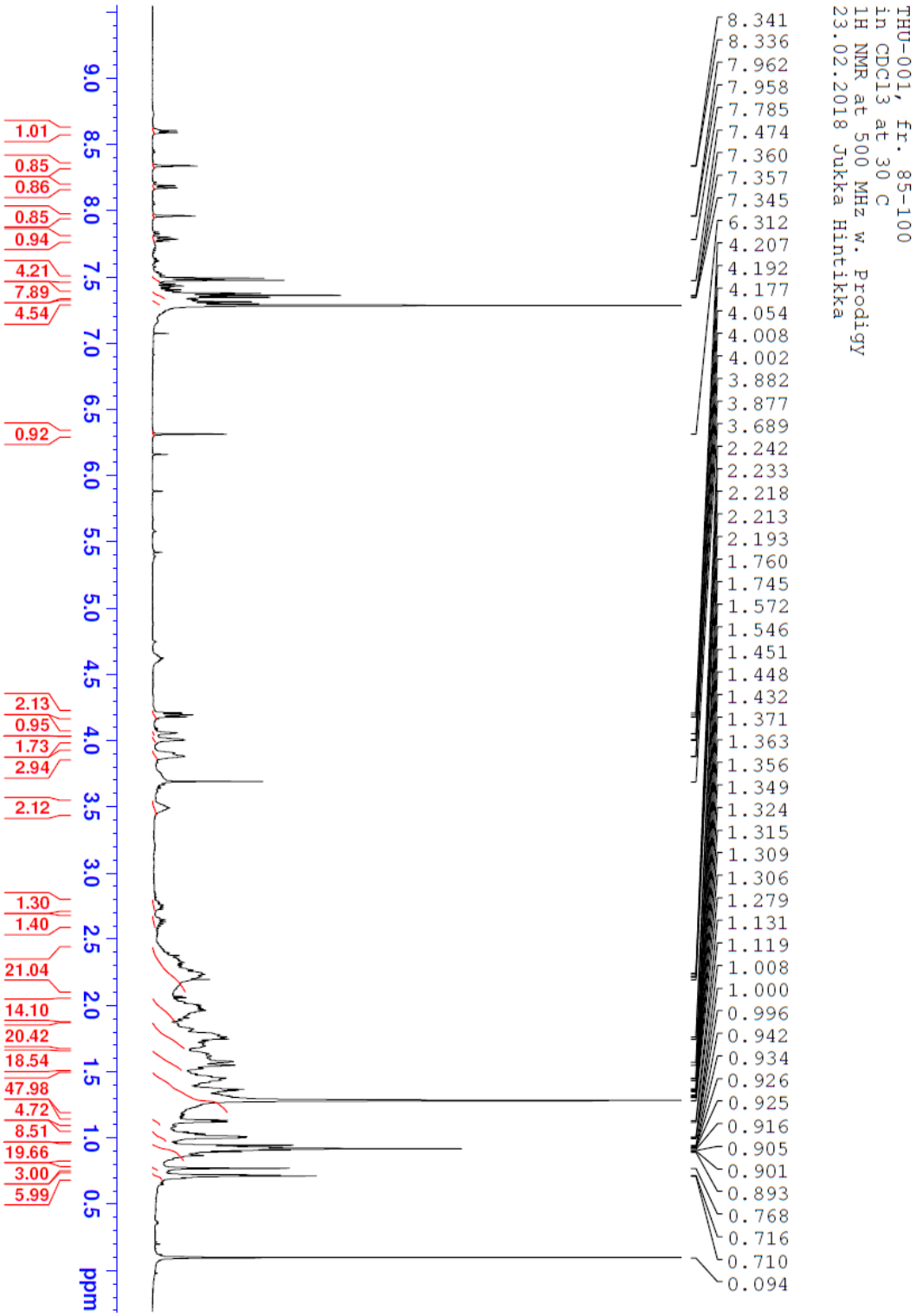

Appendix 4. ^{13}C NMR spectrum of product **1**

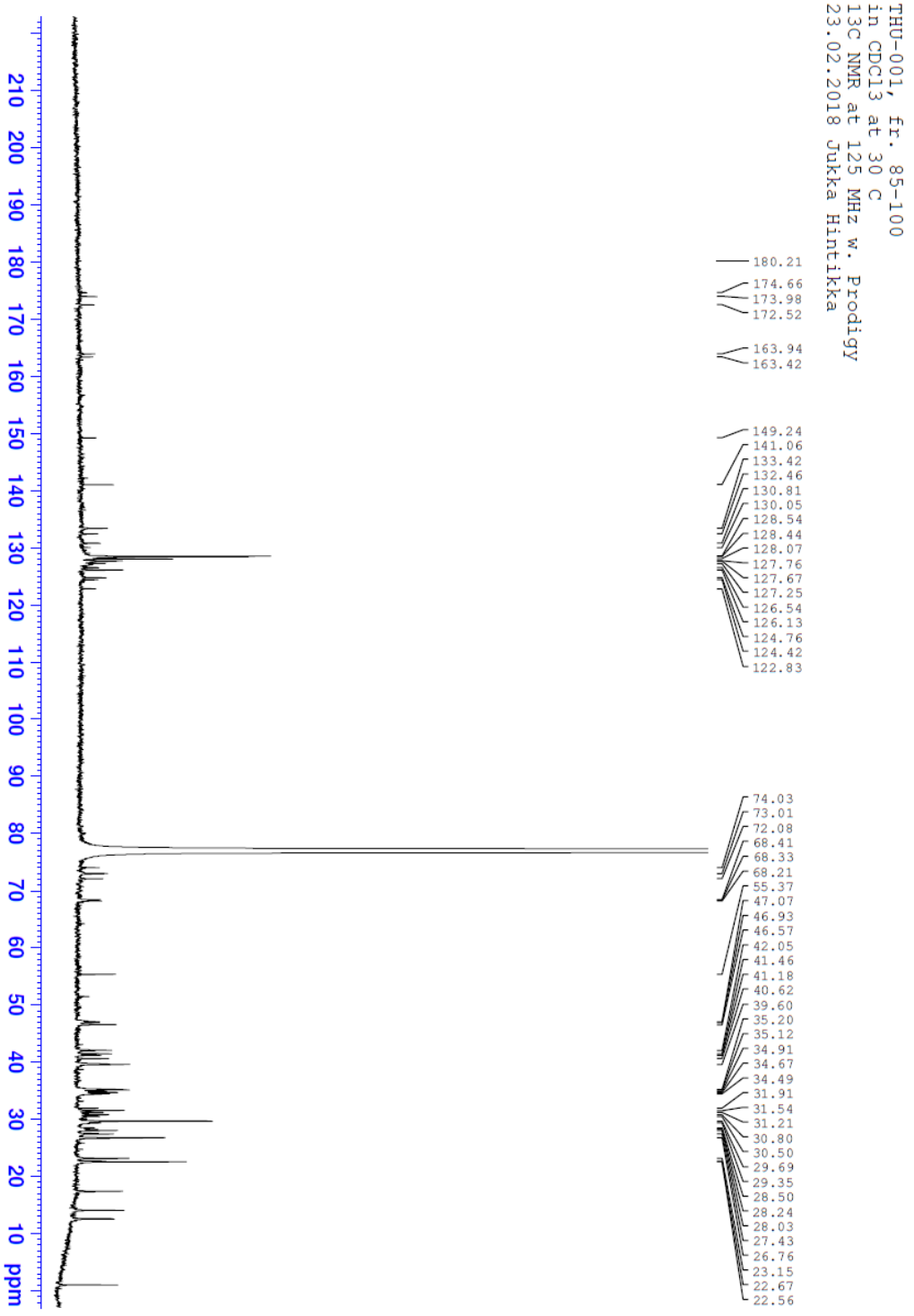

Appendix 5. Mass spectrum of product **1**

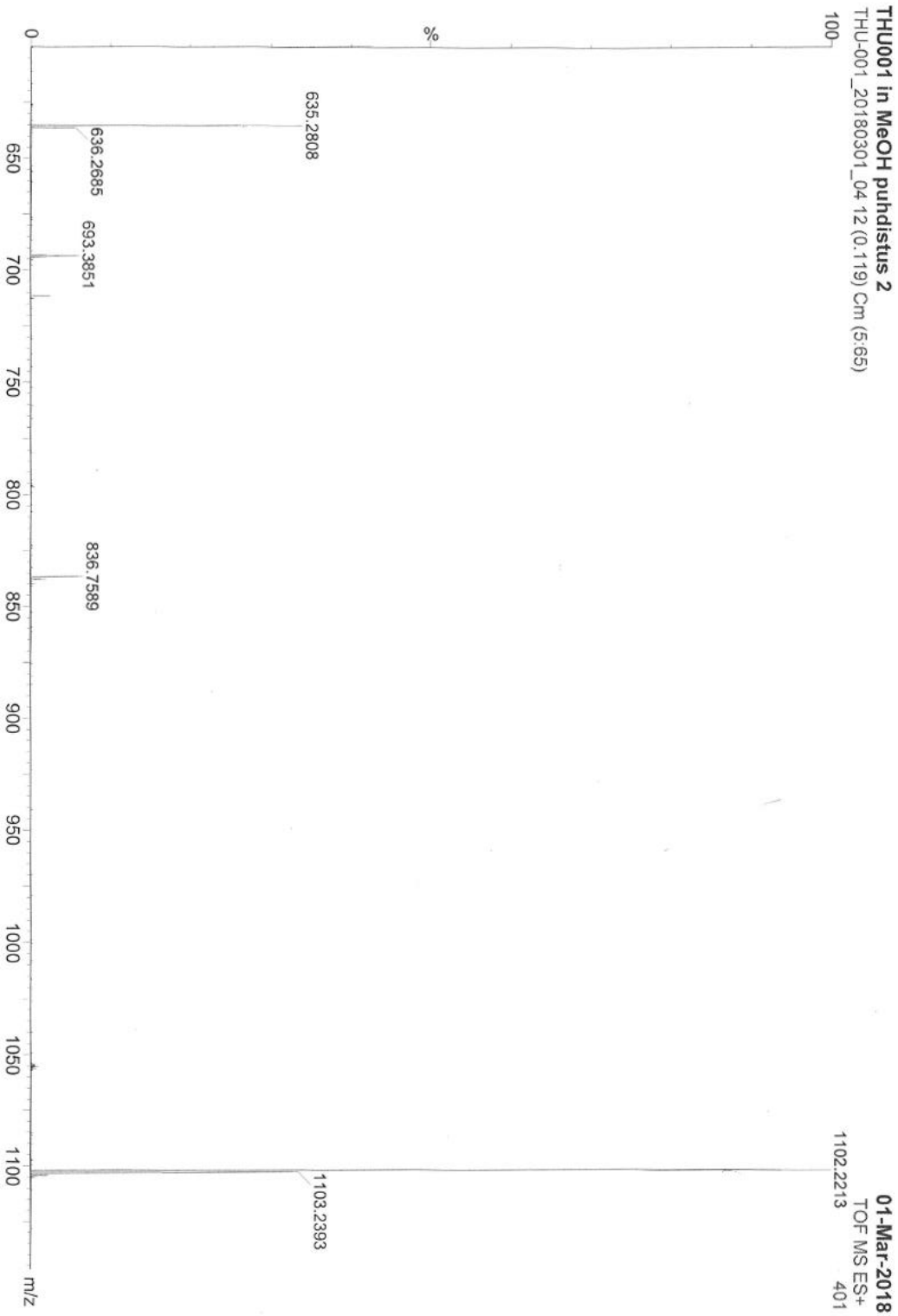

Appendix 6. ^{1}H NMR spectrum of product **2**

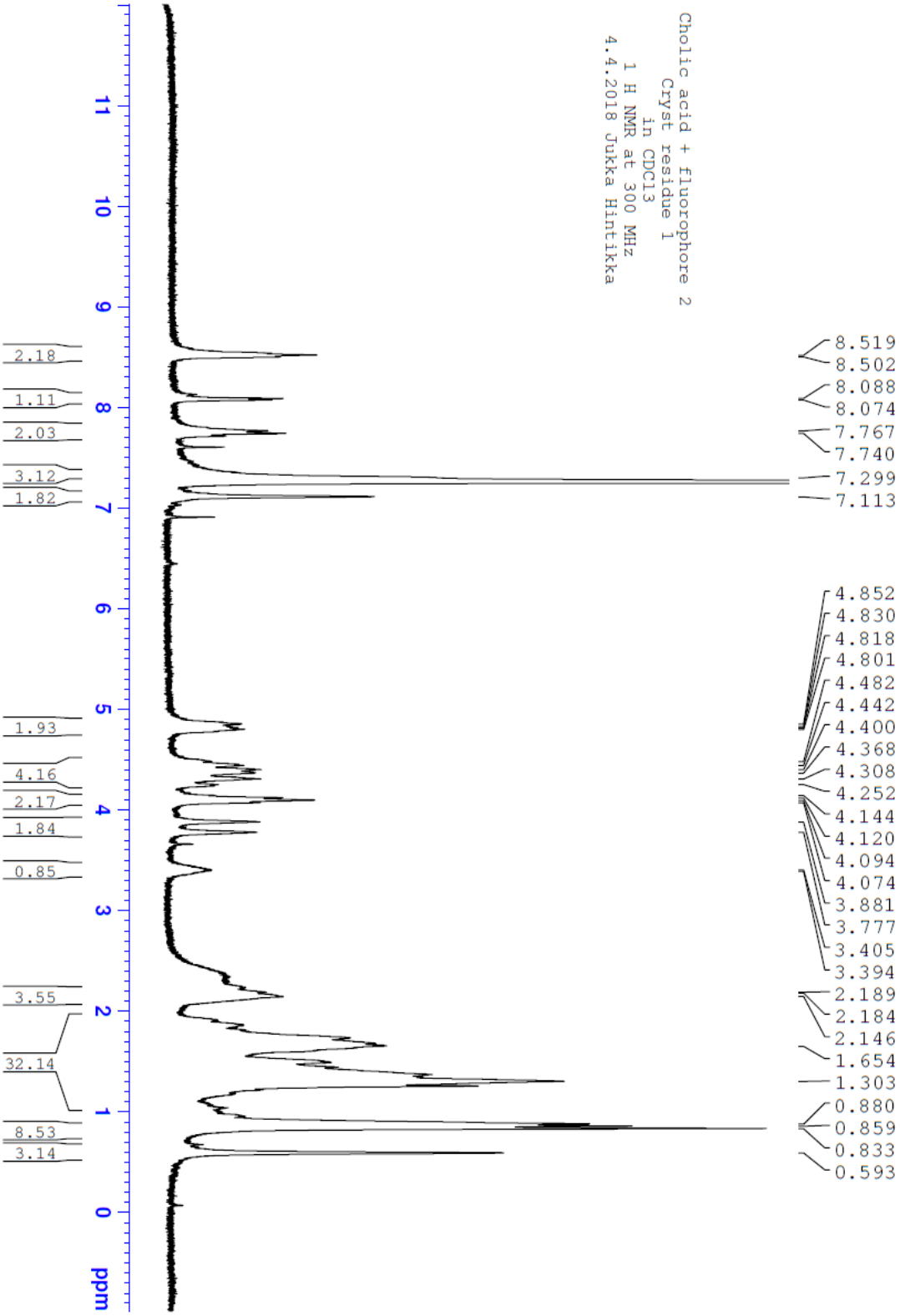

Appendix 7. ^{13}C NMR spectrum of product **2**

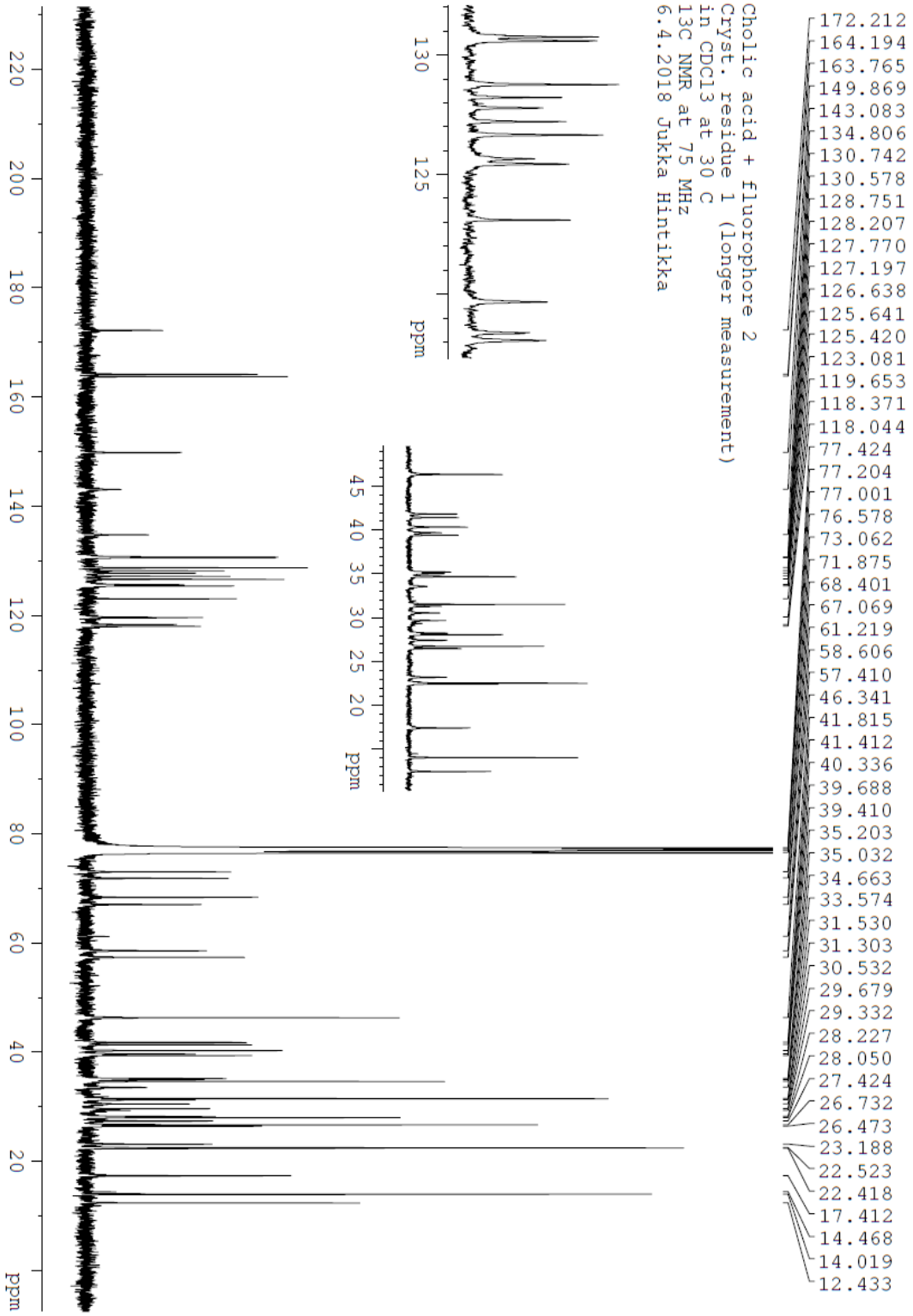

Appendix 8. Mass spectrum of product **2**

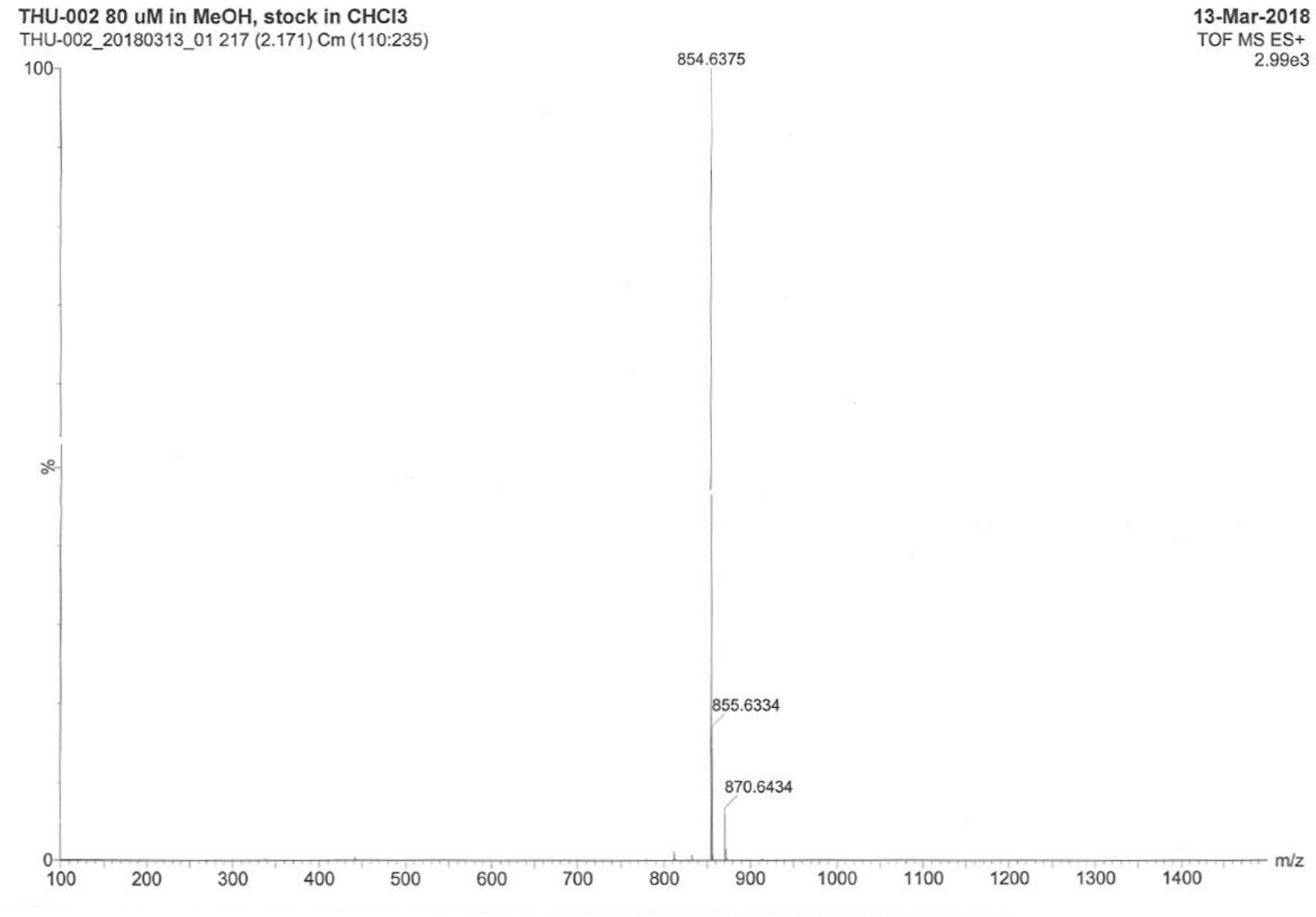

Appendix 9. ^{1}H NMR spectrum of product **2b**

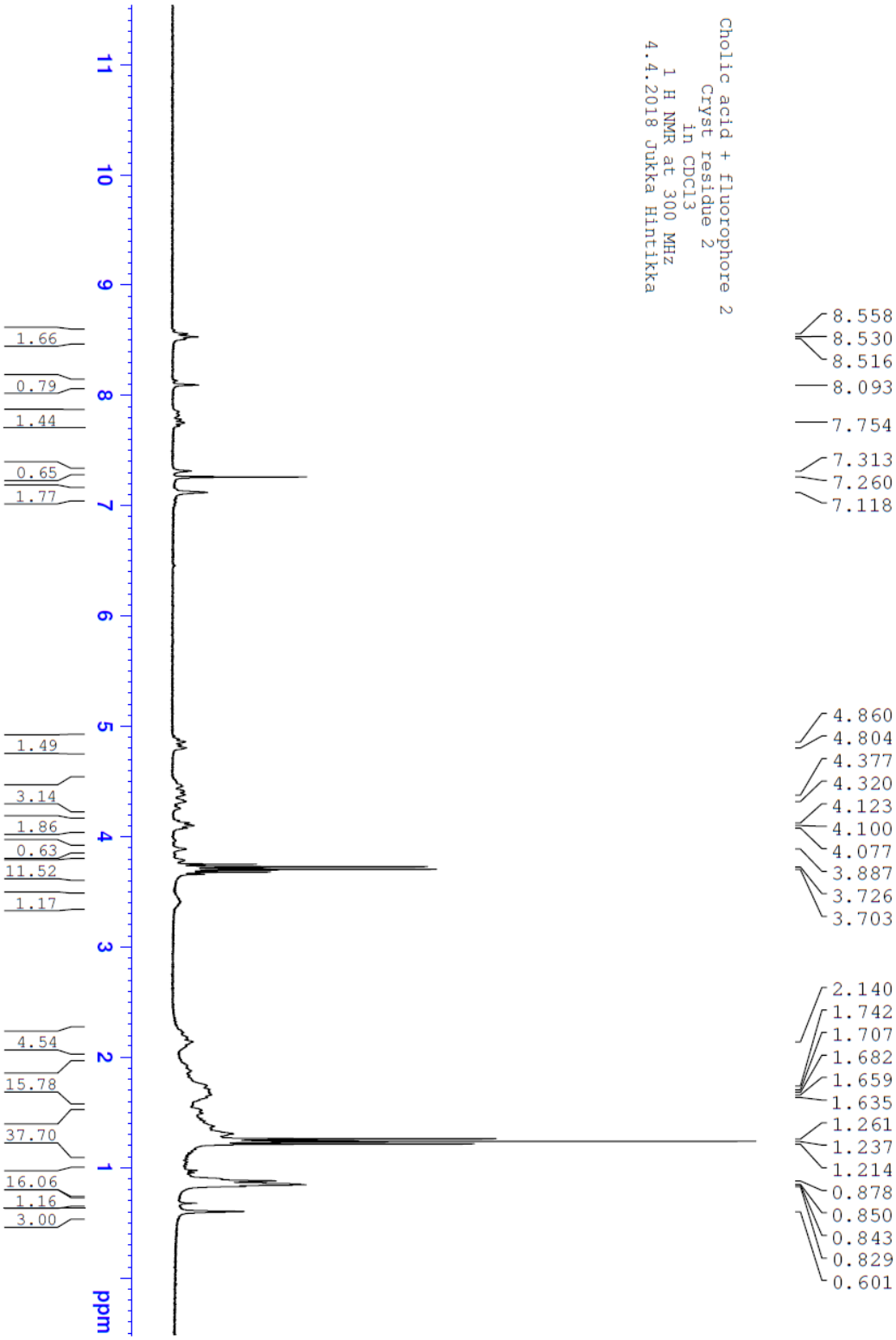

Appendix 10. ^{1}H NMR spectrum of product **3**

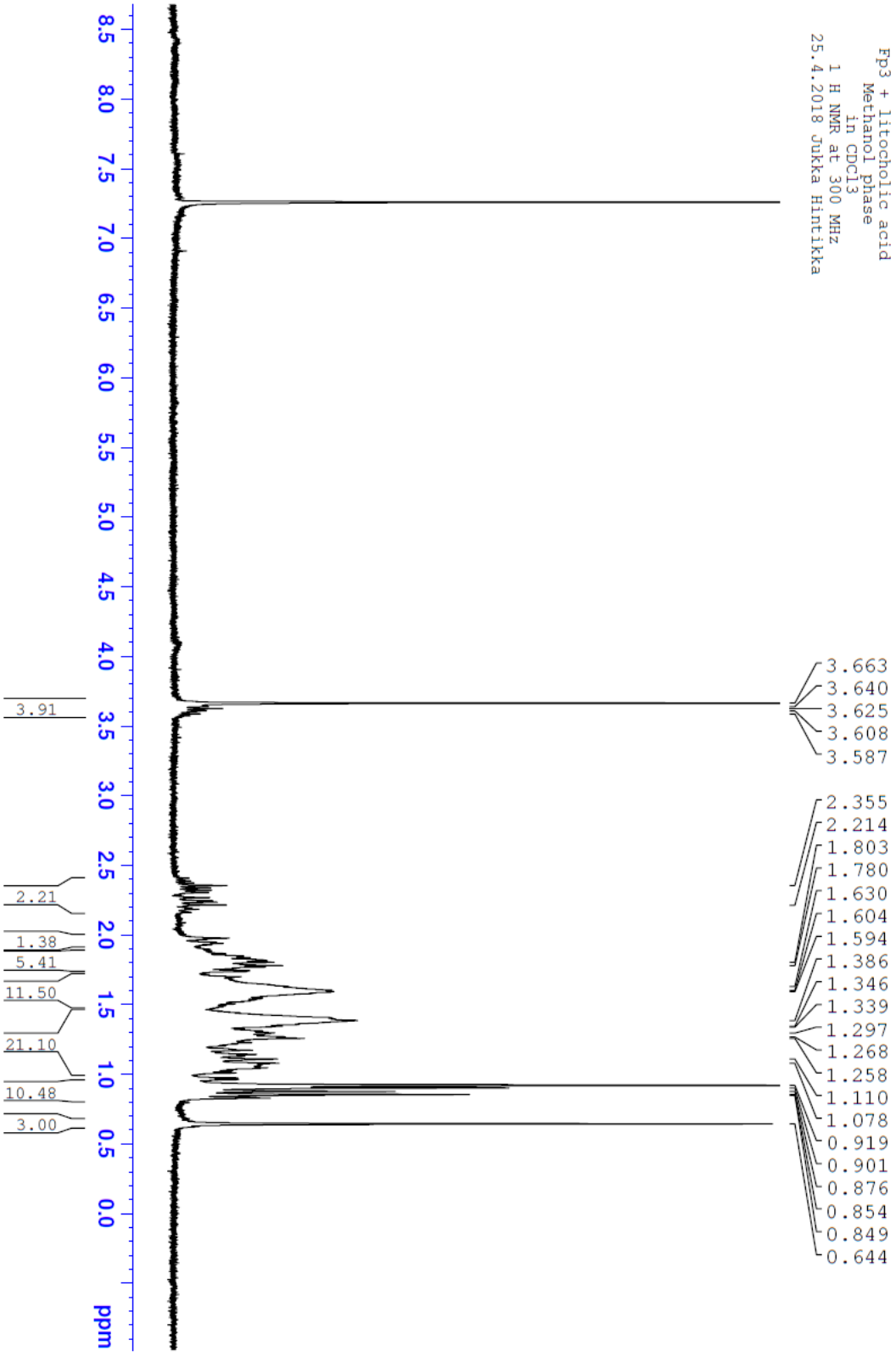

Appendix 11. ^{13}C NMR spectrum of product **3**

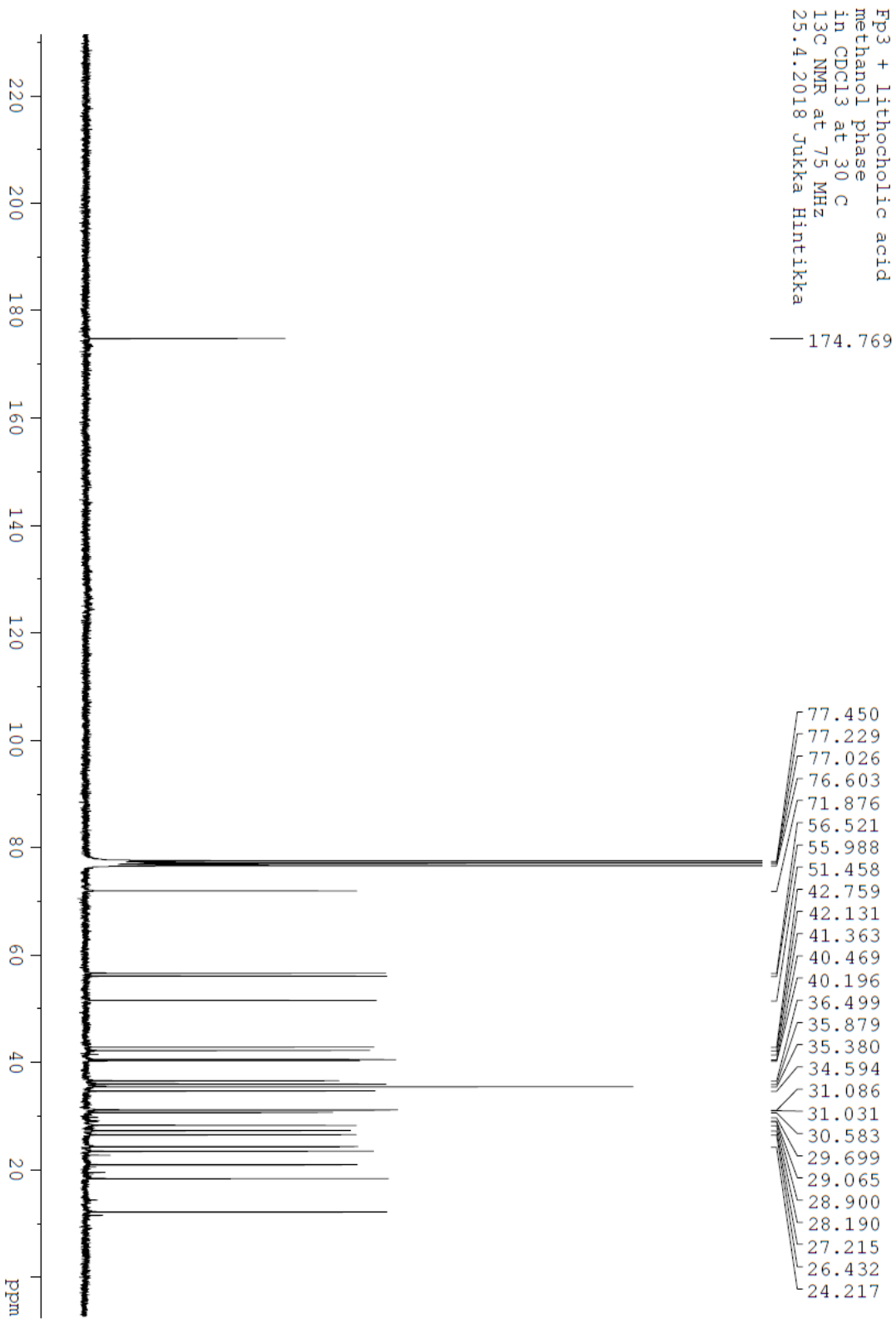

Appendix 12. Mass spectrum of product **3**

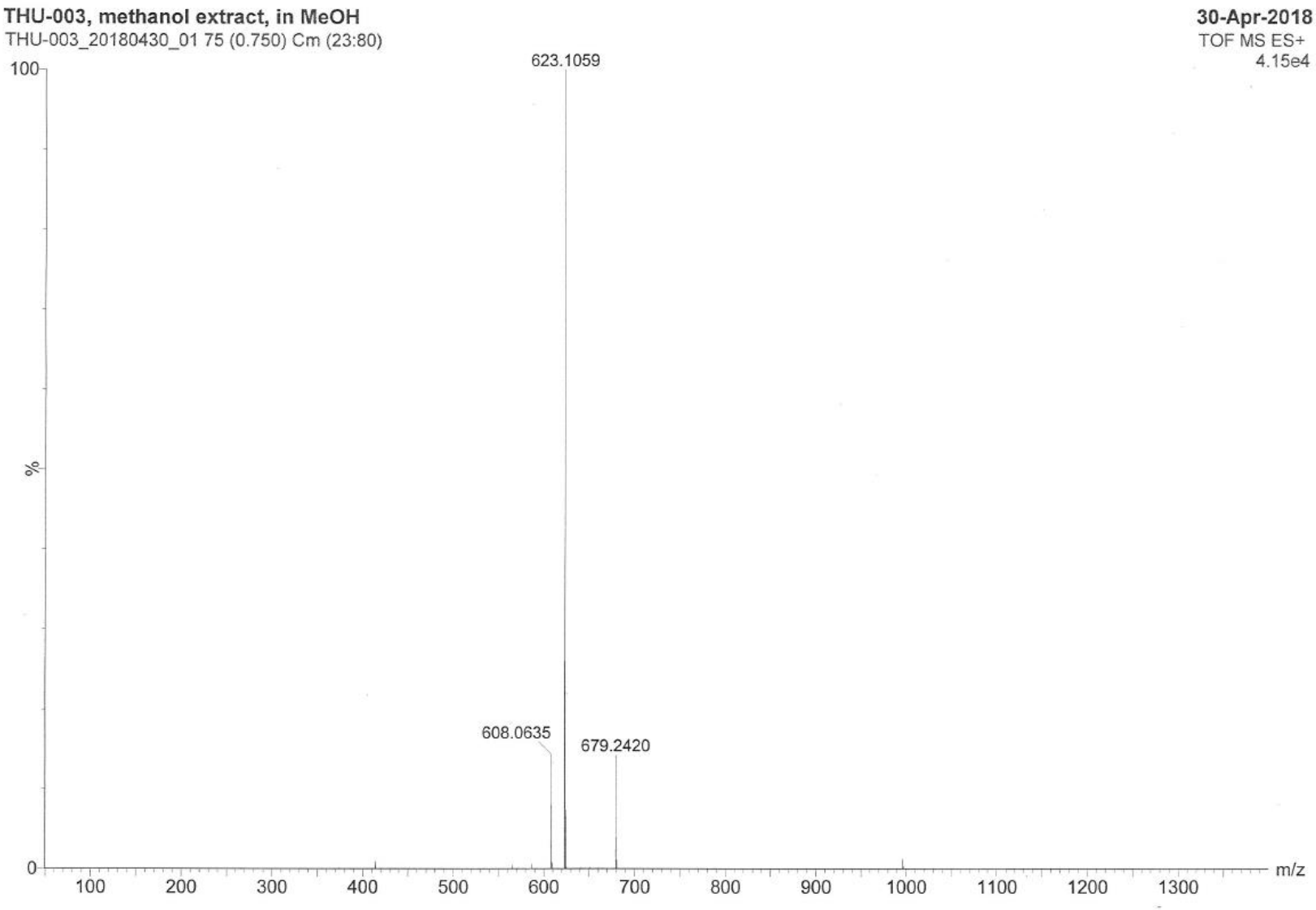

Appendix 13. ^{1}H NMR spectrum of product **3b**